NTIA Report 83-134

FM SPECTRAL MODELING AND FDM/FM SIMULATION PROGRAMS

CESAR A. FILIPPI

U.S. DEPARTMENT OF COMMERCE
Malcolm Baldrige, Secretary

David J. Markey, Assistant Secretary
for Communications and Information

OCTOBER 1983

TABLE OF CONTENTS

LIST OF TABLES

TABLE OF CONTENTS (CONTINUED)

LIST OF FIGURES

TABLE OF CONTENTS(CONTINUED)

LIST OF FIGURES

ABSTRACT

This report is concerned with the spectral representation of analog FM signals, with particular attention to FDM/FM satellite communication systems. The FM spectral modeling and gaussian approximation principles are analyzed and extended to develop computer simulation programs capable of providing representative FM spectra. A generalized program is developed to accommodate a variety of baseband and preemphasis characteristics, and adapted to generate FDM/FM telephony spectra. The program features the automatic validation and generation of the gaussian spectrum model if applicable, or the automatic simulation of the modulation process to generate the FM spectrum samples otherwise. The program is used to simulate a collection of satellite FDM/FM telephony spectra, which are to be applied as input data into other available interference analysis programs, as part of a major automated computer capability dedicated to the comprehensive assessment of orbital congestion and spectrum resource management concerns pertinent to national and international satellite communication systems scenarios.

KEY WORDS

FM Spectrum Models
Gaussian Spectral Approximation
FM Spectrum Simulation
FDM/FM Telephony Spectra

SECTION 1

GENERAL INTRODUCTION

The National Telecommunications and Information Administration (NTIA) is responsible for managing the radio spectrum allocated to the U.S. Federal Government. Part of NTIA's responsibility is to: "...establish policies concerning spectrum assignment, allocation and use, and provide the various Departments and agencies with guidance to assure that their conduct of telecommunications activities is consistent with these policies" (Department of Commerce, 1980). In support of these requirements, NTIA performs spectrum resource assessments to identify existing or potential spectrum utilization and compatibility problems among the telecommunication systems of various departments and agencies. NTIA also provides recommendations to resolve any spectrum usage or allocation conflicts, and to improve the spectrum management functions and procedures.

NTIA is engaged in the development of an automated computer capability to be used by the Federal Government for the comprehensive assessment of national and international satellite communication systems. The program will feature both interference evaluation and logical optimization of a varying systems population, thus supporting the orbit and spectrum resource management functions. The effective coexistence of multiple satellite systems and service signal transmissions represents a critical concern from the orbital congestion, communications interference and service reliability standpoints.

The orbital and spectrum congestion introduces unwanted signals into the antennas and receivers of dedicated satellites and earth stations. The interfering signals processed by the satellite transponder and earth station receiver equipment ultimately appear as degradation effects on the desired output information, whether it be analog messages or digital symbols. The link geometries and power budgets of the various satellite systems establish desired and interference signal levels at the receiving station inputs, which need to be converted into output degradation effects so as to guide the logical assessment of the operational scenarios.

The development of receiver transfer characteristics to evaluate the interference degradation effects requires accurate spectral representations of the signals involved (Jeruchim and Kane, 1970; Pontano, et al, 1973; Das and Sharp, 1975). Many existing models and formulations contain simple qualitative assumptions or restricted parametric conditions as validity constraints, with more accurate spectral representations needed to employ the available results or develop new ones as required. For example, the compact formulations available for analog FM applications are conditioned on extreme high or low modulation indices, with representation uncertainties hindering their usage in intermediate index situations.

The sections that follow are concerned with the spectral representation for analog FM applications. The spectral modeling and gaussian approximation principles are first identified in Section 2, and then extended to develop effective FM spectrum simulation programs capable of resolving the modeling concerns and providing representative FM spectra. The programs developed consist of a specific one dedicated to a particular baseband modulation, plus a

generalized one capable of handling a wide variety of modulation characteristics. The specific program presented in Section 3 features the only nontrivial modulation case where a compact formulation results for the output spectra. The program algorithm reproduces the output spectrum formula, thus bypassing the need to simulate the modulation process itself.

The generalized simulation program of Section 4 then accommodates a variety of baseband and preemphasis characteristics with minimal assumptions, by actually simulating the modulation process via equivalent block functions and transform processors. This program was further adapted to produce FDM/FM telephony spectra by including a baseband spectrum driver and CCIR preemphasis, with the high and low baseband frequencies and the rms multichannel frequency deviation selectable by the user. It also features an adjustable bandwidth expansion parameter that accounts for the FM spectral expansion while controlling the distortion and aliasing effects of the discrete representations.

The validity of the gaussian approximation for the FM spectral representation under high modulation index conditions was analyzed using both the specific and generalized FM spectrum programs. A gaussian spectrum generation algorithm was included in each program, and spectral comparisons were performed to identify the modulation index constraints needed for the gaussian spectral approximation to hold. The programs can thus deliver either the simulated FM spectra or their wideband gaussian approximation as needed, and can be used as inputs to other programs dedicated to evaluate receiver transfer characteristics from given spectral representations of the desired and interference signals.

The generalized FM spectrum generation program was employed to generate a collection of FDM/FM telephony spectra representative of existing and planned satellite communication systems. The available system specifications are used to provide the input parameters needed for the spectral generation, and the FDM/FM output spectra resulting from the simulation program are automatically computed and plotted along with the gaussian spectral representation for comparison purposes.

The FDM/FM spectral simulation results are presented in Section 4. The evolution of the gaussian spectral approximation as the modulation index increases is noted to be really governed by the equivalent rms phase deviation parameter, which depends both on the rms modulation index and the low/high frequency ratio of the multichannel baseband modulation. An effective formulation of this dependence is provided in Section 5, and incorporated into the simulation program to automatically trigger the gaussian spectral approximation when valid.

The generalized spectrum simulation program is now operational and automated to deliver the FDM/FM system spectra in an efficient way. The user selects an equivalent set of modulation parameters, and the program first computes the rms phase deviation to decide on the gaussian spectral approximation validity. If the latter is valid, the program next computes the appropriate standard deviation for the gaussian curve from the input parameters, and proceeds to generate the gaussian spectrum samples. Otherwise, the program negates the gaussian logic and proceeds with the FM simulation process to deliver the proper FM spectrum samples.

SECTION 2

FM SPECTRAL MODELING AND GAUSSIAN REPRESENTATIONS

The FM signal spectrum models presently employed only have a compact formulation in certain cases. At low modulation indices, the FM output spectrum is effectively approximated by a discrete carrier component plus a double-sideband continuous spectrum. The latter has the same shape as the equivalent lowpass spectrum that phase modulates the carrier under low index conditions. In particular, such lowpass spectrum will be identical to the input baseband spectrum when ideal FM preemphasis (parabolic power weighting) is employed.

At high modulation indices, the FM output spectrum is characterized by a small discrete carrier component plus a predominant continuous gaussian spectrum centered around the carrier component. The relative power distribution between these discrete and continuous components is uniquely specified by the rms phase deviation. The only other information needed to specify the FM output spectrum is then the gaussian standard deviation or variance parameter, which controls the effective width of the continuous gaussian portion of the spectrum. This parameter has been formulated in terms of the rms phase or frequency deviation employed, and renders the FM spectrum model characterization under high index conditions.

The gaussian spectrum model is assumed to hold regardless of the input baseband spectrum or preemphasis characteristic, as long as the high modulation index exists. However, the identification of what represents a high index condition remains somewhat arbitrary. Also, the variety of baseband spectra, preemphasis characteristics, modulation indices and frequency deviations employed in the different FM signals of interest spans a considerable range of spectral shapes and parameter values, which hinders the spectral approximation evaluation. Hence, the FM spectral modeling issue should be given due attention to assure accurate signal characterizations and permit reliable interference analyses.

Another pertinent issue consists of the parametric value assignment in the gaussian spectrum model. The standard deviation parameter in the gaussian formula is sometimes specified from the rms phase deviation in a PM formulation, and sometimes from the rms frequency deviation in an FM formulation, as discussed in what follows. The conversion is tractable in most baseband cases without preemphasis, but the preemphasized baseband cases can lead to computational difficulties. The preemphasis network can be designed to preserve the rms phase or frequency deviation but not both in general, and the evaluation of the one not being preserved may be difficult yet required if the gaussian spectral representation is to be employed.

GAUSSIAN SPECTRAL APPROXIMATION PRINCIPLES

The original principle supporting the gaussian spectral approximation under high index conditions is based on Woodward's theorem (Blackman and McAlpine, 1969). It states that the limiting form of the FM power density spectrum as the index increases is given by the probability distribution of the instantaneous

modulating frequency. Hence, the assumption of gaussian statistics in the baseband modulating signal (with arbitrary spectrum) directly induces a limiting gaussian FM spectrum for high indices under the theorem, with the gaussian standard deviation given by the rms frequency deviation.

The modulation index magnitude needed for an effective representation by the gaussian spectrum was not resolved in Woodward's theorem. The identification of crossover index bounds is hindered by the fact that they may vary with the modulating signal spectrum, since all Woodward's theorem provides is for a gaussian spectrum convergence in the limit. There have been some theoretical extensions of the theorem, with the main results consisting of autocorrelation or spectrum error estimates or bounds as a function of the rms index or frequency deviation, as well as some spectral simulation results for specific baseband spectra. However, the error performance and criteria were found to vary in prediction accuracy capability with the modulation index value and the baseband spectral shaping involved (Blackman and McAlpine, 1969; Algazi, 1968).

Another principle supporting the gaussian spectral approximation under high index conditions relies on a power series expansion (Middleton's expansion) of the autocorrelation function of the modulated signal, again assuming baseband gaussian statistics but arbitrary spectrum (Abramson, 1963). The series terms are each characterized by a different power of the autocorrelation function of the equivalent baseband phase modulation including any preemphasis effects. The autocorrelation function of the frequency modulated signal becomes a weighted superposition of these powers of the autocorrelation function of the phase modulating signal.

The power density spectrum of the modulated signal becomes a weighted superposition of spectral terms obtained from the series expansion. Each spectral term consists of an n-th order convolution of the baseband phase modulating spectrum, with the number of convolutions varying with the series terms. Each spectral convolution is then weighted by a different coefficient and superposed to yield the resultant FM spectrum. The gaussian spectral approximation essentially consists of motivating how the weighted superposition of different spectral shapes can be manipulated under high index conditions to result in a gaussian spectrum (Abramson, 1963).

Analysis of the Series Expansion Representation

The equivalent phase modulating signal is assumed to be a stationary gaussian process with zero mean and fixed standard deviation (β radians). It modulates a sinusoidal carrier of fixed amplitude (A) and frequency (ω_c radians per second), so that the correlation function $R_y(t)$ of the modulated signal y(t) can be expressed in terms of the correlation function $R_x(t)$ of the modulating signal x(t) as (Abramson, 1963):

$$R_y(t) = \frac{A^2}{2} \cdot e^{-[R_x(o)-R_x(t)]} \cdot \cos \omega_c t \qquad (1)$$

The values $R_x(o) = \beta^2$ and $R_y(o) = A^2/2$ represent the average power in the modulating and modulated signals, respectively. It is convenient to use normalized (unit power) correlation functions $r(t) = R(t)/R(o)$ and corresponding power density spectra $s(f) = S(f)/R(o)$ for both signals, and to work with an equivalent lowpass spectral version of the modulated signal (which need only be shifted and scaled to the carrier frequency to obtain the actual spectrum). The equivalent lowpass correlation function and power spectrum of the modulated signal are given by (Abramson, 1963):

$$r_y(\tau) = e^{-\beta^2 \cdot [1-r_x(\tau)]} = e^{-\beta^2} \cdot \sum_{n=o}^{\infty} \frac{\beta^{2n}}{n!} [r_x(\tau)]^n \qquad (2)$$

and

$$s_y(f) = e^{-\beta^2} \cdot \{\delta(f) + \sum_{n=1}^{\infty} \frac{\beta^{2n}}{n!} [s_x(f) \overset{n}{*} s_x(f)]\} \qquad (3)$$

The power spectrum expression consists of a weighted superposition of the form $s_y(f) = \Sigma a_n C_n(f)$, where the n=o spectral term corresponds to the discrete carrier component with $C_o(f) = \delta(f)$. The other $C_n(f) = s_x(f) \overset{n}{*} s_x(f)$ spectral terms are each an n-th order convolution of the normalized modulating spectrum $s_x(f)$. Each of these $C_n(f)$ spectral terms has a unit area, since $s_x(f)$ has this property and it is preserved through the successive convolutions (e.g., $s_x(f)$ has statistical p.d.f. properties and $C_n(f)$ behaves like the p.d.f. of a sum of independent identical random variables).

The weighting coefficients are given by $a_n = e^{-\beta^2} \cdot \beta^{2n}/(n!)$ so that they are poisson distributed over (n) with parameter $\lambda = \beta^2$. These non-negative coefficients add to unity so that each represents the fraction of the total power $(A^2/2)$ in the modulated signal that is being contributed by each series term (since the $C_n(f)$ spectra all contribute unit power). In summary, the equivalent spectrum of the modulated signal has been developed as a weighted superposition of spectral terms, where the $C_n(f)$ convolution functions control the spectral shapes being superimposed, while the a_n weights control their relative magnitudes and specify their power contribution to the total modulated signal power.

At low rms phase deviations (β), only the first few series coefficients are needed to essentially reproduce the total signal power. As the β-value increases, the power distribution becomes more spread out (rather than concentrated) on many (rather than few) terms with intermediate values of (n), with other terms having small or large (n) values contributing little power. Hence, the significant terms needed to preserve a given power percentage in a truncated (at both sides) series representation can be readily identified from the statistical poisson distribution, which specifies the a_n coefficient magnitudes. The procedure is presented in TABLE 1 as a function of the rms phase deviation (β) for various power percentages (90,95,99%) to be preserved in the modulated signal.

TABLE 1

SIGNIFICANT TERMS (VALUES OF n) VS RMS PHASE DEVIATION (β)
FOR VARIOUS POWER PERCENTAGES

$\lambda = \beta^2$	β	n(90%)	n(95%)	n(99%)
1	1.000	0-2	0-4	0-4
2	1.414	0-5	0-5	0-6
3	1.732	1-6	0-6	0-8
4	2.000	1-7	1-8	0-9
5	2.236	2-9	1-9	0-11
6	2.449	2-10	2-11	1-13
7	2.646	3-11	2-12	1-14
8	2.828	4-13	3-13	2-16
9	3.000	4-13	4-15	2-17
10	3.162	5-15	4-16	3-18
11	3.317	6-16	5-17	4-20
12	3.464	7-18	6-19	4-21
13	3.606	7-18	6-20	5-23
14	3.742	8-20	7-21	5-24
15	3.873	9-21	8-23	6-25
16	4.000	10-23	9-24	7-27
17	4.123	10-23	9-25	7-28
18	4.243	11-24	10-26	8-29
19	4.359	12-26	11-27	9-31
20	4.472	13-27	12-29	10-32

These results can be directly used for the selection of the number of series terms and spectral convolutions needed in a truncated representation or simulation of the modulated signal spectrum. The entries in TABLE 1 show that up to nine terms besides the carrier component may be needed for $\beta < 2$ radians, with the number reaching 17, 27, 32 terms as the index increases to 3, 4, 5 radians. Some spectral simulations of FDM/FM telephony are available in the open literature for $\beta = 1$ to 5 radians, but employing only ten series terms in the truncated representation (Ferris, 1968). The results of TABLE 1 illustrate that not only more terms are actually needed for such range, but that the first ten terms have a negligible or secondary contribution once the rms phase deviation exceeds four radians.

Analysis of the Gaussian Spectral Approximation

The gaussian spectrum approximation for high β-values must account for both the spectral shaping provided by the convolution terms and the power distribution provided by the weighting coefficients. The shape of each of the convolution functions $C_n(f)$ approaches a gaussian form as (n) increases based on the central limit theorem. All these limiting gaussian spectra have zero mean if $s_x(f)$ is a lowpass spectrum, but their standard deviations are different for each (n) value. Indeed, their respective variances are given by $\sigma_n^2 = n \cdot B_x^2$ where $B_x^2 = \int f^2 s_x(f) df$ is the rms bandwidth squared of the phase modulating signal. Hence, even though all high-order spectral convolutions are approximately gaussian, each converges to a distinct gaussian spectrum with their rms spectral widths varying with (n) according to $\sigma_n = \sqrt{n} \cdot B_x$.

The poisson distribution of the weighting coefficients (a_n) can itself be approximated for β^2 large by discrete point samples from a gaussian envelope with mean $\lambda = \beta^2$ and variance $\lambda = \beta^2$ as shown in Figure 1. The solid lines represent the actual poisson values whose center location and width distribution varies with $\lambda = \beta^2$, but which follow the dotted gaussian envelope approximation when $\lambda = \beta^2$ is large. The poisson distribution peaks at $n = \lambda = \beta^2$ (i.e., the nearest integer to $\lambda = \beta^2$) with a magnitude $a_n \approx (2\pi\beta^2)^{-\frac{1}{2}}$ based on the gaussian envelope peak. The other coefficients on both sides are reduced by a factor of $\exp [-(n-\beta^2)^2/2\beta^2]$ relative to the peak based on the gaussian envelope decay.

In summary, the superposition $s_y(f) = \Sigma a_n C_n(f)$ of poisson-weighted, spectral convolution functions must account for the distinct convergence behavior of the coefficients a_n and the convolutions $C_n(f)$ when motivating the gaussian spectral approximation. The distinct limiting representations involved for each series term are formulated below. They are governed by the gaussian envelope approximation to the poisson distribution for the weighting coefficients, and by the gaussian spectrum approximation via the central limit theorem for the convolution functions.

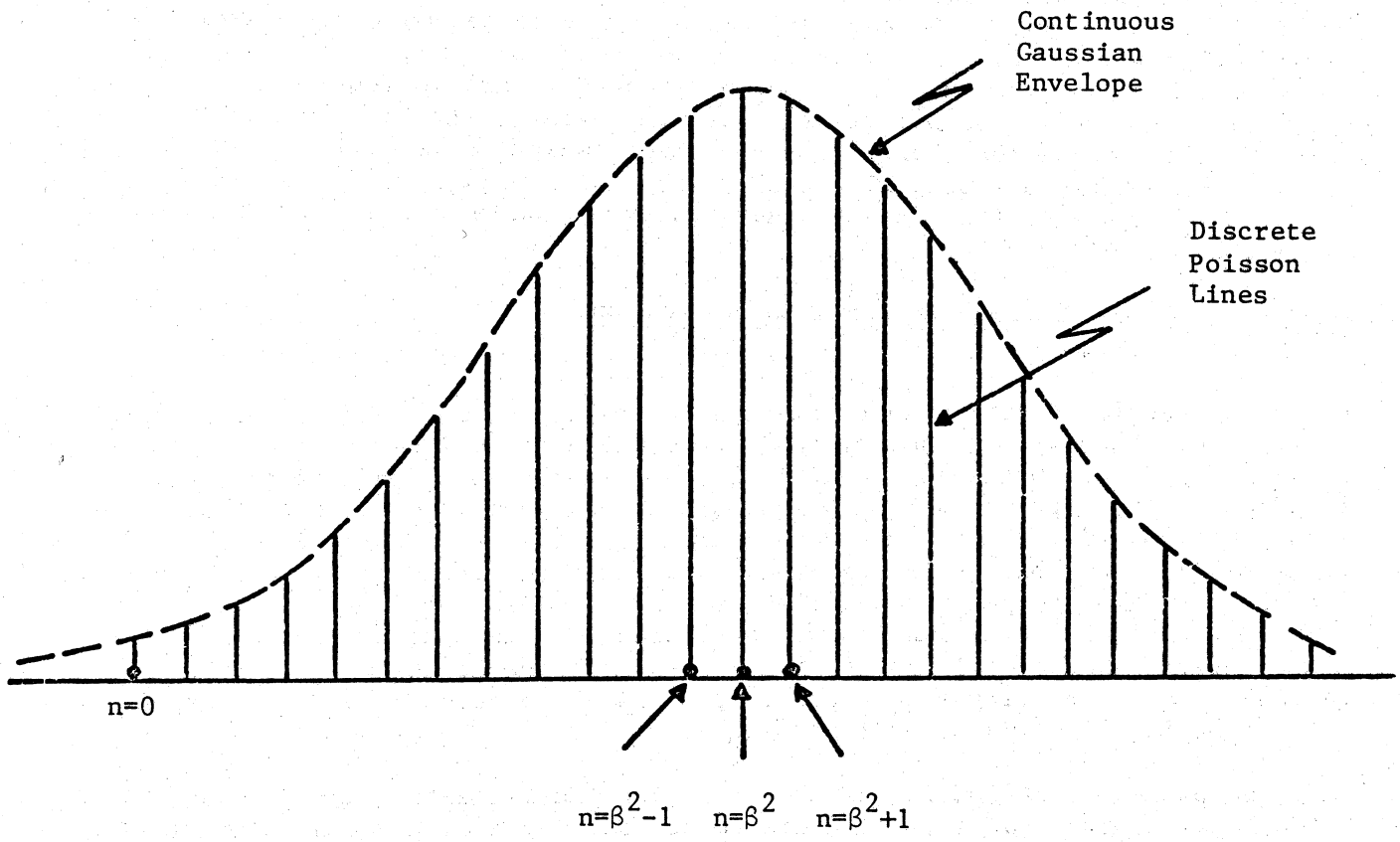

Figure 1. The Gaussian Envelope Approximation to the Poisson Weighting Coefficients.

Poisson Lines: $$a_n = \left[\frac{e^{-\beta^2}\cdot\beta^{2n}}{n!}\right]$$

Gaussian Envelope: $$a_n \approx \left[\frac{e^{-(n-\beta^2)^2/2\beta^2}}{\sqrt{2\pi\beta^2}}\right]$$ for $n \approx \beta^2$ and β^2 large

$$a_n\, C_n(f) = \left[\frac{e^{-\beta^2} \cdot \beta^{2n}}{n!}\right] \cdot \left[s_x(f) \overset{n}{*} s_x(f)\right] \tag{4a}$$

$$\approx \underbrace{\left[\frac{e^{-(n-\beta^2)^2/2\beta^2}}{\sqrt{2\pi\beta^2}}\right]}_{\text{gaussian envelope approximation to poisson-distributed weighting coefficients (for } \beta^2 \text{ large)}} \cdot \underbrace{\left[\frac{e^{-f^2/2nB_x^2}}{\sqrt{2\pi n B_x^2}}\right]}_{\text{gaussian spectrum approximation to n-th order convolution function (for n large)}} \tag{4b}$$

The fact that each convolution function $C_n(f)$ approaches a distinct gaussian shape does not imply that their weighted superposition can also be assumed to be gaussian. The following rationale is also involved in motivating the gaussian spectral representation:

(a) Only those series terms with $n \approx \beta^2$ will have significant weighting coefficients and need be kept.

(b) Their associated $C_n(f)$ functions can all be approximated by the same curve by letting $n = \beta^2$ for all terms kept, which removes the spectral width variation with n.

(c) The series has now been reduced to $(\Sigma a_n) \cdot C(f)$, where $C(f) = C_n(f)$ with $n = \beta^2$, and the sum of coefficients can be approximated by unity since only significant terms were kept.

(d) The series has now become just C(f), which is a gaussian spectral function with standard deviation $\sigma = \beta \cdot B_x$ as obtained by setting $n = \beta^2$ in $\sigma_n = \sqrt{n} \cdot B_x$.

(e) The equivalent lowpass power spectrum of the modulated signal is thus approximated by

$$s_y(f) \approx \frac{e^{-(f^2/2\beta^2 B_x^2)}}{\sqrt{2\pi\beta^2 B_x^2}} \tag{5}$$

This development emphasizes that the gaussian spectral representation of the modulated signal under high rms phase deviation conditions is not a straightforward approximation. It not only requires that each convolution term $C_n(f)$ be gaussian approximated, but also that the weighting coefficients a_n selectively cooperate to remove the spectral width variations with n and approximate a single gaussian spectrum from the superposition of distinct approximately gaussian spectra. Also, the standard deviation $\sigma = \beta \cdot B_x$ of the gaussian spectral approximation can be noted to be a function of the rms phase deviation (β) and the rms bandwidth (B_x) of the equivalent phase modulating signal.

The critical role of the weighting coefficient distribution is further emphasized by considering the special case where the modulating signal has itself a gaussian spectrum, i.e.,

$$S_x(f) = \beta^2 \cdot \frac{e^{-(f^2/2B_x^2)}}{\sqrt{2\pi B_x^2}} \tag{6}$$

In this case the $C_n(f)$ convolution functions in (4a) will all be exactly gaussian with zero mean and variance $\sigma_n^2 = n \cdot B_x^2$ as in (4b), except for the n = 0 discrete carrier component. The gaussian shape of each convolution term is now exact rather than approximate, and it is up to the distribution of the weighting coefficients to render an approximately gaussian spectrum from the superposition of exact but distinct gaussian spectra. This case clearly illustrates that it does not suffice to have each of the spectral convolutions converge to a gaussian shape via the central limit theorem. These distinct gaussian shapes must still be weighted and superimposed to yield a single gaussian representation which is not an automatic result (DeRosa, 1976).

SECTION 3

RECTANGLE CONVOLUTION PROGRAM FOR FM SPECTRUM SIMULATION

The previous sections have shown that the gaussian spectral approximation for FM signals remains to be validated insofar as the modulation index constraints and the baseband spectrum dependence is concerned. A possible approach consists of comparing the gaussian spectrum to the actual FM spectrum obtained from theoretical, simulation or empirical results. One tractable case that features a compact theoretical formulation compatible with computer simulation implementation is considered in this section.

The case in question consists of a lowpass rectangular baseband spectrum that phase modulates the sinusoidal carrier. This case corresponds to a parabolic frequency modulating spectrum, so that it can represent a rectangular baseband spectrum followed by a parabolic preemphasis characteristic in FM applications. The normalized phase modulating spectrum is given by $s_x(f) = 1/W$ for $|f| \leq W/2$, and the interest is to derive the n-th order convolutions $C_n(f)$ of this spectrum, so as to form their weighted superposition with the coefficient distribution governed by the rms phase deviation assumed.

A computer program was developed at NTIA to simulate the compact mathematical formulation representing the n-th order spectral convolutions $C_n(f)$. There is no need to simulate the actual convolution operations, as exact expressions for $C_n(f)$ are available in an iterative form for any (n) value. The computer simulation only requires the development of effective algorithms to implement the iterations involved, and to generate the (a_n) weighting coefficients so as to form the $\Sigma a_n C_n(f)$ superposition representing the FM signal spectrum. The gaussian spectral approximation of (5) was also implemented so as to compare it to the actual FM spectrum obtained.

THE RECTANGLE CONVOLUTION PROGRAM PRINCIPLES

A transformation to a unit width rectangle (W = 1) defined over the unit interval (0, 1) is convenient to exploit available theoretical results. If the n-th order convolution function obtained under these conditions is denoted by $F_n(f)$, with n=1 corresponding to the initial rectangle, then the transformation

$$C_n(f) = \frac{1}{W} F_n\left(\frac{f}{W} + \frac{n}{2}\right) \tag{7}$$

yields the convolution functions of interest. The argument shift by n/2 centers all the $F_n(f/W)$ functions at the origin, and the scaling of the frequency variable and the function magnitude removes the unit width premise.

The $F_n(f)$ functions span the (o, n) interval and exhibit a peak at f = n/2, since they represent n-th order convolutions of a unit rectangle. The $F_n(f)$ functions can be decomposed into unit width segments as shown in Figure 2, and the notation $F_n^{(k)}(f)$ is used to denote the k-th segment of the n-th function

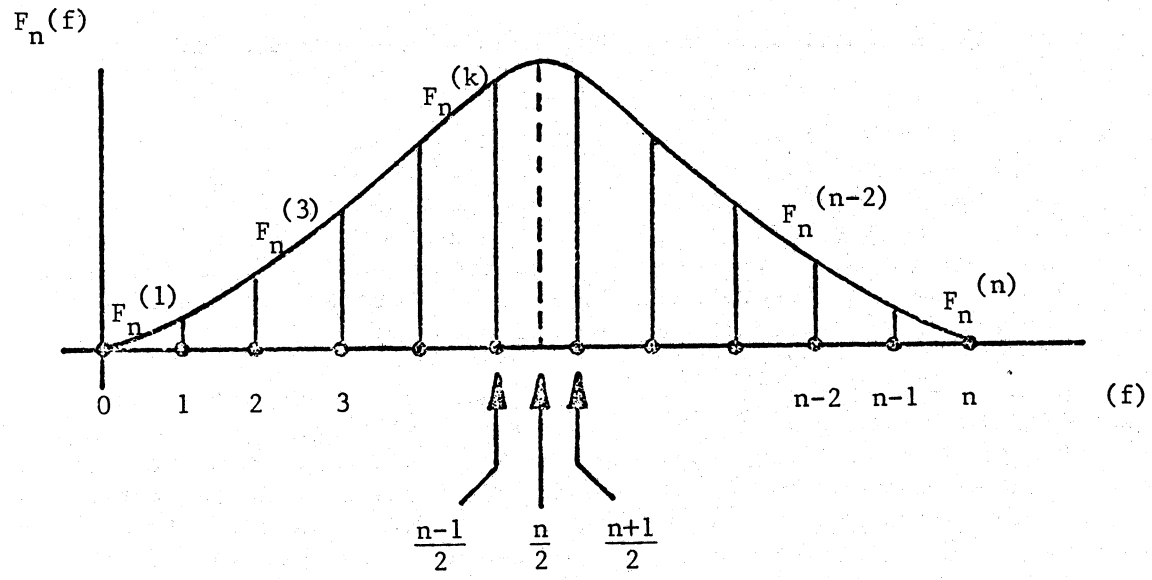

Case of n-odd: Peak Occurs at Middle of Midsegment

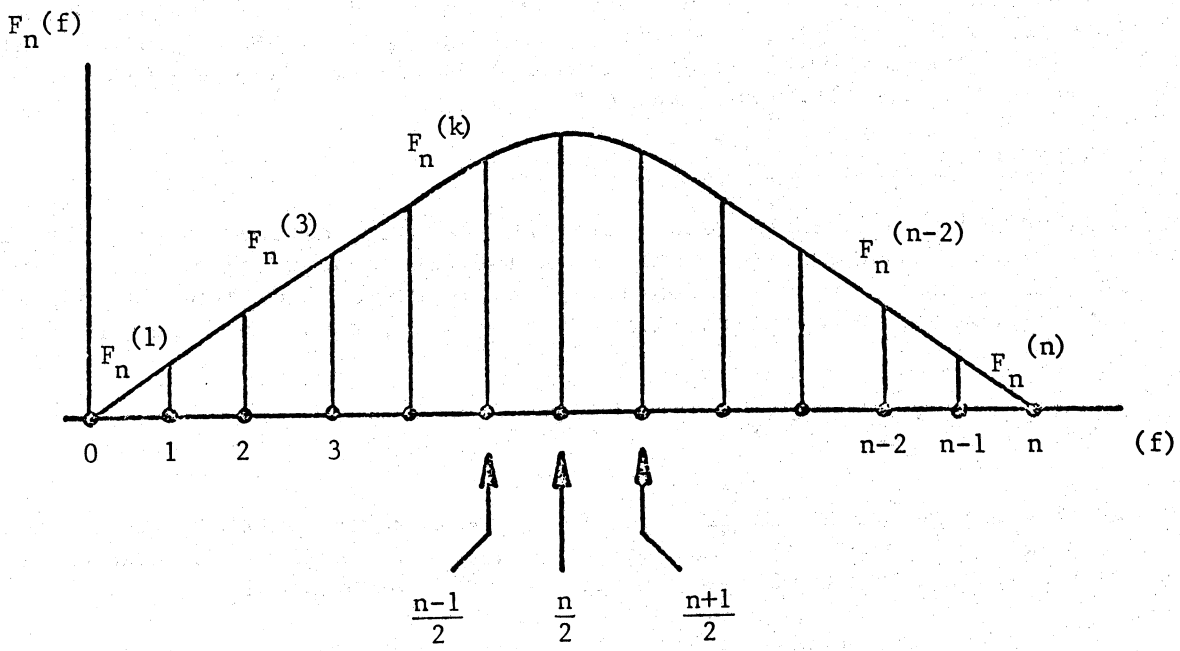

Case of n-even: Peak Occurs at Boundary of Midsegments

Figure 2. Decomposition of $F_n(f)$ into $F_n^{(k)}(f)$ segments.

where $1 \leq k \leq n$. The motivation for this decomposition is that there exist compact expressions for the $F_n^{(k)}(f)$ segments, with an iterative formulation over (k) and (n) that can be exploited in a computer simulation to generate an entire function from one segment (k iteration) and to superpose the weighted functions to obtain the spectrum (n iteration).

The general expression for an arbitrary k-th segment ($1 \leq k \leq n$) of an arbitrary n-th function ($n \geq 1$) is given by (Cramer, 1945):

$$F_n^{(k)}(f) = \frac{1}{(n-1)!} \sum_{j=0}^{k-1} (-1)^j \binom{n}{j} (f-j)^{n-1} \quad , \; k-1 \leq f \leq k \tag{8}$$

and the segment iteration over (k) follows as

$$F_n^{(k+1)}(f) = F_n^{(k)}(f) + \frac{(-1)^k}{(n-1)!} \binom{n}{k} (f-k)^{n-1} \tag{9}$$

The validity of these formulas was verified by independently evaluating the first few convolution functions to match, and then performing induction proofs over (k) and (n) to check the general expressions. The formulas reproduced the convolution functions in question, and the induction relation was verified using binomial coefficient properties (Feller, 1968).

The $F_n(f)$ functions are symmetric about their peak at $f = n/2$, so there is only need to evaluate the segments on one side of the peak to generate the function. The evaluation was performed by developing a digital computer program that simulated the formulas and produced point samples of one-half of each function. The program also included the appropriate shifting of these samples to both sides of the origin, so as to deliver the symmetric left and right samples needed to generate the $C_n(f)$ functions centered at the origin.

The weighted superposition of the $C_n(f)$ functions as shifted versions of the $F_n(f)$ functions can be accomplished in two ways. One approach consists of first generating the entire shifted functions and then adding them on a weighted point basis. This method requires careful selection of the sampling points in the unshifted $F_n(f)$ functions to assure the overlap of the shifted samples from different functions. Another approach consists of first fixing the shifted sample points and only adding the specific weighted samples needed from each unshifted function.

Both methods were investigated for computer simulation, and the first one was implemented in the program. An effective overlap of the shifted samples from different functions was provided by taking an even number of samples per segment in the unshifted functions. The peak of the unshifted functions lies at the

middle of the midsegment if (n) is odd and at the boundary between two symmetric midsegments if (n) is even. The use of an even sampling rate per segment assures the peak coverage regardless of whether (n) is odd or even, and the shifted sample overlaps become assured when the peak overlaps are provided.

The weighting coefficients a_n were generated by the program for a given rms phase deviation (β) using the poisson distribution formula. The number of coefficients needed was established according to TABLE 1 as a function of β for a given power preservation criterion. The n = 0 carrier component with magnitude exp $(-\beta^2)$ was independently evaluated, since the weighted superposition algorithm excluded such discrete component to avoid the impulse simulation. A dB transformation of the discrete and continuous spectral magnitudes was also implemented.

THE RECTANGLE CONVOLUTION PROGRAM RESULTS

The results of the simulation program just described are presented in this section. The normalized FM spectral densities for various β-values are shown in Figures 3(a) to 3(f) with linear scale and in Figures 4(a) to 4(f) in dB scale. The first set of figures illustrates the variation of the FM spectrum from rectangular to gaussian shape as β increases, while the second set serves to discriminate the spectral tail magnitudes obtained. The rms phase deviation is given by β radians, and the carrier component magnitude of $-\beta^2 \log_{10} e$ dB is indicated in all plots.

The number of spectral convolutions (series terms) employed was selected according to TABLE 1 to provide a 99 percent power preservation in the FM spectrum. A minimum of five convolutions was performed for those cases where less would have sufficed. The effectiveness of the procedure was also verified by performing more and less convolutions than required, and verifying that no significant differences were obtained with the extra convolutions.

Some typical verification results are presented in Figures 5(a) and 5(b), where the nominal number of convolutions required is indicated in the legend. A smaller number of convolutions proves to be insufficient for the nominal reproduction, whereas a larger number matches the nominal reproduction in the significant spectral region. The differential effects of the extra convolutions appear in the spectral tail regions as evidenced by the dB plots of Figures 6(a) and 6(b).

The interest is to compare the gaussian spectrum approximation to the FM spectrum obtained via the spectral convolution series. The baseband phase modulating spectrum has the normalized form $s_x(f) = 1/W$ for $|f| \leq W/2$, from which the rms bandwidth follows as $B_x = W/\sqrt{12}$. Hence, the gaussian spectrum approximation has a standard deviaton given by $\sigma = \beta . B_x = \beta W/\sqrt{12}$, so that the gaussian formula (5) becomes

$$s_y(f) = \frac{\sqrt{6}}{\pi} \cdot (\beta W)^{-1} . e^{-6(f/\beta W)^2} \qquad (10)$$

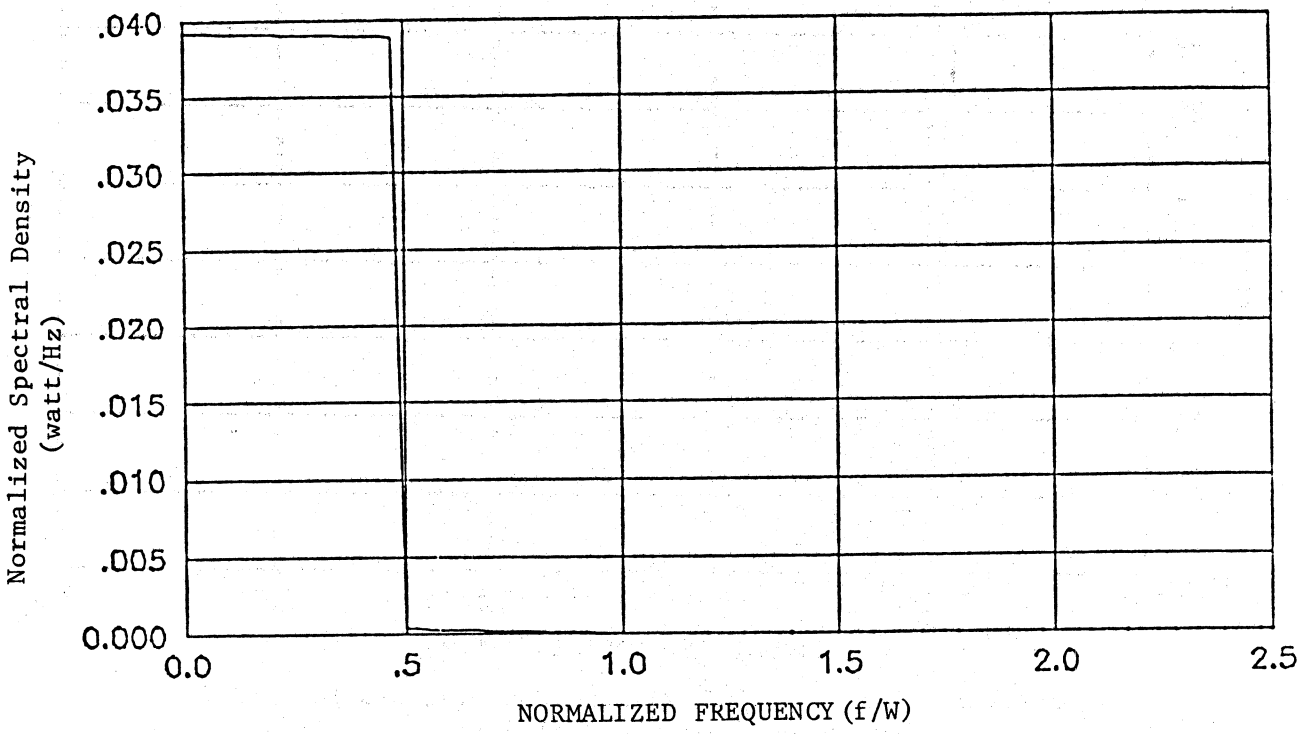

Figure 3(a). Sum of N=5 Weighted Convolutions for β=0.2
(carrier level = -0.174 dBW)

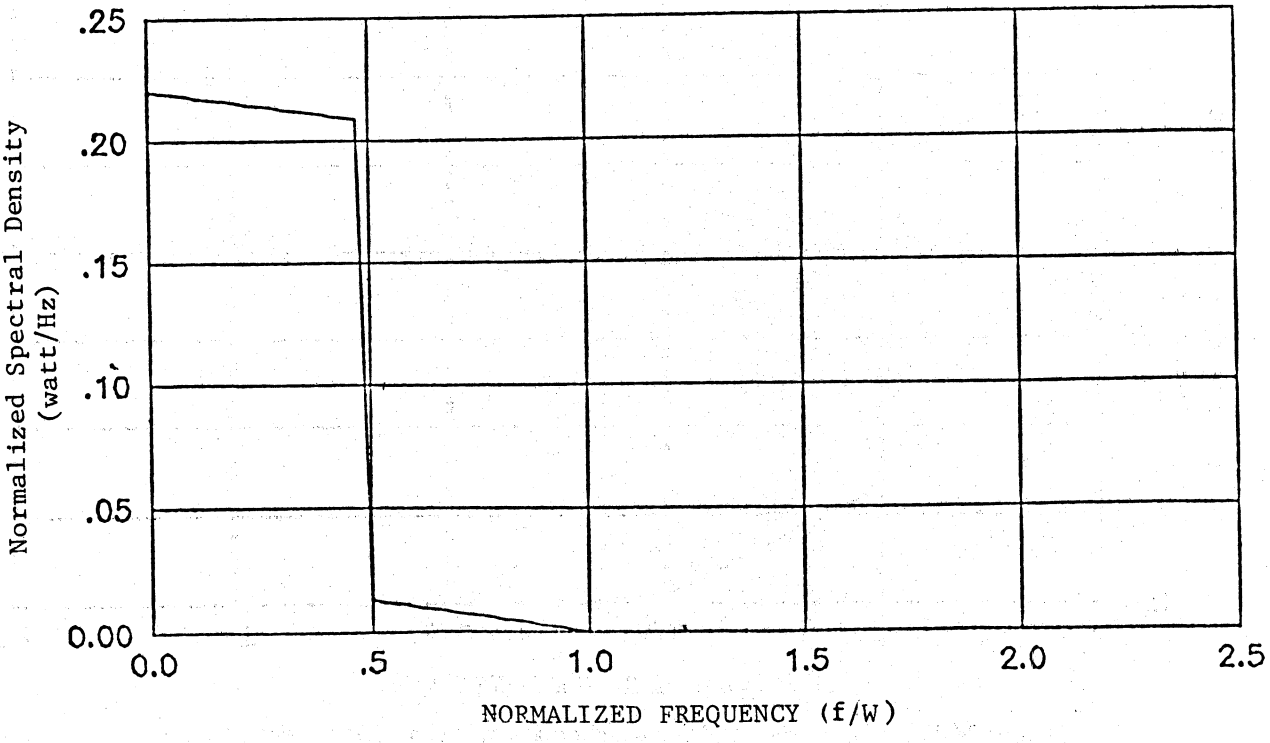

Figure 3(b). Sum of N=5 Weighted Convolutions for β=0.5
(carrier level =-1.086 dBW)

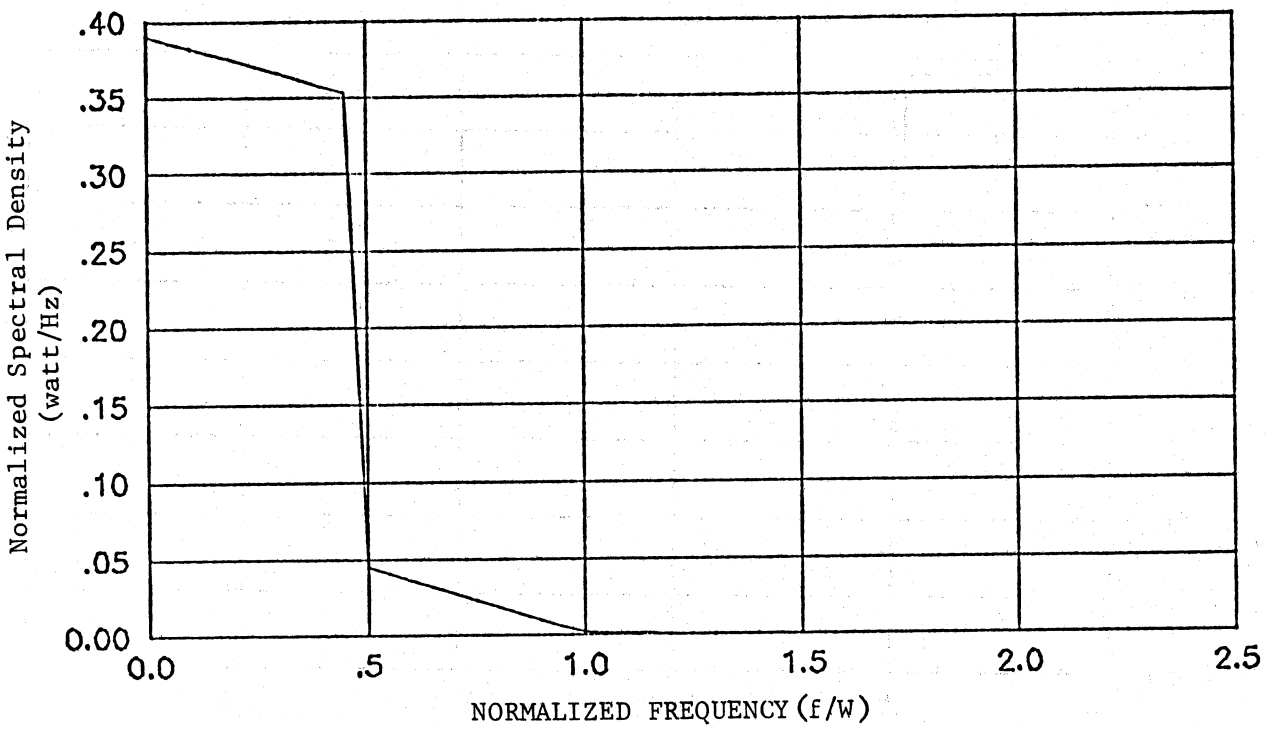

Figure 3(c). Sum of N=5 Weighted Convolutions for β=0.7
(carrier level = -2.171 dBW)

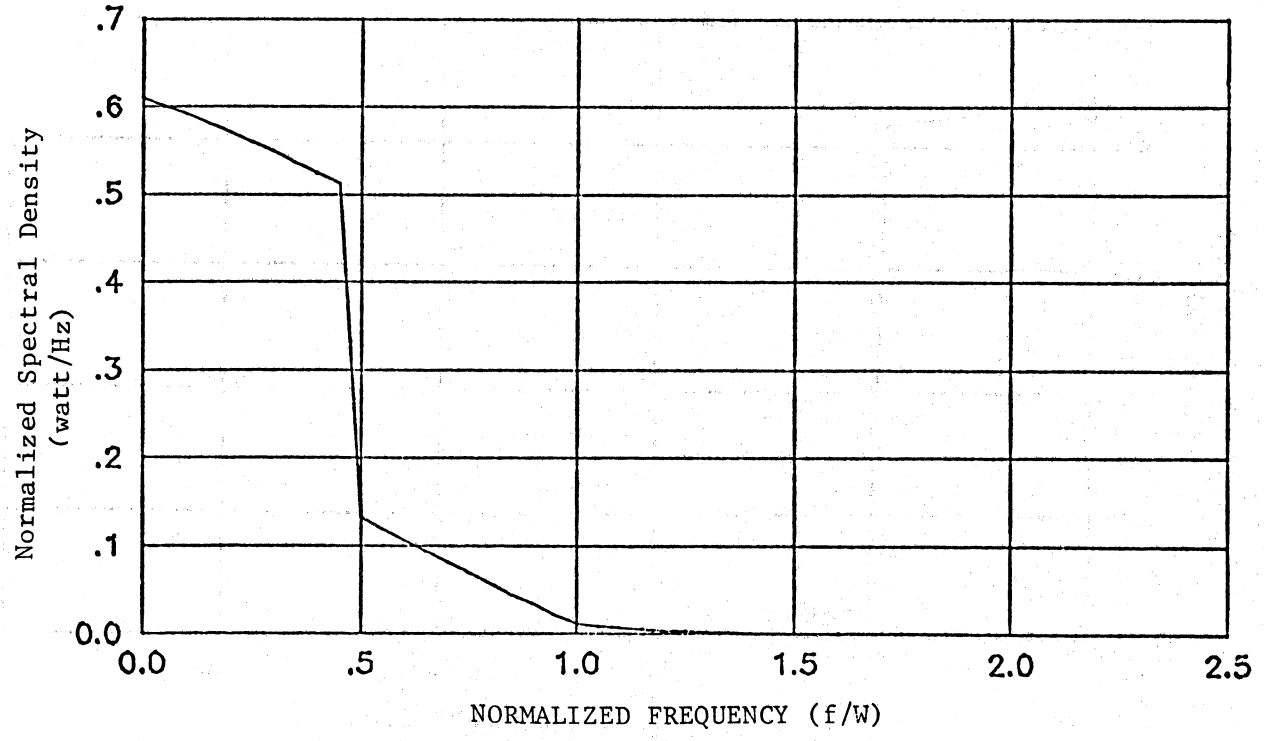

Figure 3(d). Sum of N=5 Weighted Convolutions for β=1.0
(carrier level = -4.343 dBW)

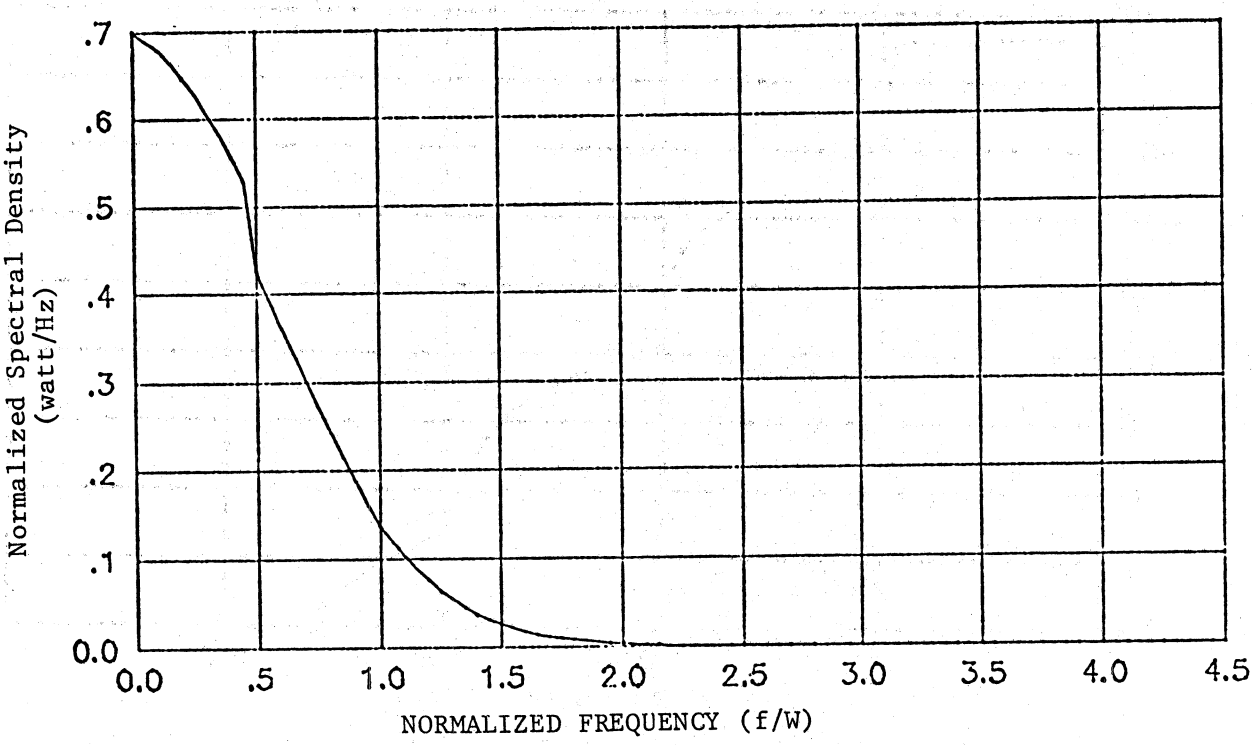

Figure 3(e). Sum of N=9 Weighted Convolutions for β=2.0
(carrier level = -17.372 dBW)

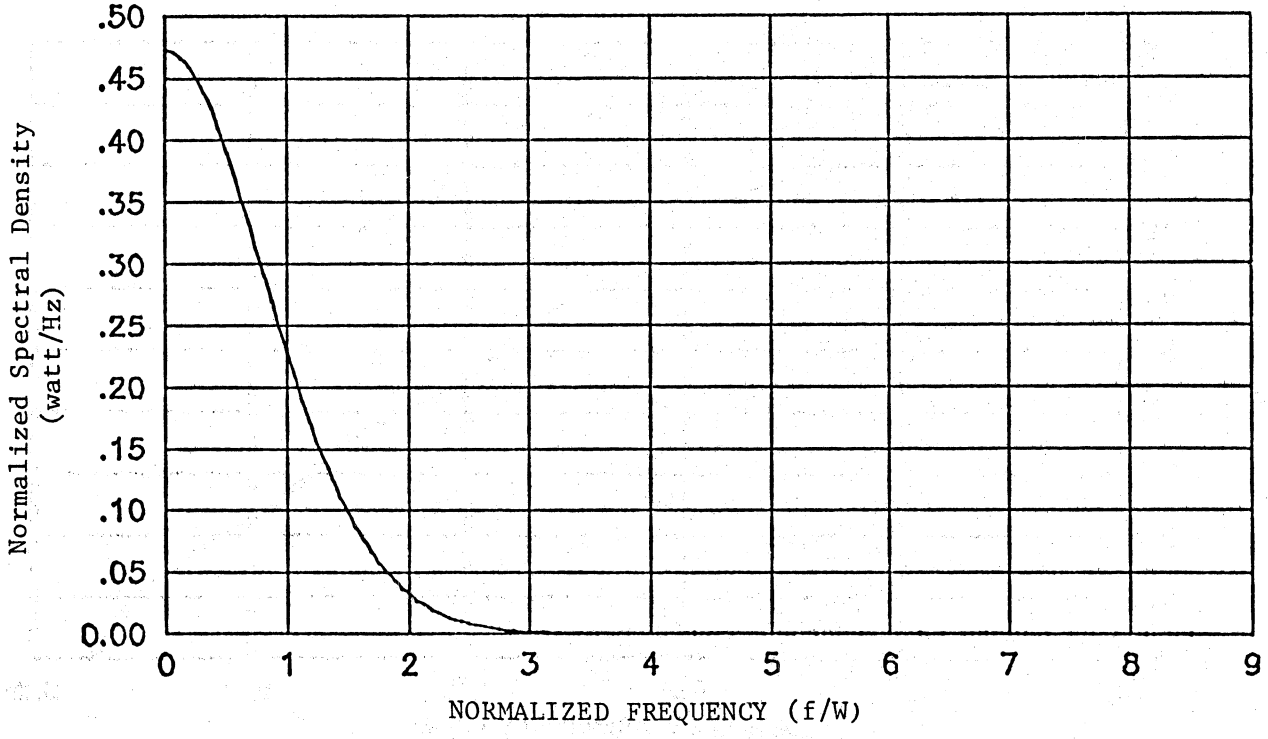

Figure 3(f). Sum of N=17 Weighted Convolutions β=3.0
(carrier level = -39.087 dBW)

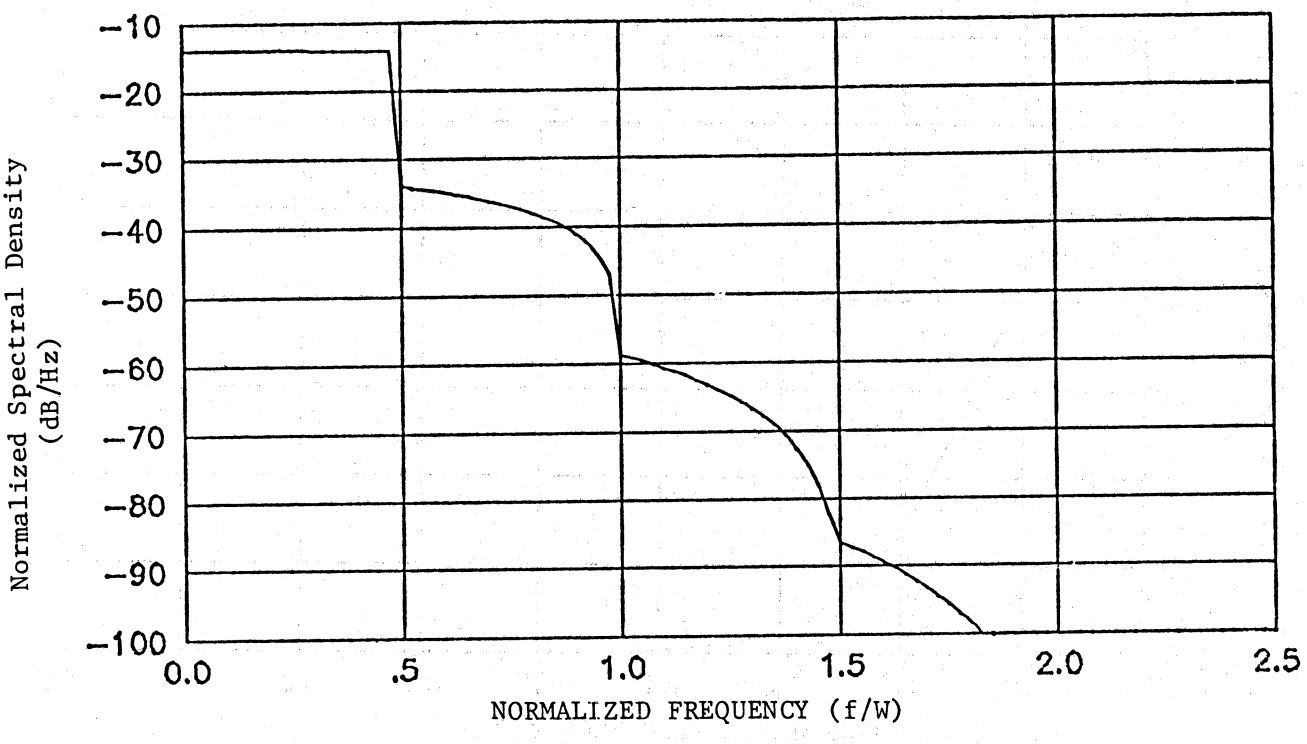

Figure 4(a). Case of N=5 Weighted Convolutions for β=0.2 (carrier level = -0.174 dBW)

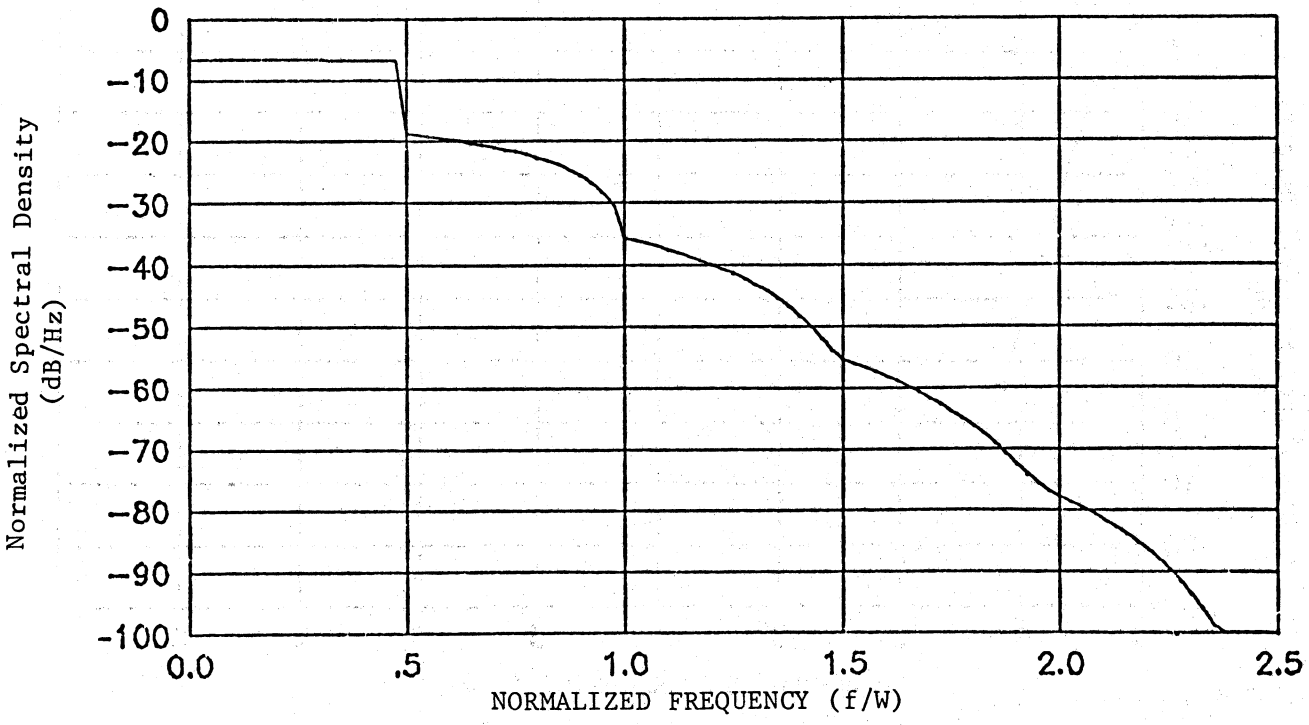

Figure 4(b). Case of N=5 Weighted Convolutions for β=0.5 (carrier level = -1.086 dBW)

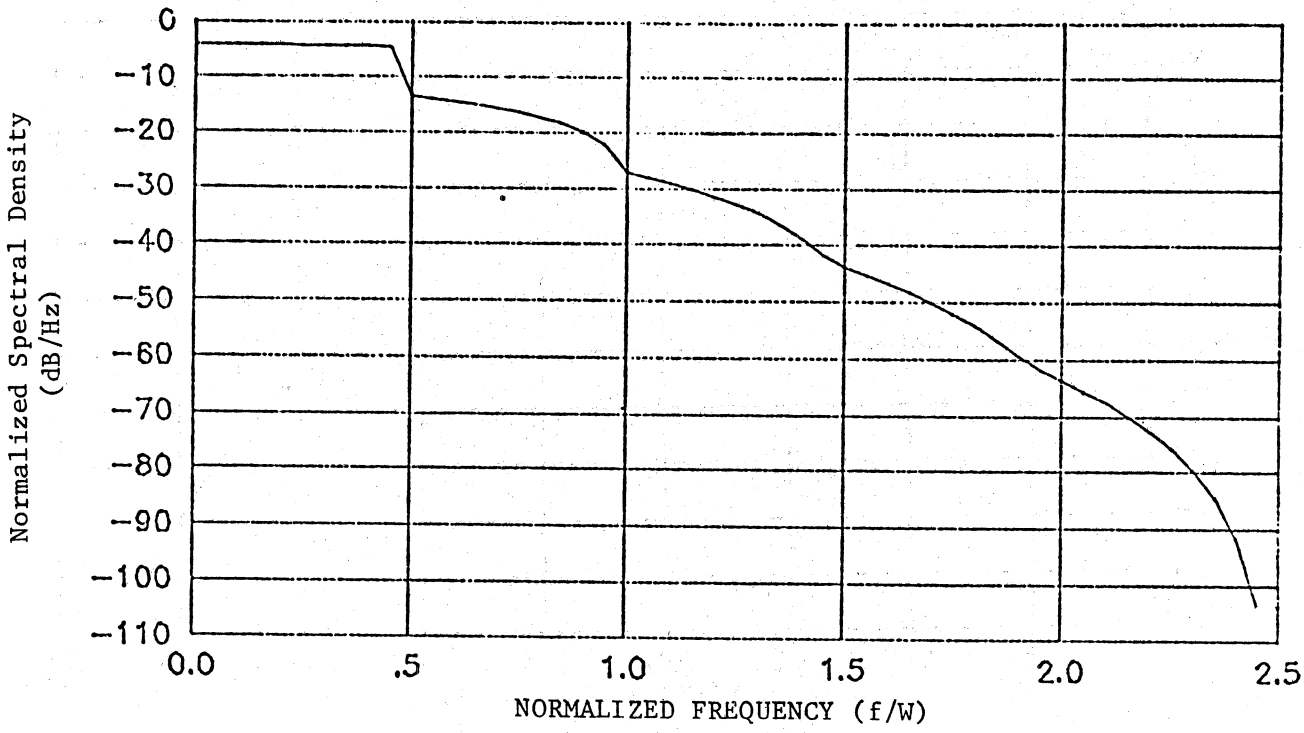

Figure 4(c). Case of N=5 Weighted Convolutions for $\beta=0.7$
(carrier level = -2.171 dBW)

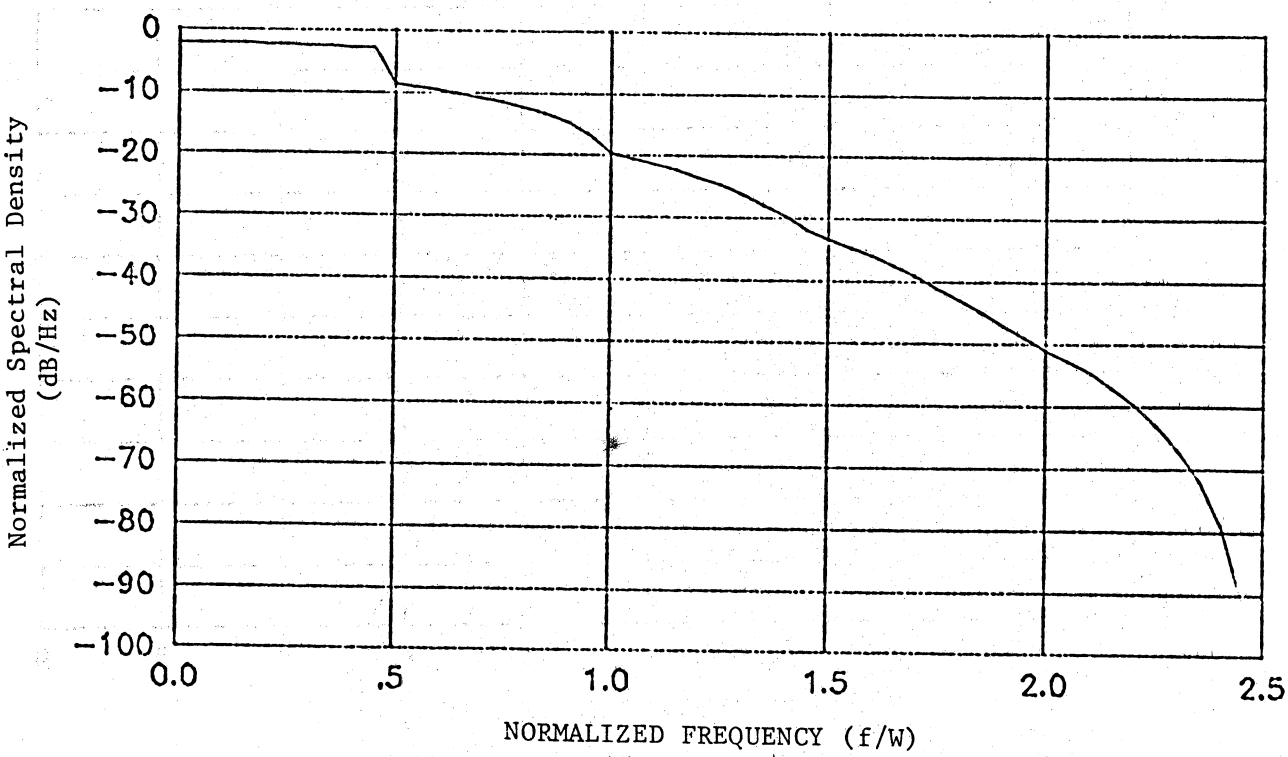

Figure 4(d). Case of N=5 Weighted Convolutions for $\beta=1.0$
(carrier level = -4.343 dBW)

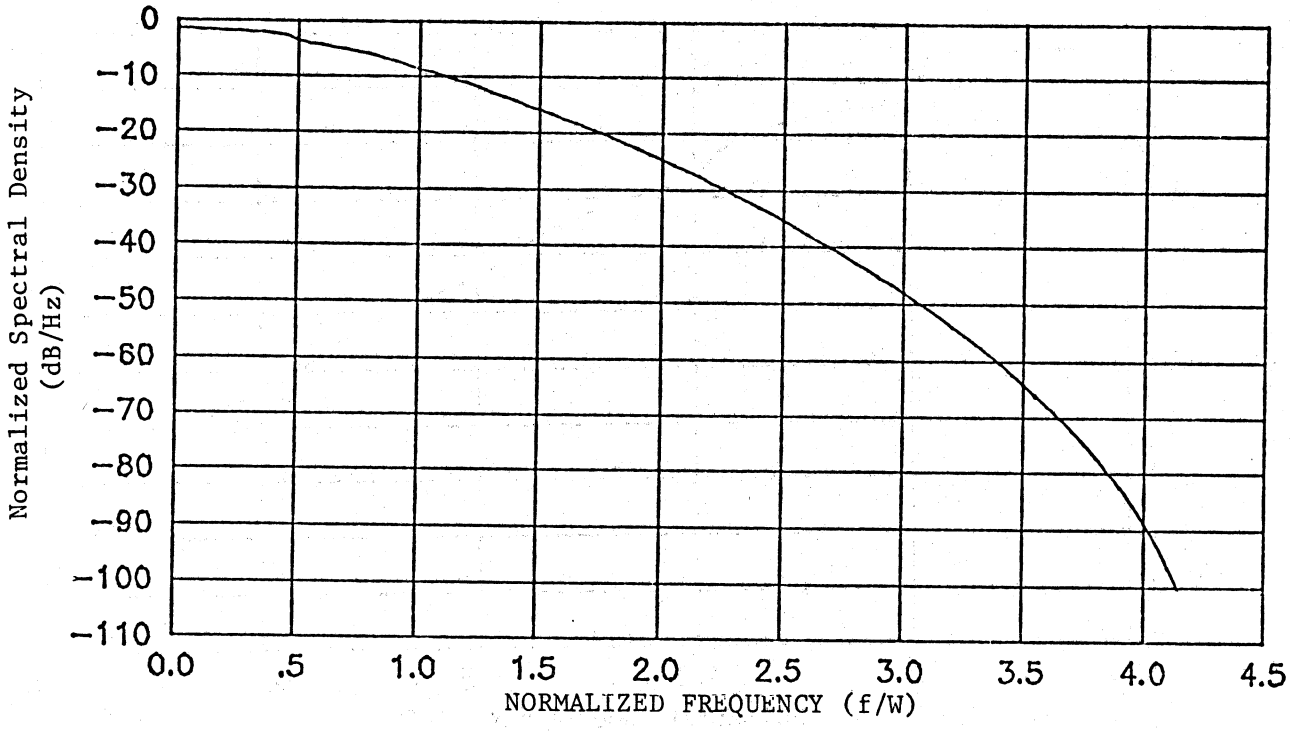

Figure 4(e). Case of N=9 Weighted Convolutions for β=2.0
(carrier level = -17.372 dBW)

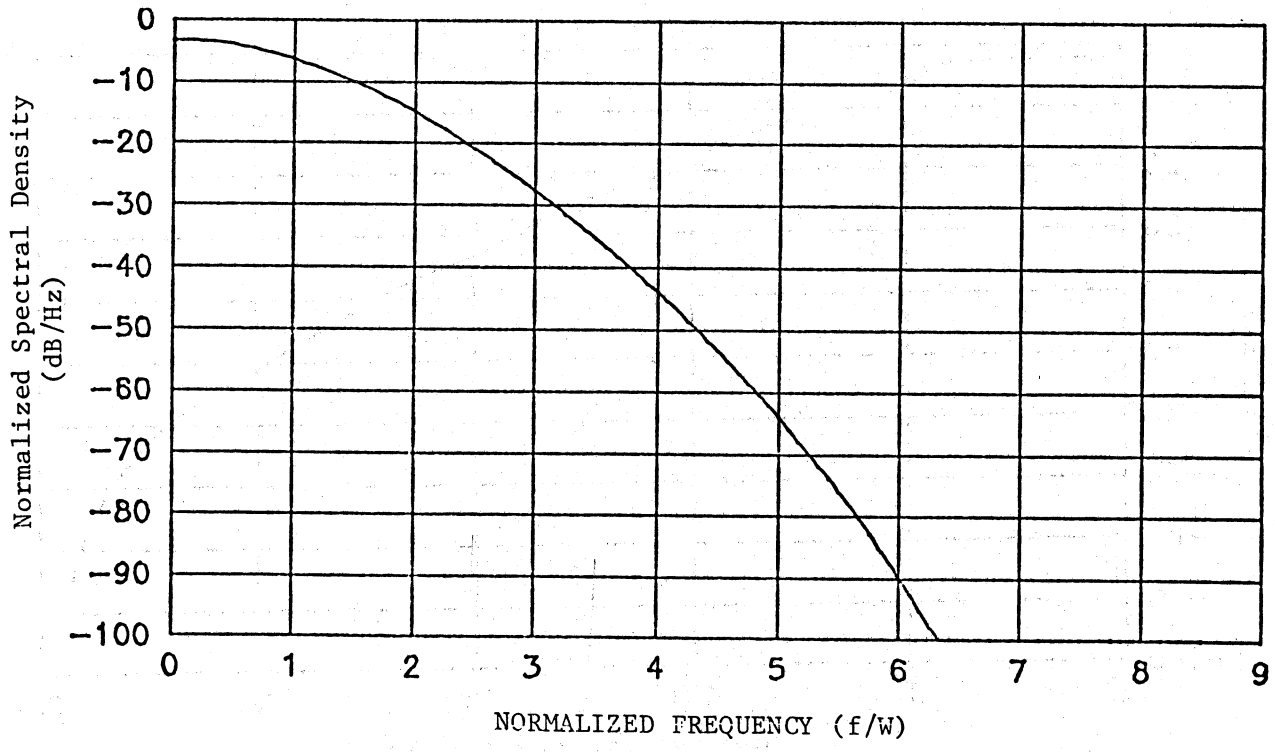

Figure 4(f). Case of N=17 Weighted Convolutions for β=3.0
(carrier level = -39.087 dBW)

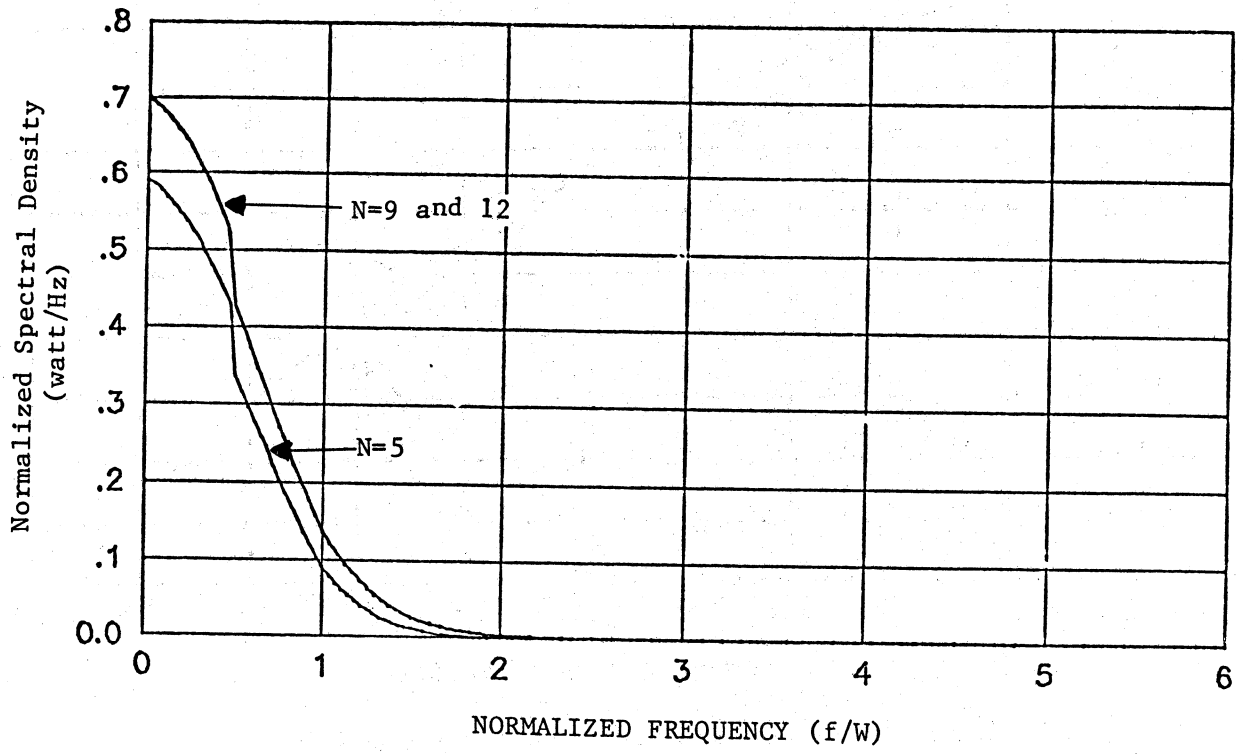

Figure 5(a). Various Convolutions for β=2.0 (Note: 9 is the nominal number of convolutions)

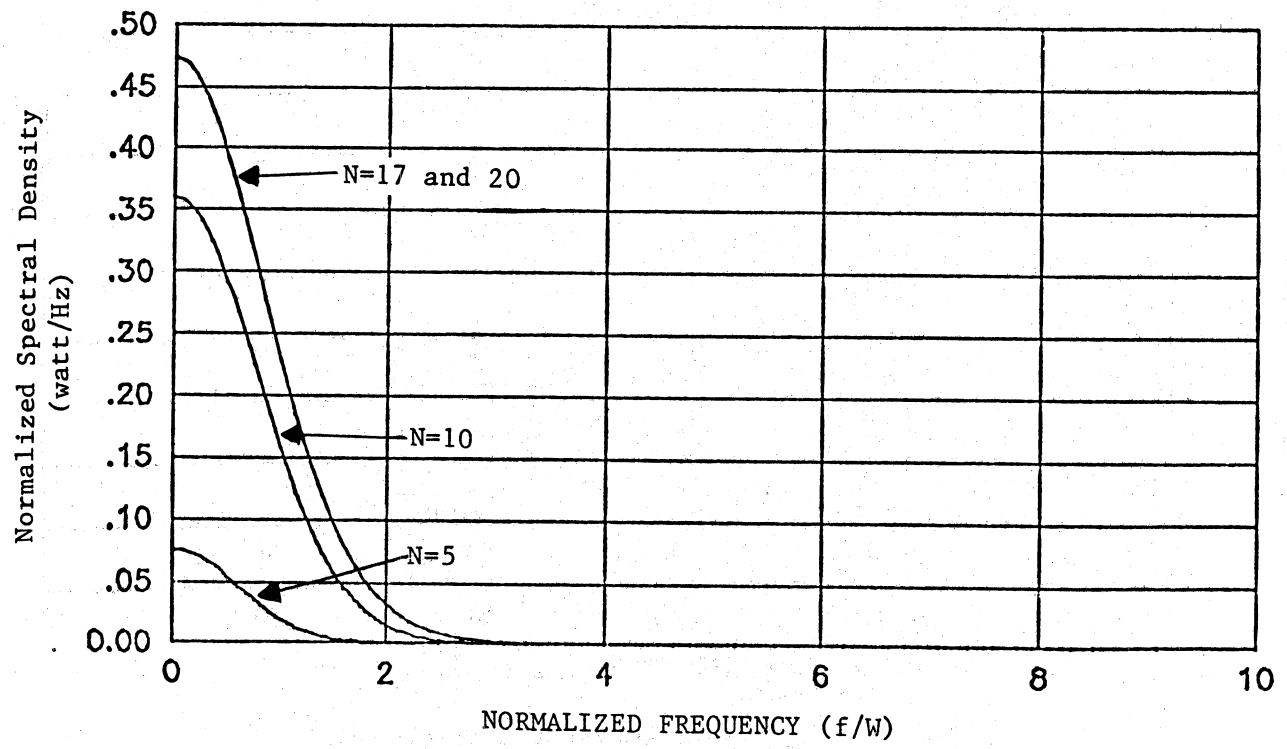

Figure 5(b). Various Convolutions for β =3.0 (Note: 17 is the nominal number of convolutions)

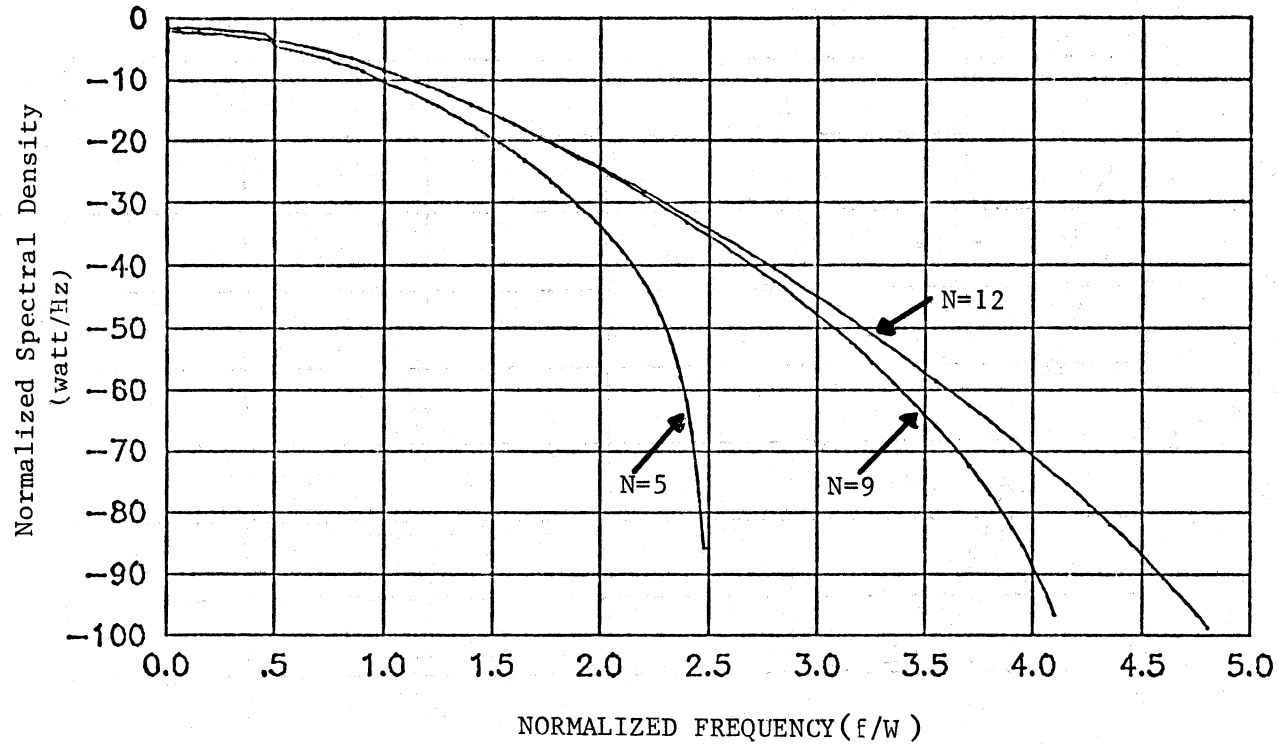

Figure 6(a). Various Convolutions for β=2.0
(Note: 9 is the nominal number of convolutions)

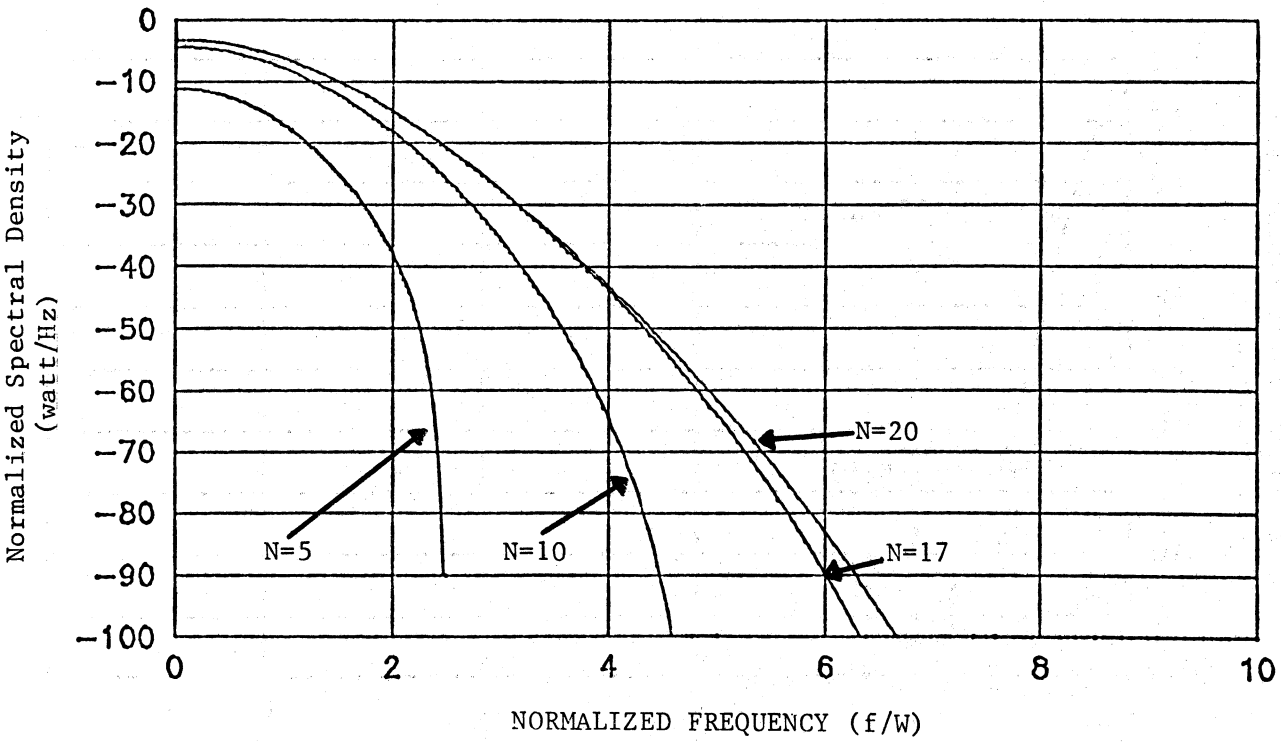

Figure 6(b). Various Convolutions for β=3.0
(Note: 17 is the nominal number of convolutions)

This expression can be compared to the spectral convolution series simulation by setting W=1. The comparison results are presented in Figures 7(a) to 7(l), which show that the gaussian approximation is still poor at $\beta = 1$ but has become effective before $\beta = 2$ is reached. The corresponding db differential between each pair is also presented in Figures 8(a) to 8(l), where the plots show 10 log (y_1/y_2) with (y_1) as the gaussian spectrum approximation and (y_2) as the spectral convolution series. Hence, a negative dB differential in these plots implies that the series spectrum exceeds the gaussian spectrum by that amount.

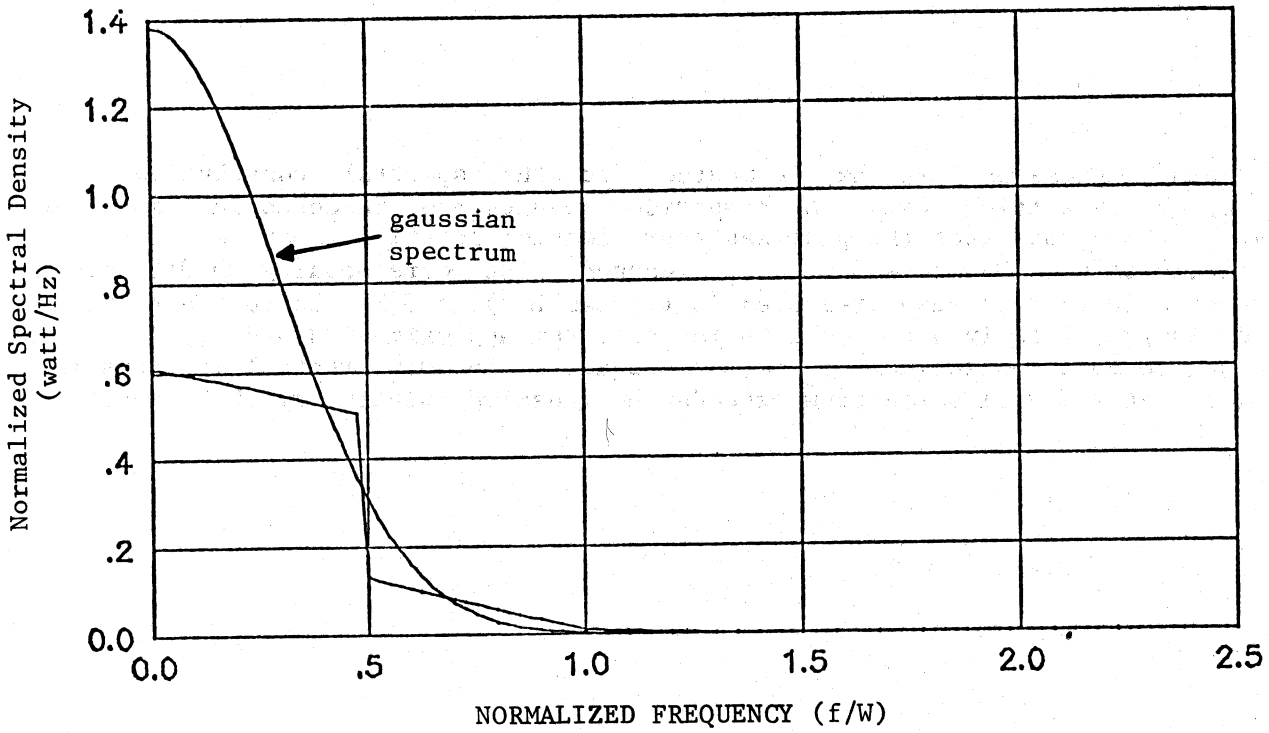

Figure 7(a). Sum of N=5 Weighted Convolutions for β=1.0
(carrier level = -4.343 dBW)

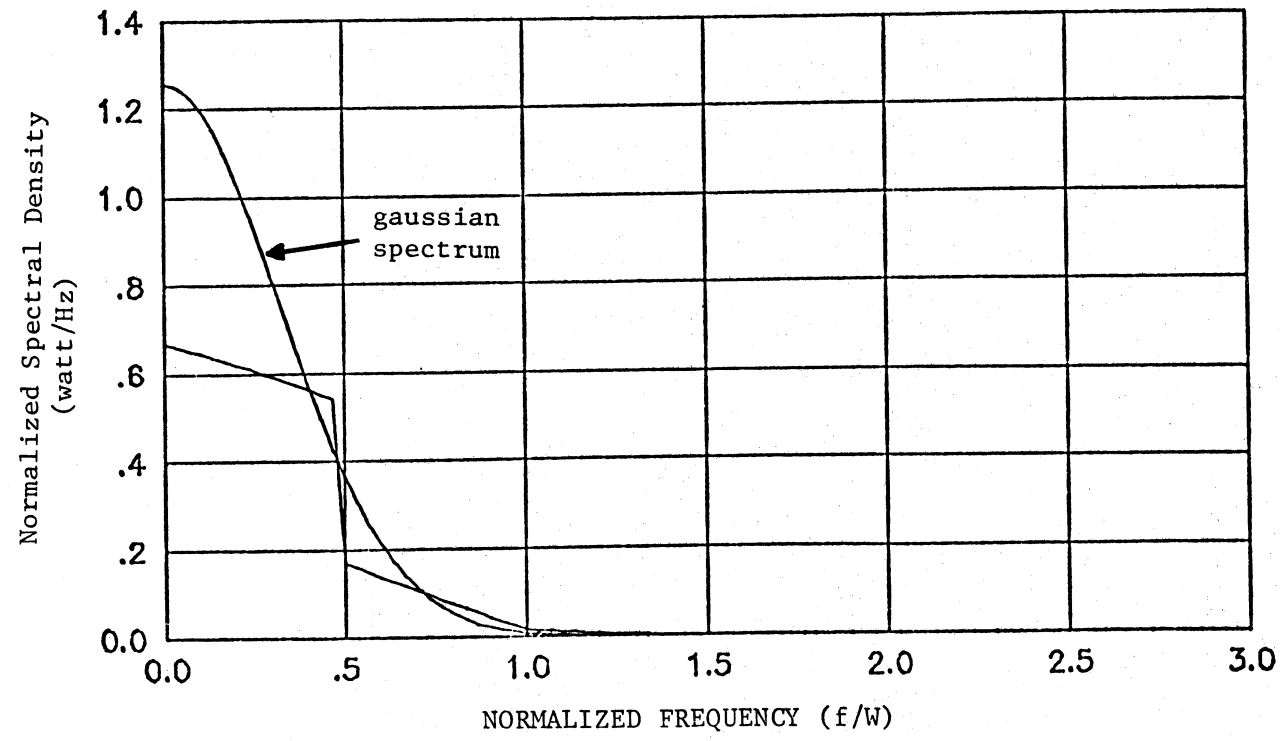

Figure 7(b). Sum of N=6 Weighted Convolutions for β=1.1
(carrier level = -5.255 dBW)

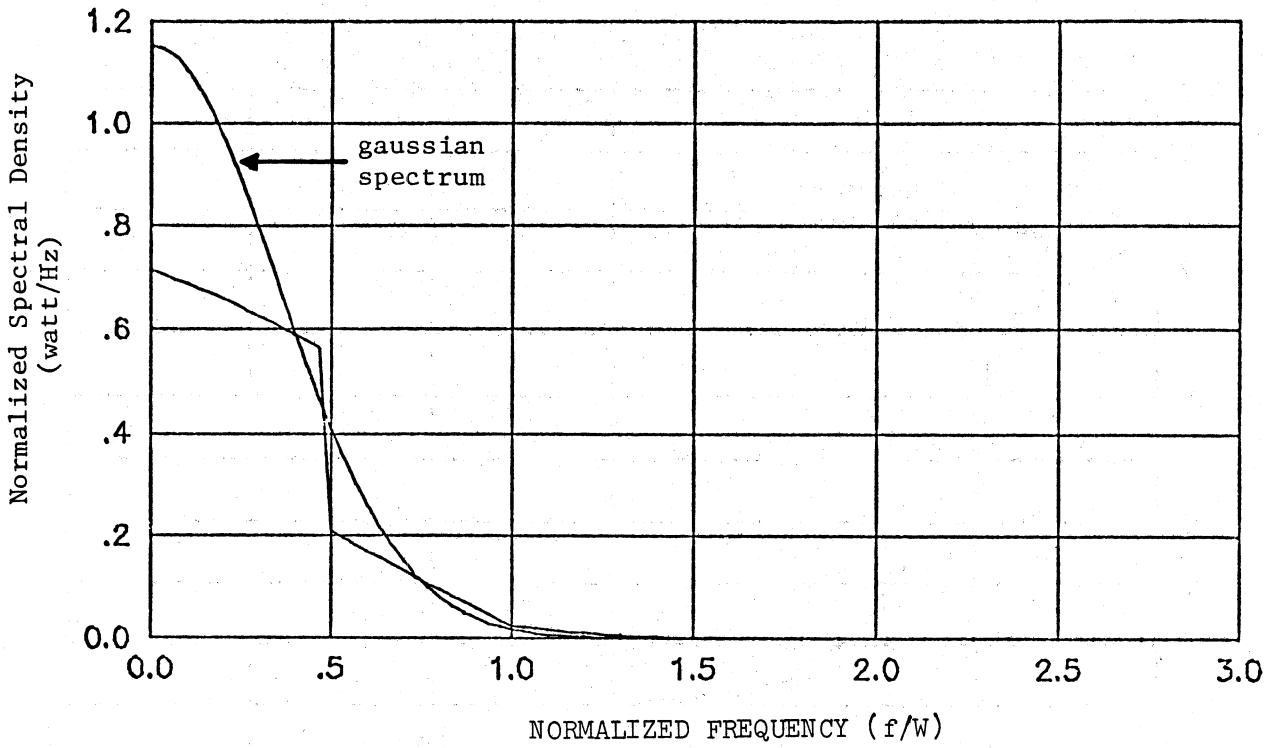

Figure 7(c). Sum of N=5 Weighted Convolutions for β=1.2
(carrier level = -6.254 dBW)

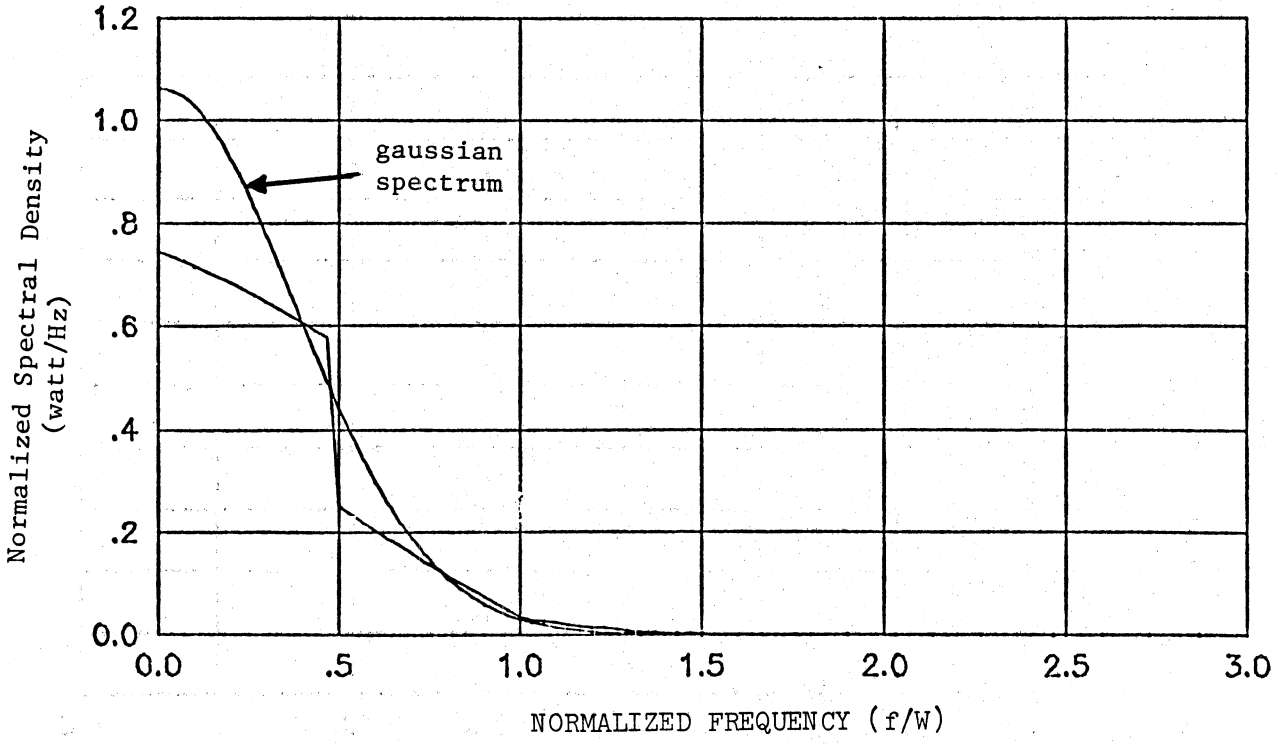

Figure 7(d). Sum of N=6 Weighted Convolutions for β=1.3
(carrier level = -7.340 dBW)

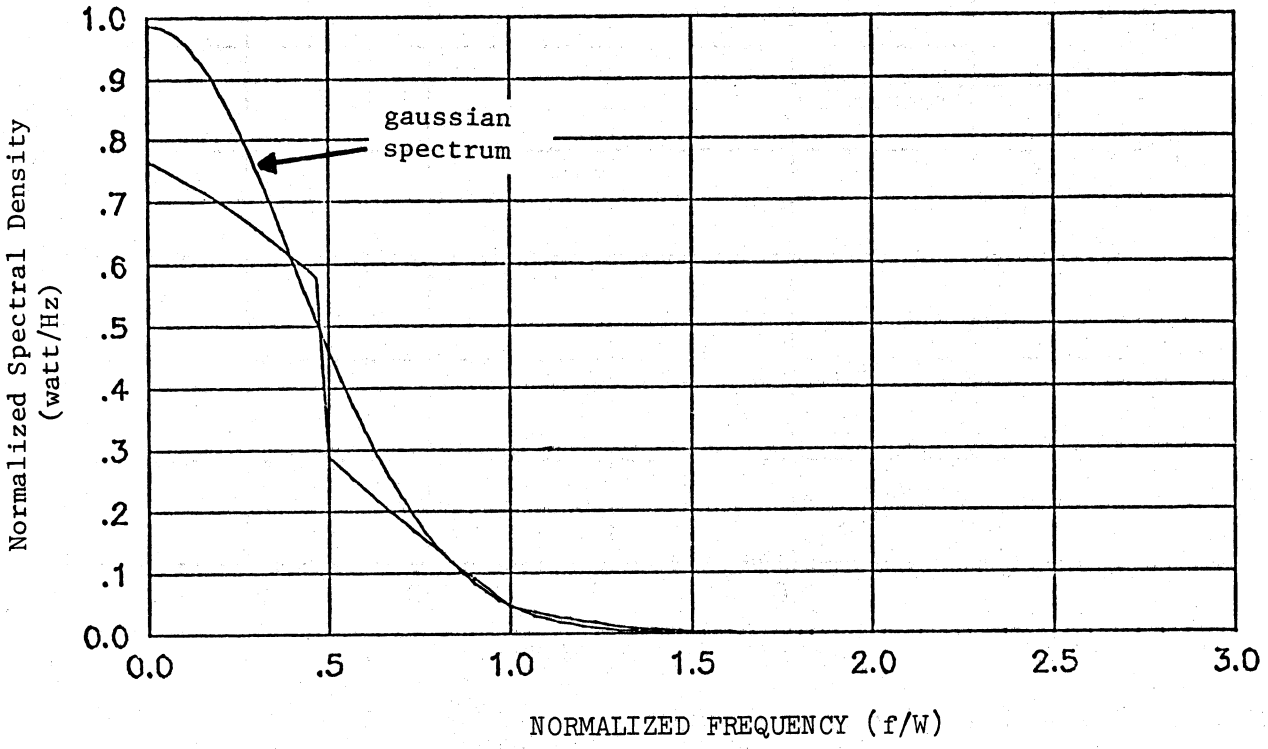

Figure 7(e). Sum of N=6 Weighted Convolutions for β=1.4
(carrier level = -8.512 dBW)

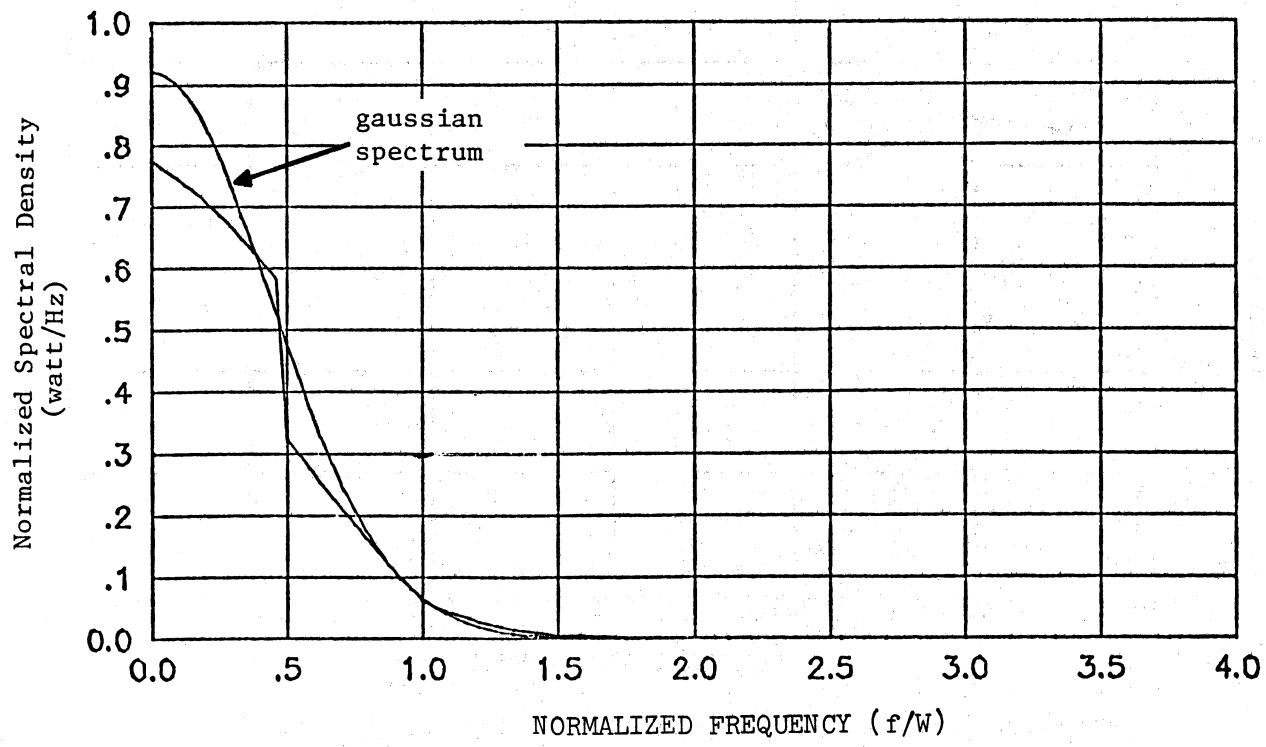

Figure 7(f). Sum of N=8 Weighted Convolutions for β=1.5
(carrier level = -9.772 dBW)

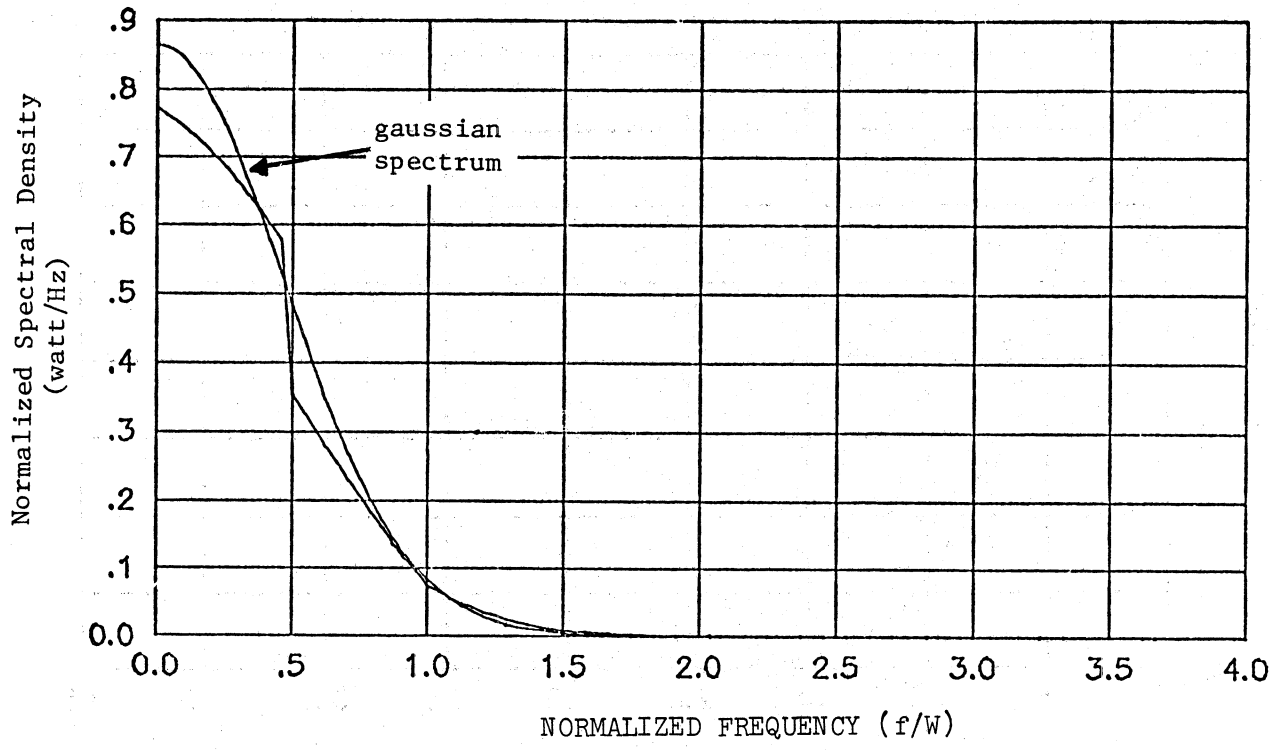

Figure 7(g). Sum of N=8 Weighted Convolutions for β=1.6
(carrier level = -11.118 dBW)

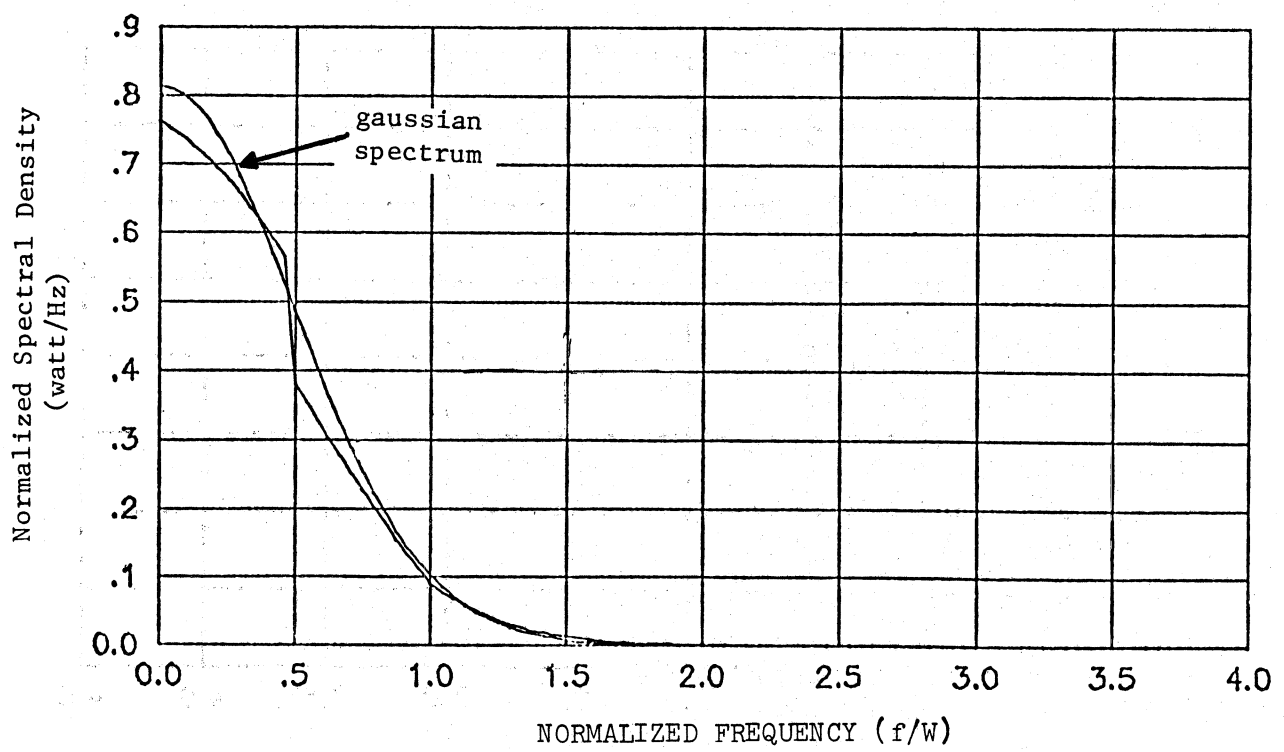

Figure 7(h). Sum of N=8 Weighted Convolutions for β=1.7
(carrier level = -12.551 dBW)

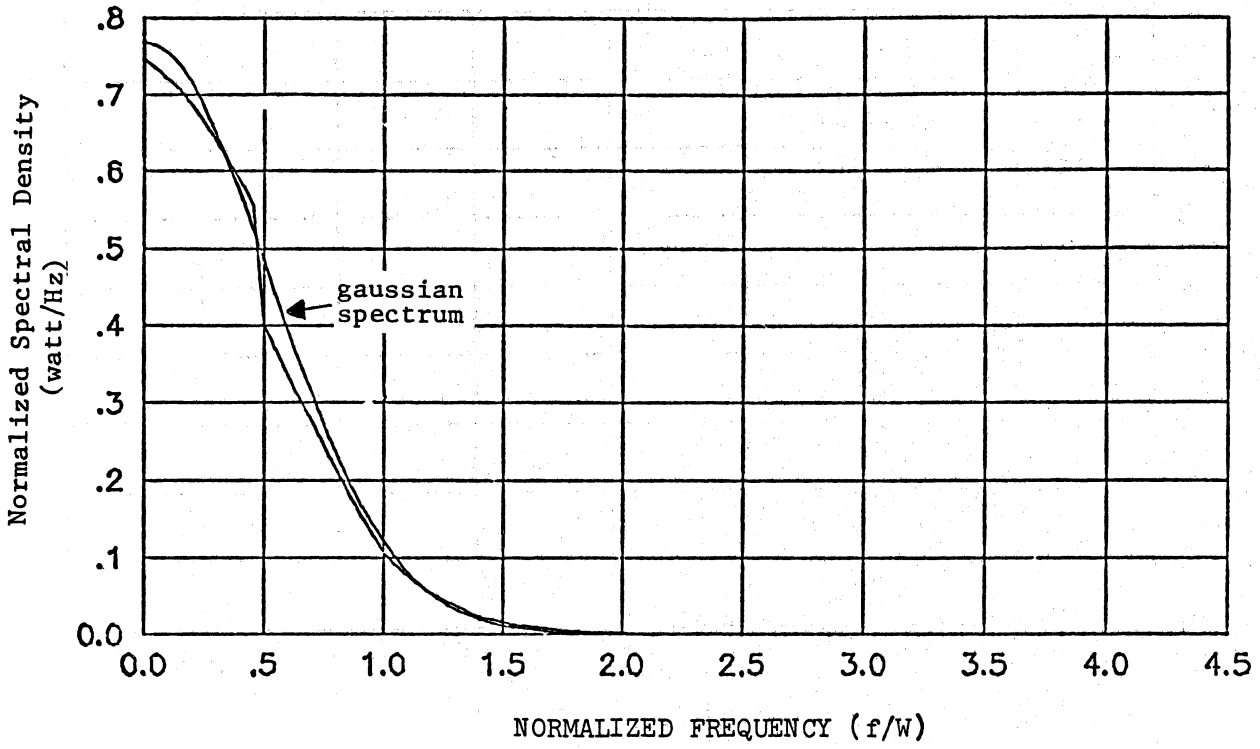

Figure 7(i). Sum of N=9 Weighted Convolutions for β=1.8
(carrier level = -14.071 dBW)

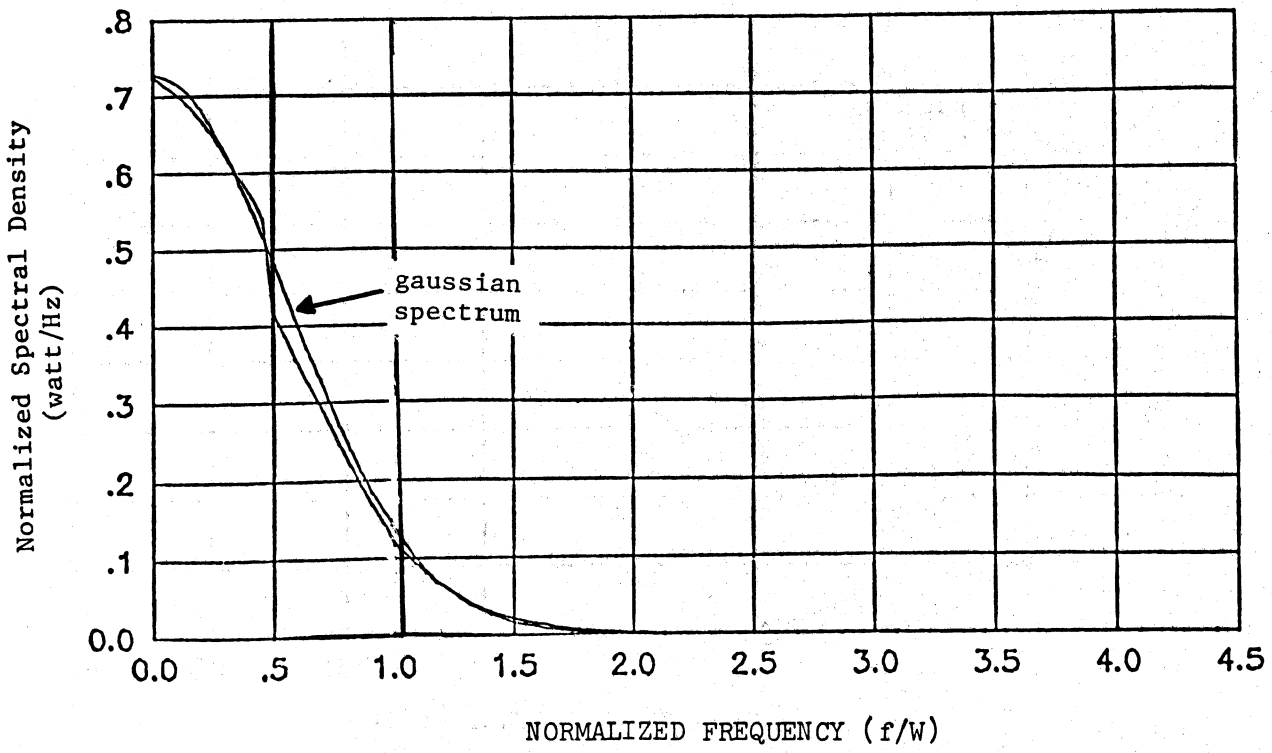

Figure 7(j). Sum of N=9 Weighted Convolutions for β=1.9
(carrier level = -15.678 dBW)

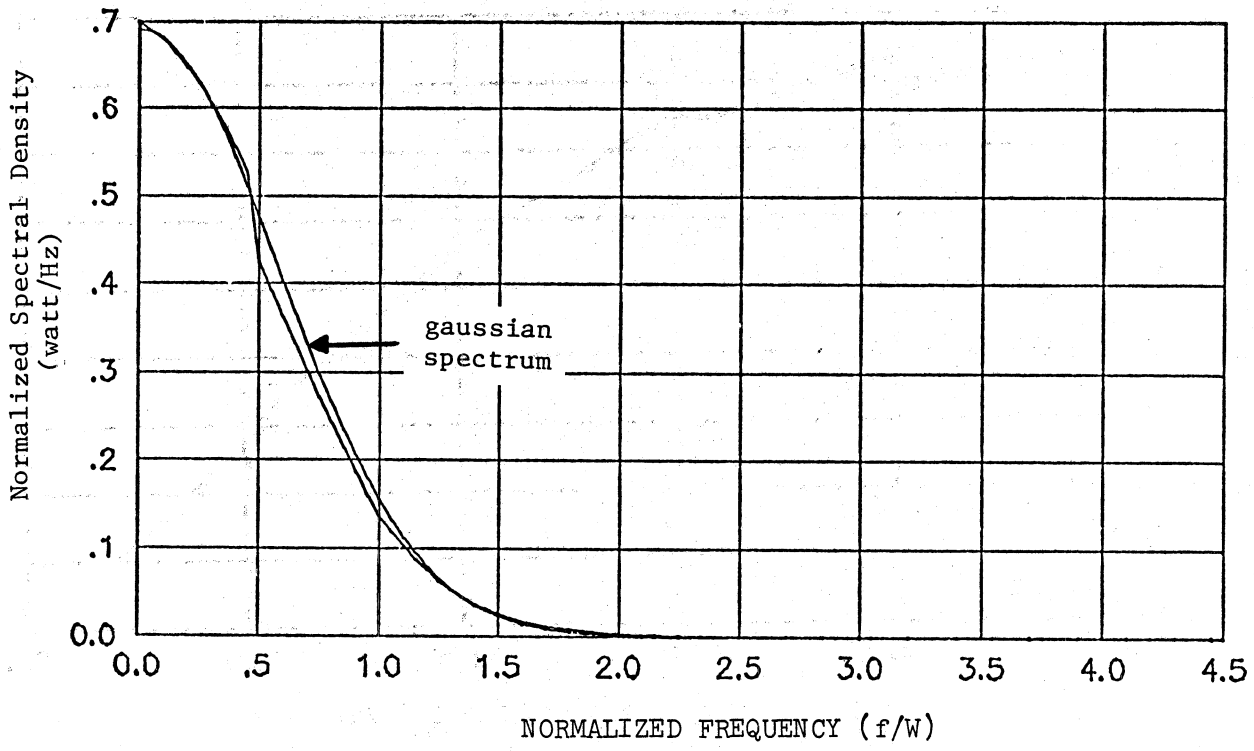

Figure 7(k). Sum of N=9 Weighted Convolutions for β=2.0
(carrier level = -17.372 dBW)

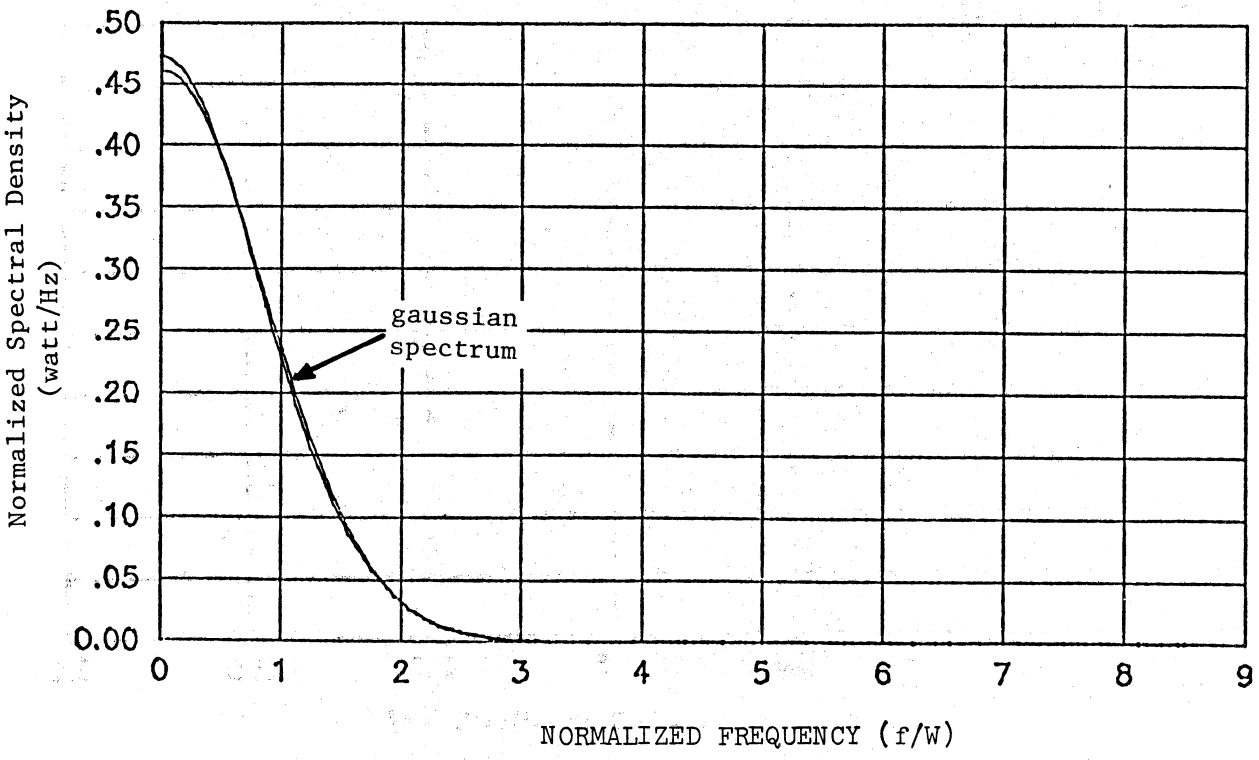

Figure 7(l). Sum of N=17 Weighted Convolutions for β=3.0
(carrier level = -39.087 dBW)

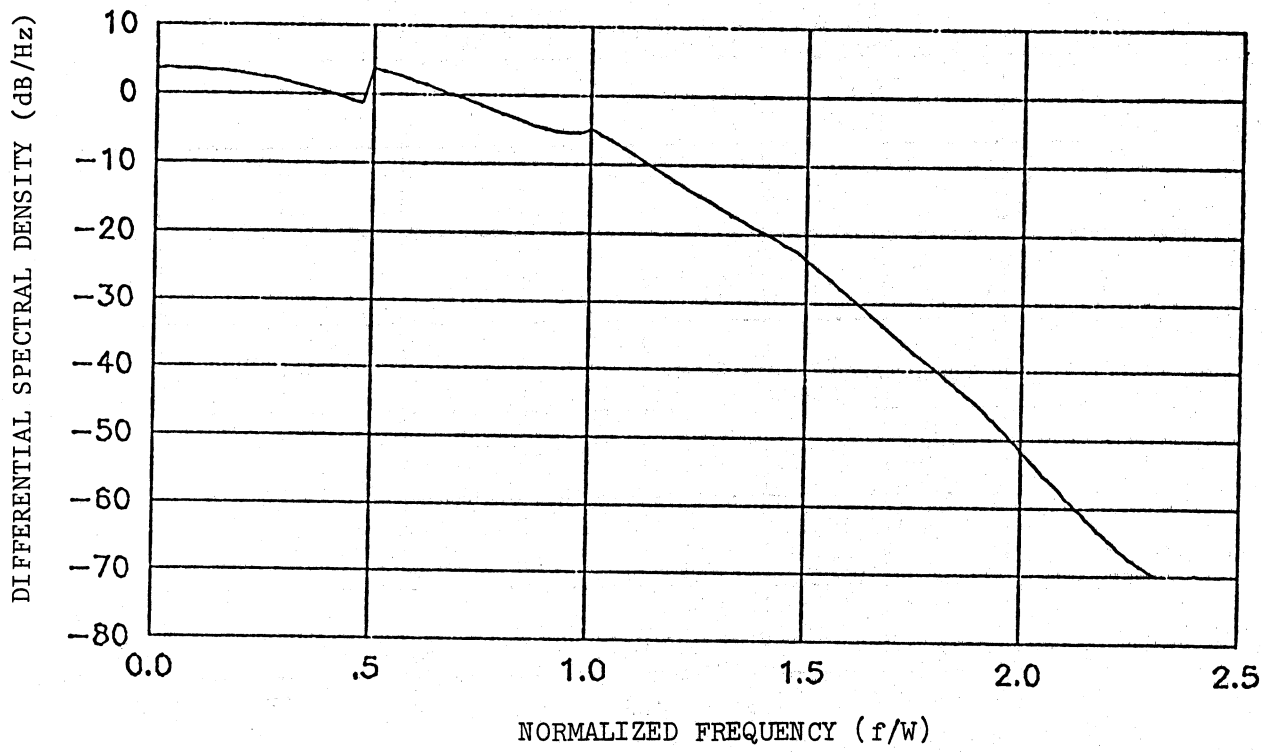

Figure 8(a). Case of N=5 Weighted Convolutions for β=1.0 (carrier level = -4.343 dBW)

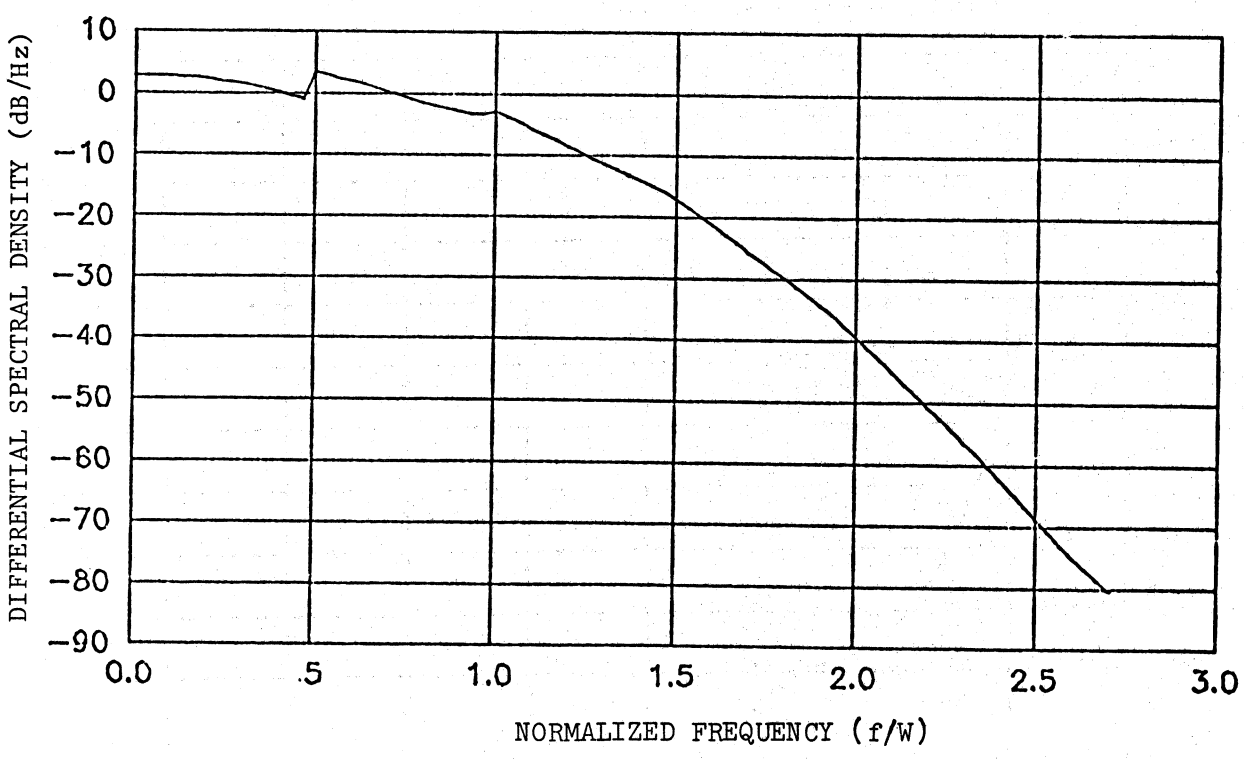

Figure 8(b). Case of N=6 Weighted Convolutions for β=1.1 (carrier level = 5.255 dBW)

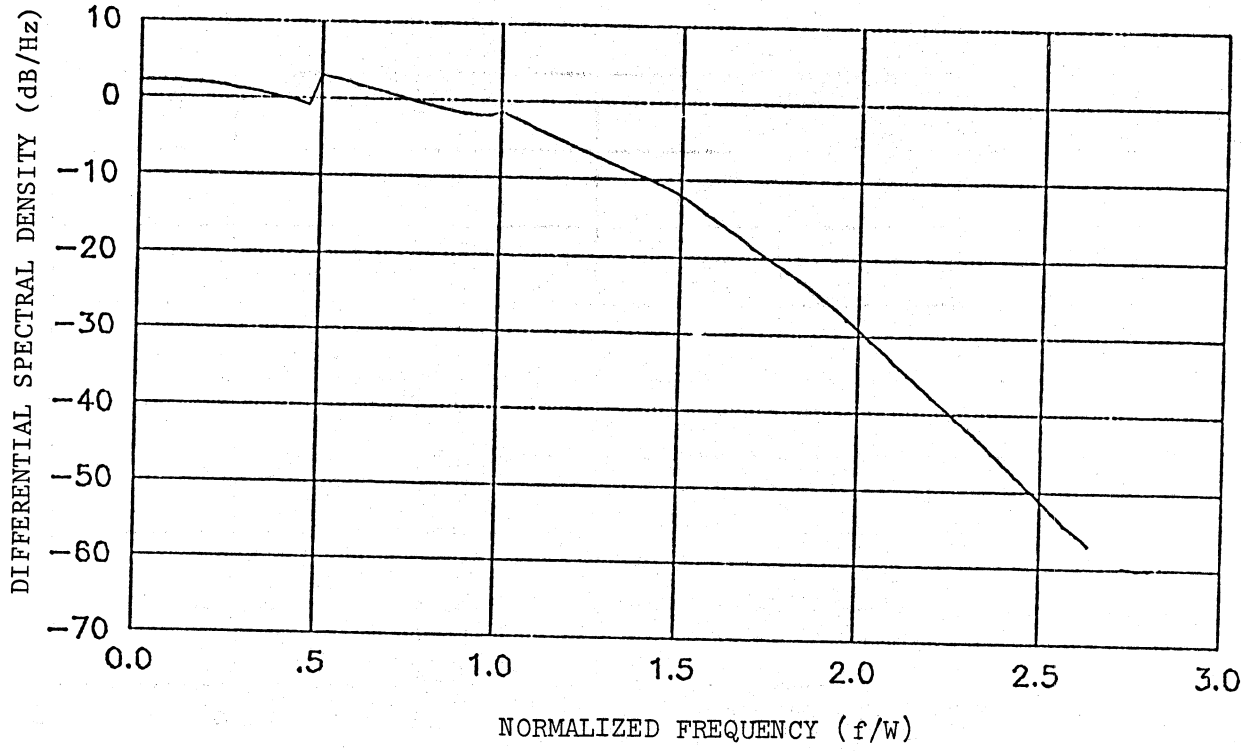

Figure 8(c). Case of N=6 Weighted Convolutions for β=1.2 (carrier level = -6.254 dBW)

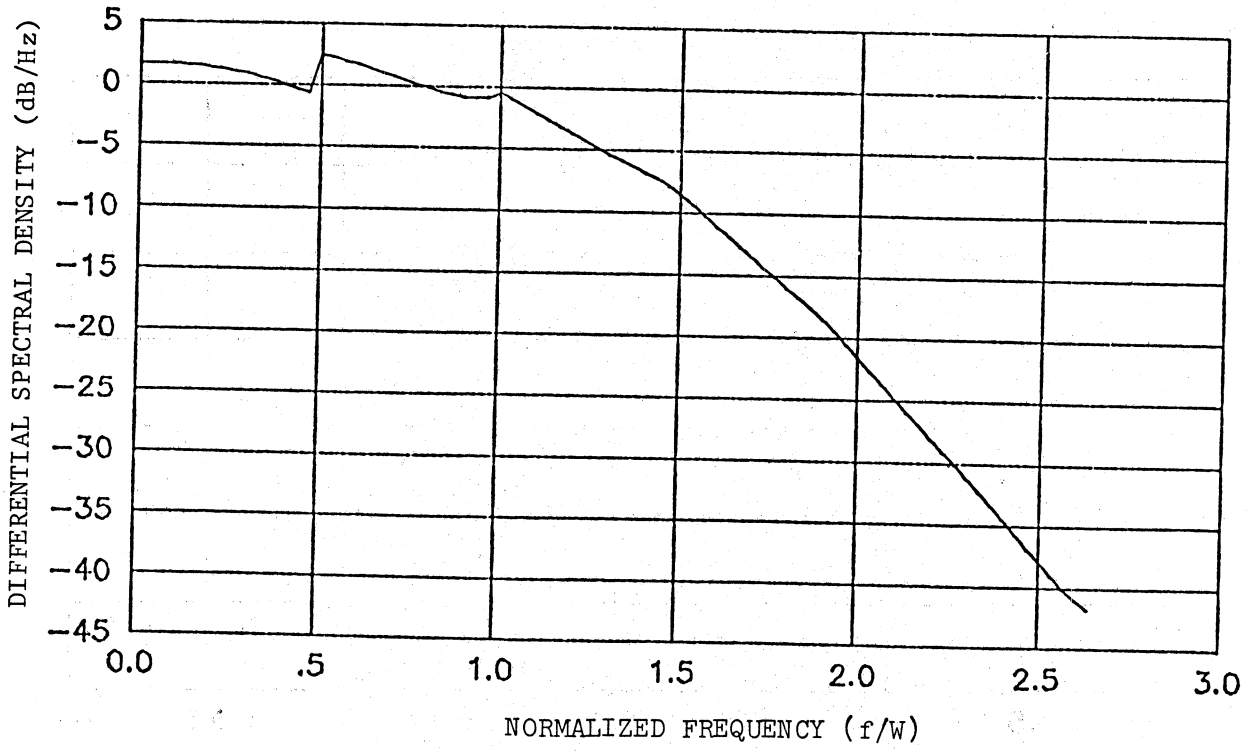

Figure 8(d). Case of N=6 Weighted Convolutions for β=1.3 (carrier level = -7.340 dBW)

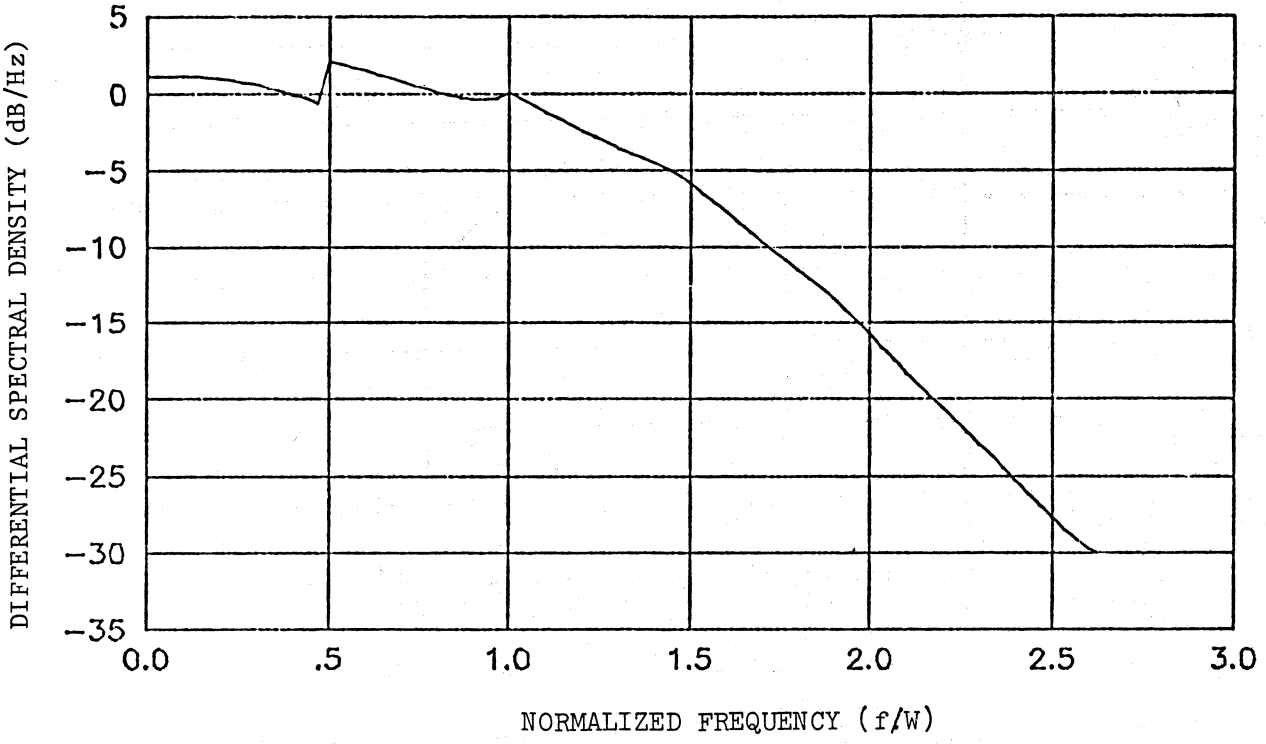

Figure 8(e). Case of N=6 Weighted Convolutions for β=1.4 (carrier level = -8.512 dBW)

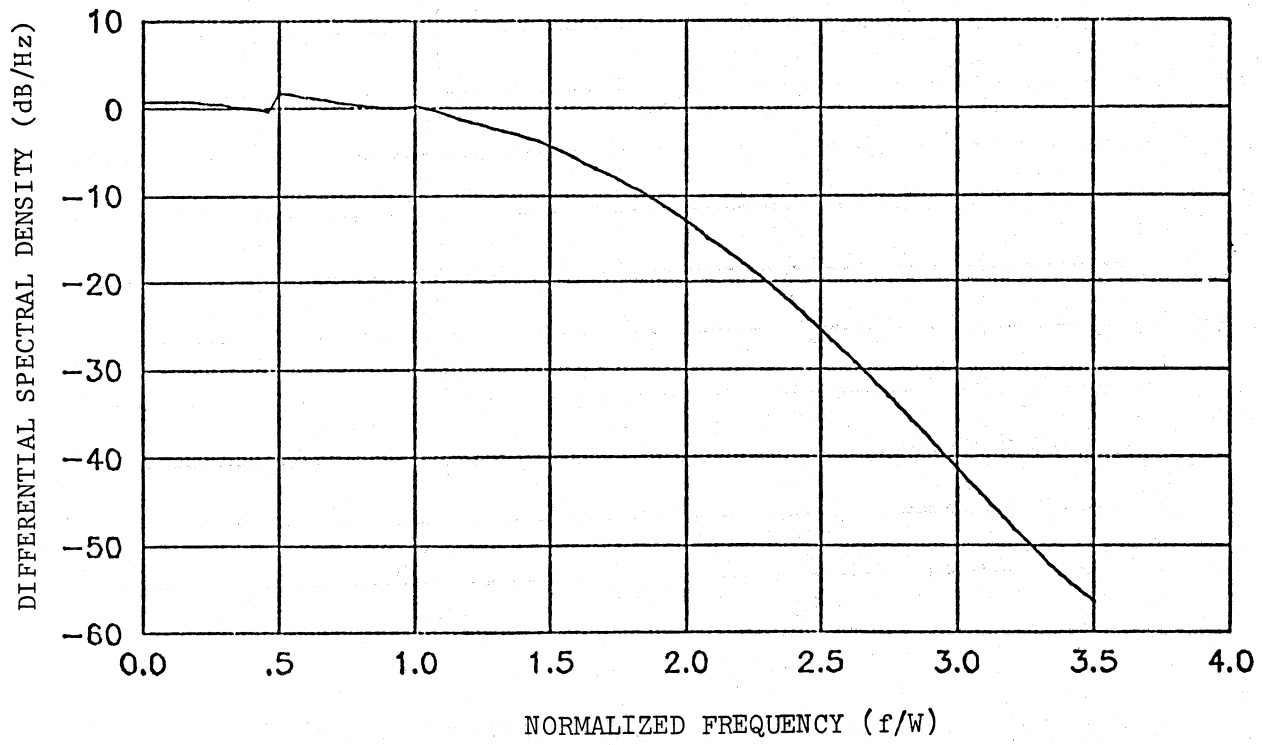

Figure 8(f). Case of N=8 Weighted Convolutions for β=1.5 (carrier level = -9.772 dBW)

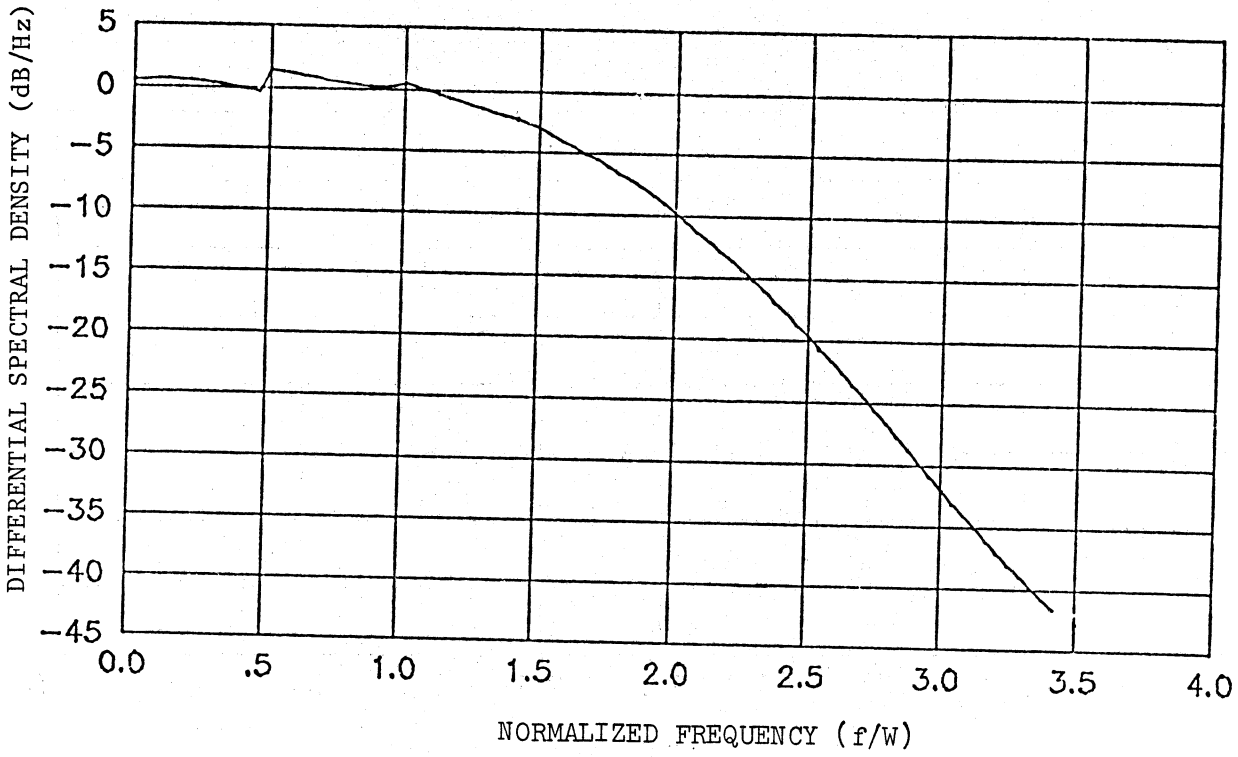

Figure 8(g). Case of N=8 Weighted Convolutions for β=1.6 (carrier level = -11.118 dBW)

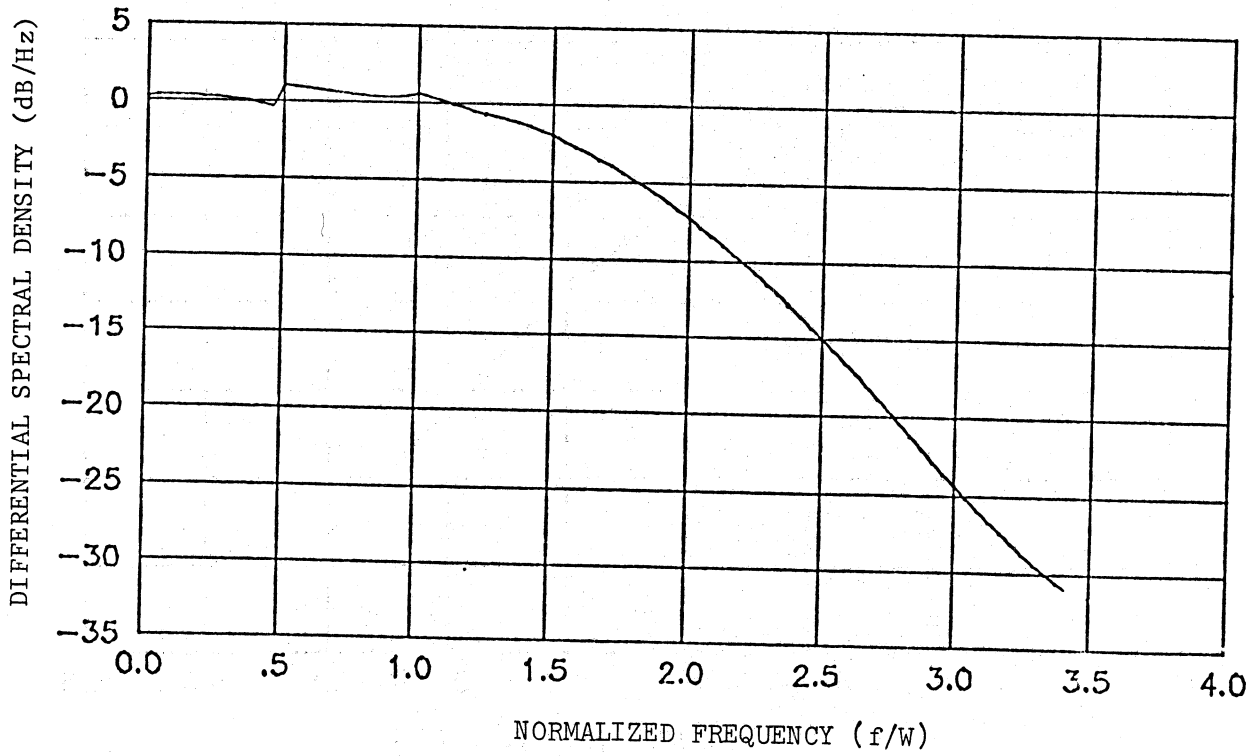

Figure 8(h). Case of N=8 Weighted Convolutions for β=1.7 (carrier level = -12.551 dBW)

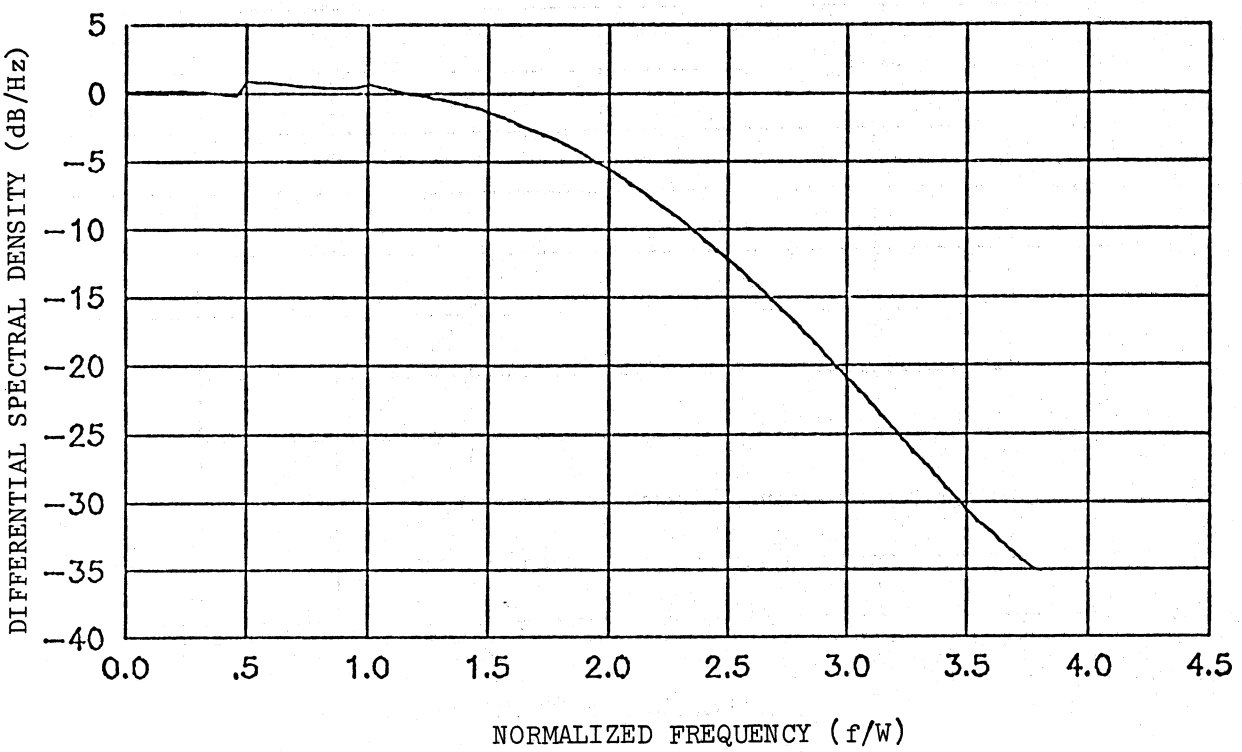

Figure 8(i). Case of N=9 Weighted Convolutions for β=1.8 (carrier level = -14.071 dBW)

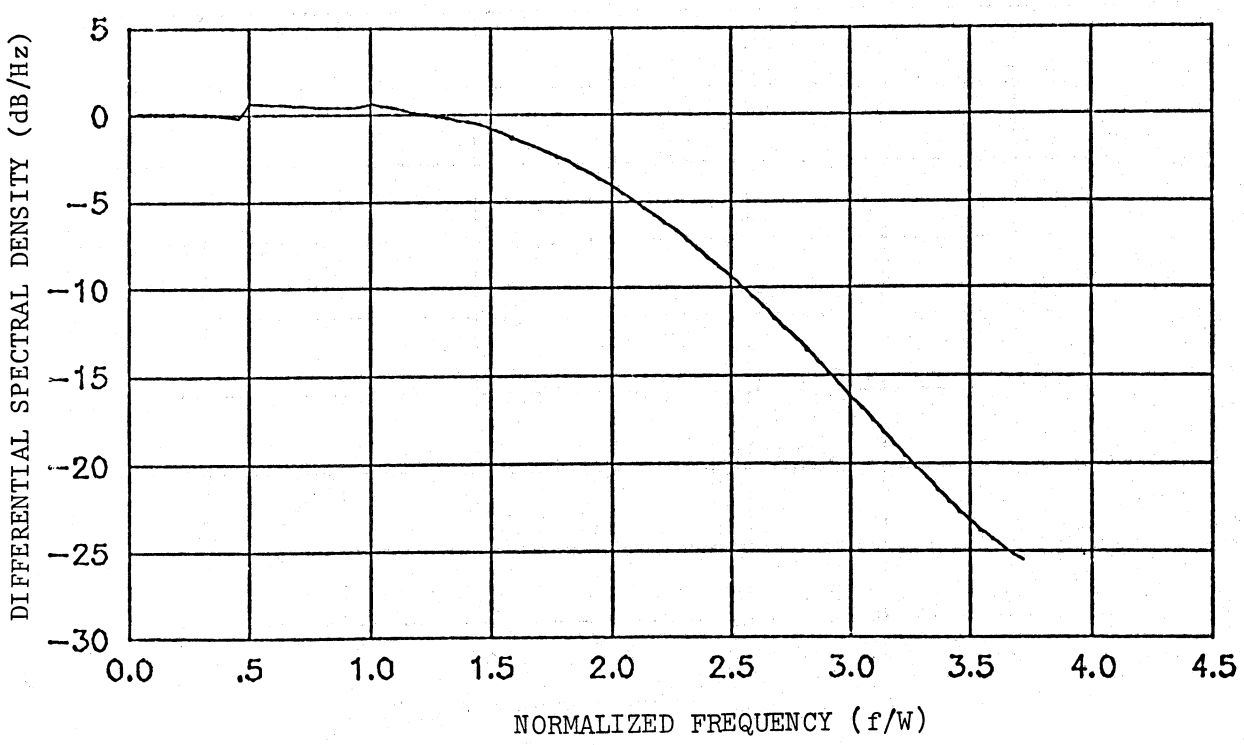

Figure 8(j). Case of N=9 Weighted Convolutions for β=1.9 (carrier level = -15.678 dBW)

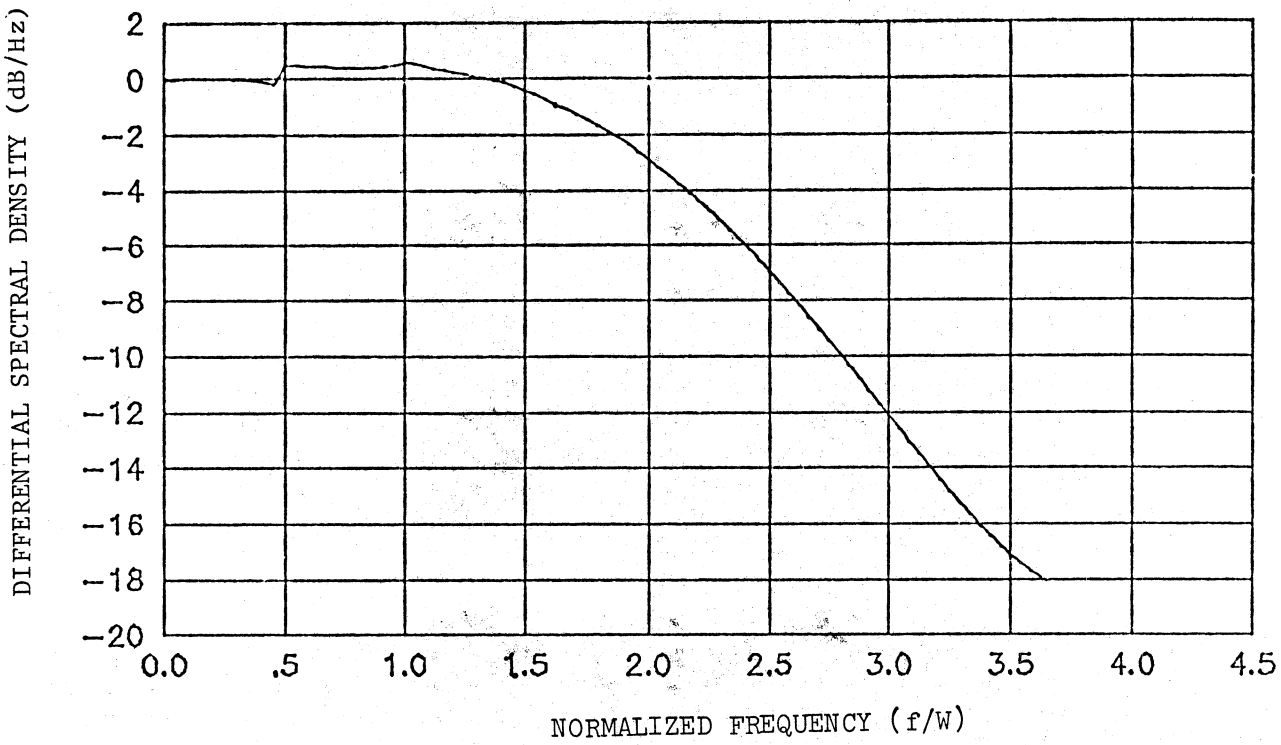

Figure 8(k). Case of N=9 Weighted Convolutions for β=2.0 (carrier level = -17.372 dBW)

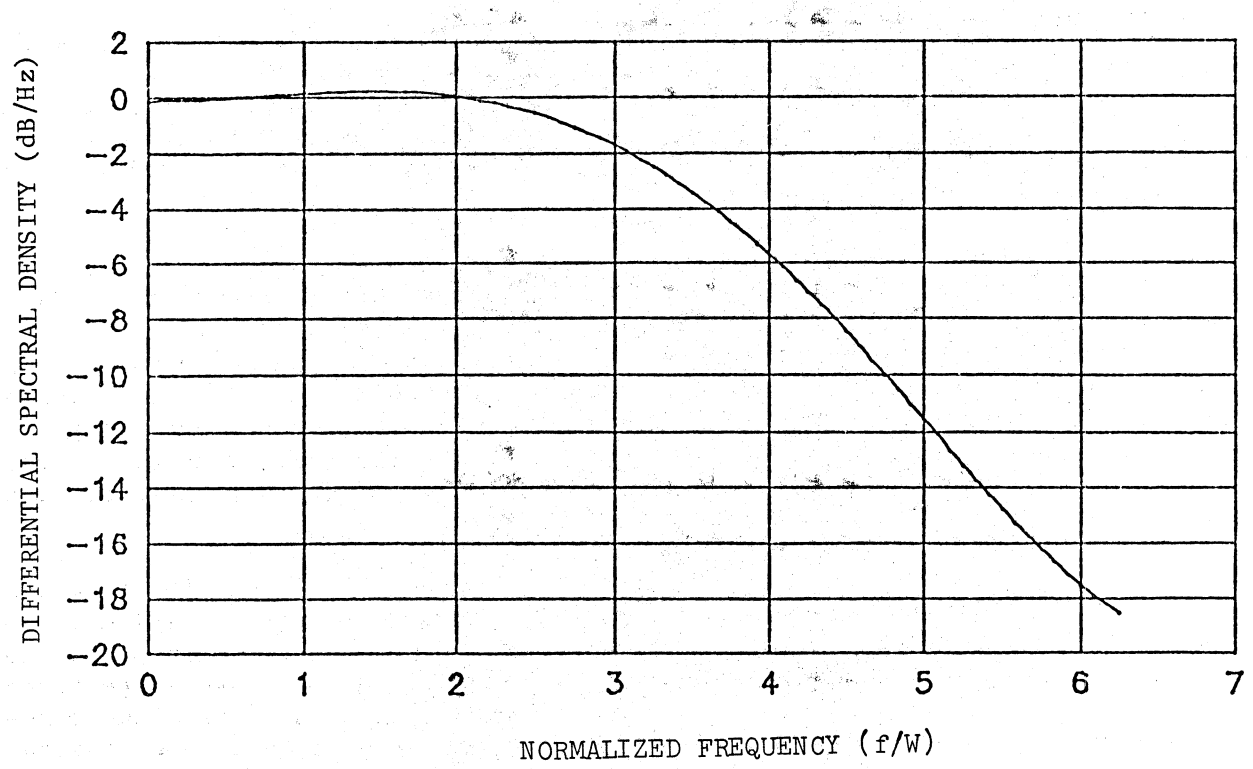

Figure 8(l). Case of N=17 Weighted Convolutions for β=3.0 (carrier level = -39.087 dBW)

SECTION 4

GENERALIZED FM SPECTRUM GENERATION PROGRAM

The rectangle convolution program results are limited to the baseband modulation case considered. The existence of a wider variety of baseband spectra and preemphasis characteristics in practical applications motivates a more generalized FM spectrum simulation capability. The interest is to provide for baseband spectral shaping and parametric assignment control by the user, and the compromise is that a compact mathematical formulation of the spectral convolution terms is no longer available. The computer program must now simulate the FM spectrum generation process itself, rather than implement available expressions as done in the rectangle convolution program.

The assumption of gaussian statistics in the baseband modulating signal yields the general expression already given in (1) in terms of an equivalent phase modulating process. The formulation can be adapted to represent a generalized FM process by relating the phase-modulating power spectrum $S_x(f)$ to an arbitrary input baseband power spectrum $S_b(f)$ and preemphasis power transfer characteristic T(f). The spectral relationships are given by

$$S_x(f) = \left(\frac{\Omega}{2\pi f}\right)^2 T(f)\, S_b(f) = \left(\frac{\Delta F}{f}\right)^2 T(f)\, S_b(f) \qquad (11)$$

where $\Omega = 2\pi(\Delta F)$ is the rms frequency deviation in rad/sec if $S_p(f) = T(f) \cdot S_b(f)$ has unit power. The mean-square phase deviation is given by the integral of (11), and its magnitude depends on the baseband spectrum and preemphasis characteristic in general. For example, a uniform baseband spectrum over a frequency range (f_1, f_h) results in an rms phase deviation of $\beta = \Delta F/\sqrt{f_1 f_h}$ when no preemphasis is employed.

The generalized FM spectrum generation procedure is shown in Figure 9. The equivalent phase modulating spectrum $S_x(f)$ is first developed according to (11) for a given baseband spectrum $S_b(f)$, preemphasis characteristic T(f) and rms frequency deviation ΔF. The correlation function $R_x(t)$ of the phase modulating spectrum is next obtained via an Inverse Fourier Transform, and used to evaluate the equivalent correlation function $r_y(t)$ of the modulated signal according to the exponential transformation in (1). The spectrum $s_y(f)$ corresponding to this function is then obtained via a Direct Fourier Transform to generate the equivalent lowpass spectrum of the FM signal.

A computer program was developed at NTIA to simulate the FM spectrum generation of Figure 9. The program essentially involves the simulation of an input spectrum and four processing blocks. The input spectrum represents the nominal baseband spectrum without preemphasis, and one of the processors performs the preemphasis conversion of the baseband spectrum into an equivalent phase modulating spectrum. The other processors perform the direct and inverse

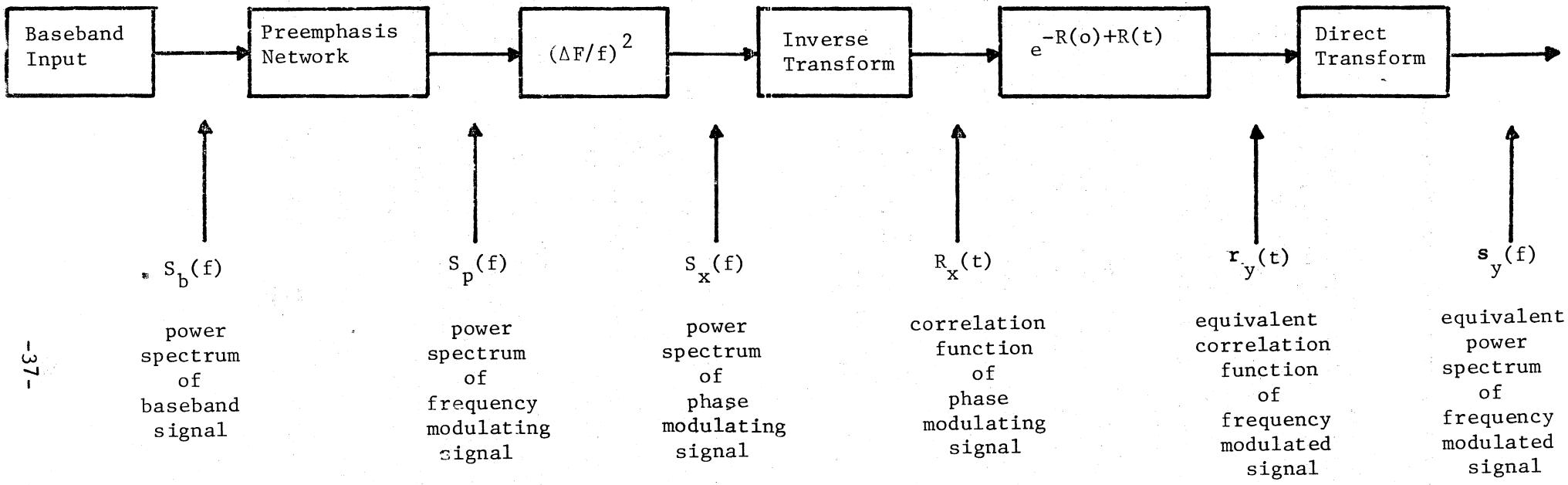

Figure 9. Generalized FM Spectrum Generation.

transforms involved, as well as the exponential transformation that simulates the modulation effect.

The continuous Fourier Transforms must be replaced by their discrete versions for computer implementation. This implies that a time-limited plus band-limited signal modeling is being provided, which represents a departure from the continuous case and requires careful accounting of distortion and aliasing effects. A systematic procedure was developed to select the number of samples for an effective discrete representation in either time or frequency domain. The procedure can handle general unknown functions where only pulse width and bandwidth measures are provided, as well as typical test functions where specific parametric formulations are available.

A Fast Fourier Transform algorithm was employed for the Discrete Fourier Transform realization. An existing in-house subroutine was analyzed and adapted by the addition of a special purpose driver dedicated to deliver the input samples in a manner convenient for spectral analysis purposes. A menu of test signals with their corresponding discrete formulations was developed to validate the transform computation under various pertinent conditions (e.g., lowpass and bandpass spectra, finite or infinite pulse widths and bandwidths). The theoretical results were reproduced accurately in all cases, with only the ideal retangular shapes requiring careful handling to accommodate the instantaneous discontinuity effects. The use of weighted mixtures of the test functions was also employed to simulate arbitrary spectral conditions and further validate the transform algorithms, by verifying that the mixture output corresponds to the weighted superposition of the individual output results.

DISCRETE FOURIER TRANSFORMS

The Discrete Fourier Transform (DFT) consists of a direct and inverse transform pair employed to relate the discrete-time and discrete-frequency domain representations of signal waveforms. The DFT provides for an accurate approximation to the continuous Fourier Transform pair, and permits its practical computation via digital computer algorithms. The Fast Fourier Transform (FFT) represents a modern efficient algorithm employed to compute the DFT.

A finite number (N) of samples is involved in the discrete time and frequency representations of the DFT. This implies that a time-limited plus band-limited signal characterization is always provided. This represents a departure from the continuous fourier transform, where a signal cannot be limited in both the time and frequency domains simultaneously. The number of samples employed must be carefully selected to assure an adequate representation when signals with an infinite domain in time or frequency are under consideration.

The direct and inverse DFT pair is specified by the formulas:

$$S(n) = \sum_{k=o}^{N-1} R(k) \exp\left[-j(2\pi/N)nk\right] = \sum_{k=o}^{N-1} R(k)\, W_N^{nk} \qquad \text{(direct)} \qquad (12a)$$

and

$$R(k) = \frac{1}{N} \sum_{n=o}^{N=1} S(n) \exp [+j (2\pi/N) nk] = \frac{1}{N} \sum_{n=o}^{N=1} S(n) W_N^{-nk} \quad \text{(inverse)} \quad (12b)$$

where R(k) represents the discrete-time samples, S(n) represents the discrete-frequency samples, and $W_N = \exp [-j (2\pi/N)]$ is noted to vary with the sample size (N). The same number of samples is employed in both the time and frequency domain representations.

The time samples R(k) and the frequency samples S(n) can in general be complex valued. The complex conjugate R*(k) of the time domain sequence can be verified to be identical to the direct DFT of the complex conjugate S*(n) of the frequency domain sequence, except for the presence of a (1/N) scaling factor. This permits the evaluation of the inverse DFT as a direct DFT with simple modifications as shown in Figure 10(a). The last conjugation can obviously be omitted for the case of real samples in time. Moreover, a real even symmetry in time implies a real even symmetry in frequency, and then the inverse DFT reduces to a direct DFT with (1/N) scaling as shown in Figure 10(b). This last case is of particular interest when evaluating autocorrelation and power spectral density functions of real signals, since these functions exhibit a real even symmetry about the origin in both time and frequency domains.

An inverse DFT is employed in Figure 9 to obtain the discrete correlation function $R_x(k)$ from the discrete power spectrum $S_x(n)$. The latter represents the samples from its continuous counterpart $S_x(f)$, but the correlation values $R_x(k)$ obtained via (12b) must be multiplied by $N \cdot \Delta f$ to represent samples from the continuous correlation function $R_x(t)$. This effect is a consequence of the incremental spacings being implicit in the DFT summation versus explicit in the continuous transform integral.

A similar effect occurs when using the direct DFT in Figure 9 to obtain the discrete power spectrum $s_y(n)$ from the discrete correlation function $r_y(k)$. The latter represents the samples from its continuous counterpart $r_y(t)$, but the spectral values $s_y(n)$ obtained via (12a) must be divided by $N \cdot \Delta f$ to represent samples from the continuous power spectrum $s_y(f)$. Notice that this division by $N \cdot \Delta f$ does not cancel the above multiplication by $N \cdot \Delta f$ since there is the nonlinear exponential transformation separating these effects in Figure 9.

The inclusion of these scaling factors is necessary to maintain dimensional analogy with the continuous signal representation. The net effect insofar as the simulation logic is concerned is shown in Figures 11(a) and 11(b). The inverse continuous transform is realized by a direct DFT plus a Δf multiplier, which corresponds to the inverse DFT with a $N \cdot \Delta f$ multiplier. The direct continuous transform is realized by a direct DFT with a $N \cdot \Delta f$ divider, and the generation of dB/Hz spectral units only requires taking 10 log (·) of the DFT output data and subtracting the constant 10 log $(N \cdot \Delta f)$.

NUMBER OF SAMPLES

The number of samples (N) employed in the DFT must be sufficient to provide an effective representation of the continuous time and frequency functions

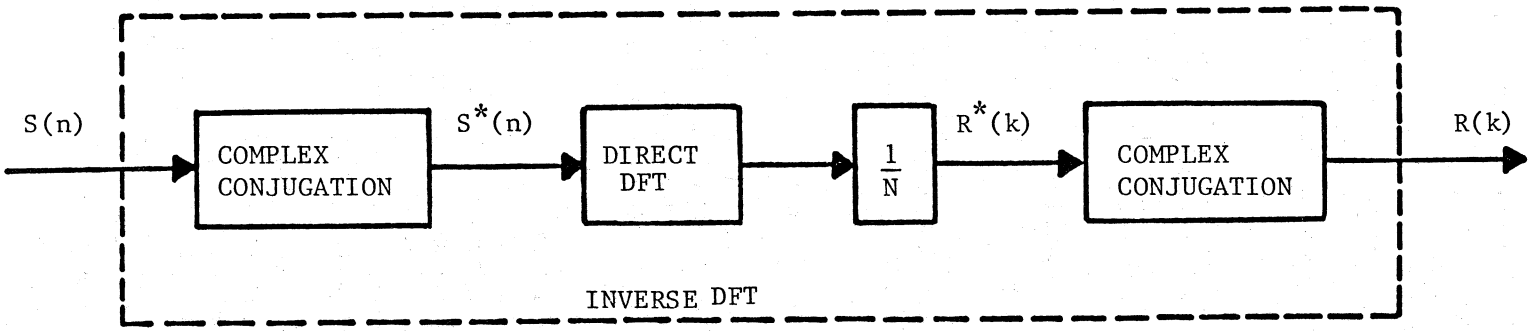

Figure 10(a). Inverse DFT Realization via Direct DFT.

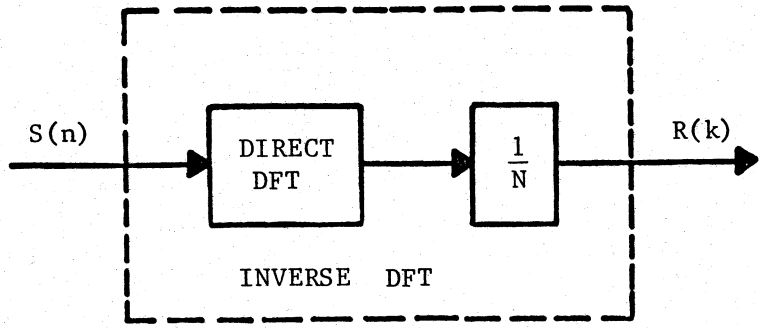

Figure 10(b). Inverse DFT Realization for Real Even Symmetry.

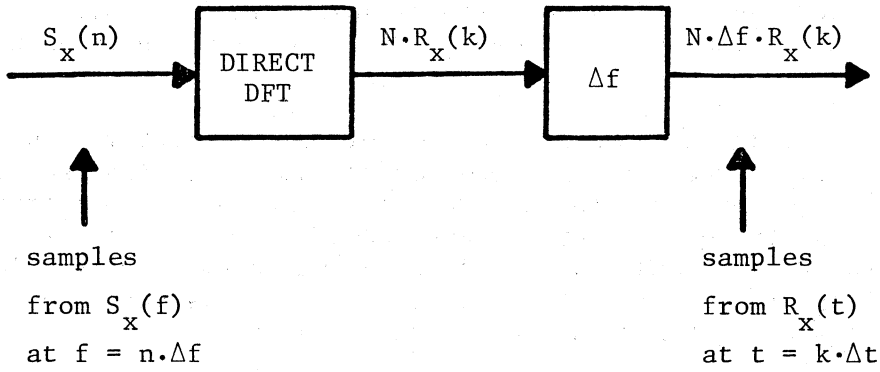

Figure 11(a). Inverse Transform Simulation with Dimensional Analogy. ($\Delta t \cdot \Delta f = 1/N$ is always satisfied in the DFT)

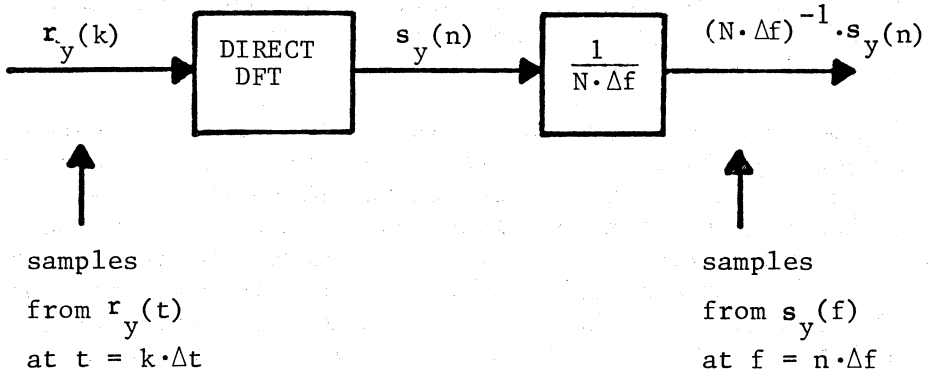

Figure 11(b). Direct Transform Simulation with Dimensional Analogy. ($\Delta t \cdot \Delta f = 1/N$ is always satisfied in the DFT)

involved. The fact that the same number of samples is used in both domain representations implies that the selection rationale must jointly provide enough time spread and spectral occupancy to cover the effective pulse widths and bandwidths involved.

A standardized procedure was developed to logically select the number of samples (N), and is applicable regardless of whether the direct or inverse DFT is being computed. The procedure can handle general unknown time or frequency functions where pulse width or bandwidth measures are the only available information, as well as specific functions where detailed parametric formulations are assumed as models. In particular, the procedure was designed to handle even-symmetric functions (autocorrelation, power density) based on the immediate application of interest here.

Consider an even-symmetric input function with a one-sided effective width measure (W_{in}). The input function will be assumed in the time domain for formulation purposes, without loss of generality since we only need to interchange the time (t) and frequency (f) variables otherwise. The number of input samples (N) needed to cover the input with a uniform incremental spacing (Δt) then satisfies $N(\Delta t) = 2\,W_{in}$. The relation $(\Delta t) \cdot (\Delta f) = 1/N$ is inherent in the DFT definition, and relates the input and output incremental spacings. Hence, a given number of samples (N) corresponds to input and output increments of $\Delta t = 2W_{in}/N$ and $\Delta f = 1/2W_{in}$, and the net output width coverage capability is given by $N(\Delta t)/2 = 1/2W_{in}$ (one-sided). This last amount must exceed the (one-sided) effective output width measure (W_{out}), which yields the requirement of $N \geq 4\,(W_{in})\,(W_{out})$ for the sample number selection. Note this condition is symmetric in its joint accounting of the time and frequency domains (pulse widths, bandwidths) as should be the case.

The selection of a baseband input spectrum is first used to establish a lower bound on the number of samples required. An input bandwidth measure is available from the spectral shape, and the associated pulse width measure can be obtained from its corresponding correlation function. This minimum number of samples is obviously insufficient for the ultimate FM output spectrum representation, since the bandwidth expansion effect must be accounted for. The bandwidth expansion can be estimated using Carson's Rule or other FM bandwidth measure selected, and the corresponding increase in the number of samples required becomes specified.

The baseband input spectrum $S_b(f)$ of Figure 9 was simulated to approximate a rectangular shape with selectable low and high cutoff frequencies. A noncentral Butterworth spectrum family was employed for this purpose, with the cutoff rate (spectral tail decay) carefully selected to assure that an effective approximation to the ideal rectangle effects are preserved through the spectral transformations of (11) leading to the equivalent phase modulating spectrum $S_x(f)$ in Figure 9.

The selection of a Butterworth spectrum instead of an ideal rectangle for simulation purposes was motivated by practical DFT representation considerations. The step discontinuities of an ideal rectangle hinder a discrete simulation,

since the sampling logic must account for the unavoidable ringing distortion. Moreover, the Butterworth discrete formulation provides for a free parameter that can be conveniently employed as a bandwidth expansion designator to automatically accommodate the increase in the number of samples required as the baseband input spectrum generates the FM output spectrum.

BUTTERWORTH BASEBAND SPECTRUM SIMULATION

A noncentral Butterworth spectrum family represents a useful approach for the simulation and shaping of the baseband power spectrum. The noncentral Butterworth family can provide control of a variety of spectral features (center location, bandwidth, cutoff rate) with a compact formulation, as well as approximate a uniform distribution over some arbitrary low (f_l) and high (f_h) frequency range.

The continuous noncentral Butterworth spectrum is specified by the three-parameter family given by

$$S_b(f) = \frac{1}{1 + \left(\frac{f - f_o}{f_r}\right)^P} \tag{13}$$

where $f_o = (1/2)\ (f_h + f_l)$ is the center location, $f_r \simeq (1/2)\ (f_h - f_l)$ is the one-sided 3 dB bandwidth from the center (with the approximation holding for P large), and $P \geq 2$ is an even integer that governs the cutoff rate of the spectral tails beyond the 3 dB breakpoints. The spectral shaping is controlled by the user via the (f_o, f_r, P) parameters, and the spectrum approximates an ideal rectangle as P increases, with the bandwidth occupancy approaching f_r as a lower bound.

A band-limited reproduction of the Butterworth bandwidth occupancy requires a spectral coverage that extends beyond $f_o + f_r$, which can be specified as $N(\Delta f) = 2\ (f_o + Mf_r)$ in a discrete representation with N samples The parameter $M \geq 1$ serves to establish the effective bandwidth measure as Mf_r, while maintaining a bandwidth definition flexibility. For example, M = 1 corresponds to the 3 dB bandwidth, while $1 < M < 1.57$ corresponds to the equivalent noise bandwidth which varies with the P value.

The correlation function corresponding to a given Butterworth spectrum varies in shape according to the P value. For example, P = 2 yields an exponential pulse, while a large P approximates a sinc pulse in the limit. The number of samples (N) must span the effective pulse widths in each case, with the relation $N\ (\Delta t) \cdot (\Delta f) = 1$ used to establish the sample size requirement. For example, the sinc pulse has zero crossings spaced by $(2Mf_r)^{-1}$ so that a one-sided coverage of K zero crossings requires $N\ (\Delta t) \geq K/(Mf_r)$ or $N > 2K\ (f_o + Mf_r)/(Mf_r)$.

It is convenient to define the parameter $Q = f_o/f_r$, so that the set (M, N, P, Q) represents the spectral design parameters in the discrete representation.

The rectangular spectrum and sinc pulse coverage then implies $N > 2K[(Q/M) + 1]$ where $Q \simeq (f_h + f_l)/(f_h - f_l)$ for large P values. For example, the range of (f_l, f_h) values employed in FDM/FM telephony for satellite communication applications corresponds to a practical range of $1 \leq Q < 2$ for spectral representation purposes.

The discrete formulation of the Butterworth spectrum family is specified by

$$S_b(n) = \frac{1}{1+\left[\left(\frac{2n}{N} - 1\right) Q + \frac{2nM}{N}\right]^P} \quad \text{for} \quad 0 \leq n < N/2 \tag{14}$$

where the other remaining samples for $N/2 \leq n \leq N-1$ are obtained as mirror images of those above due to the even symmetry of the power spectrum. A typical set of the discrete Butterworth spectra obtained via the program simulation based on these formulas is illustrated in Figure 12. The case of $Q = M = 1.5$ was arbitrarily selected since it is representative, and the condition $Q = M$ yields a center location at $n = N/4$ which is easy to verify.

The discrete correlation functions corresponding to various Butterworth spectra were obtained via the inverse FFT for further validation. Some typical results are shown in Figures 13(a) to 13(h), where the $P = 10$ and $P = 100$ cutoff cases are considered under varying central ($Q = 0$) and noncentral ($Q \neq 0$) conditions. These P values are large enough so that the nominal correlation functions effectively approximate those corresponding to the case of ideal rectangular spectra.

On this basis, the total area (power content) under the continuous Butterworth spectrum is given by $A = 2f_r(\text{sinc } \pi/P)^{-1} \approx 2f_r$ for the central ($Q = 0$) cases, and by twice this amount for the noncentral ($Q \neq 0$) cases. These values also represent the continuous correlation function peaks at the origin, which can be formulated in the discrete representation as

$$A_o = \frac{1}{M \text{ sinc } (\pi/P)} \approx \frac{1}{M} \quad \text{for} \quad Q = 0 \tag{15a}$$

and

$$A_o = \frac{2}{(Q + M) \text{ sinc } (\pi/P)} \approx \frac{2}{Q + M} \quad \text{for} \quad Q \neq 0 \tag{15b}$$

These theoretical results can be verified to hold in all the simulation plots for the discrete correlation function peaks. The actual functional dependence can also be verified by noting that the nominal continuous correlation functions are given by $R_b(t) = A \text{ sinc } (2\pi f_r t)$ for the central ($Q = 0$) cases, and by $R_b(t) = 2A \text{ sinc } (2\pi f_r t) \cos (2\pi f_o t)$ for the noncentral ($Q \neq 0$) cases. These expressions have discrete formulations given by

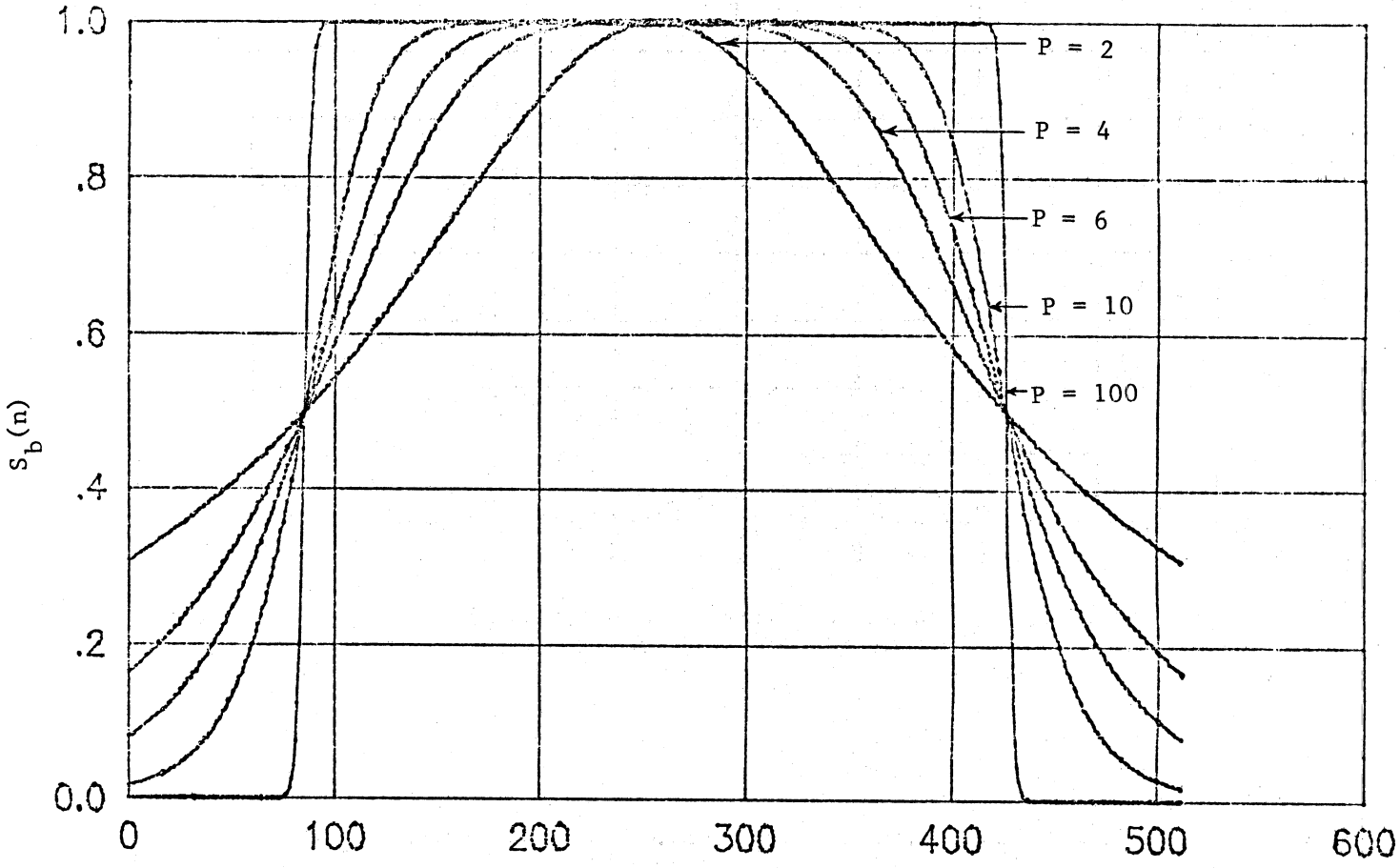

$$S_b(n) = \frac{1}{1+\left[\left(\frac{2n}{N} - 1\right) Q + \frac{2nM}{N}\right]^P} \quad \text{for} \quad 0 \leq n < N/2$$

Figure 12. Butterworth Power Density Spectra
(Q = M = 1.5, N = 1024)

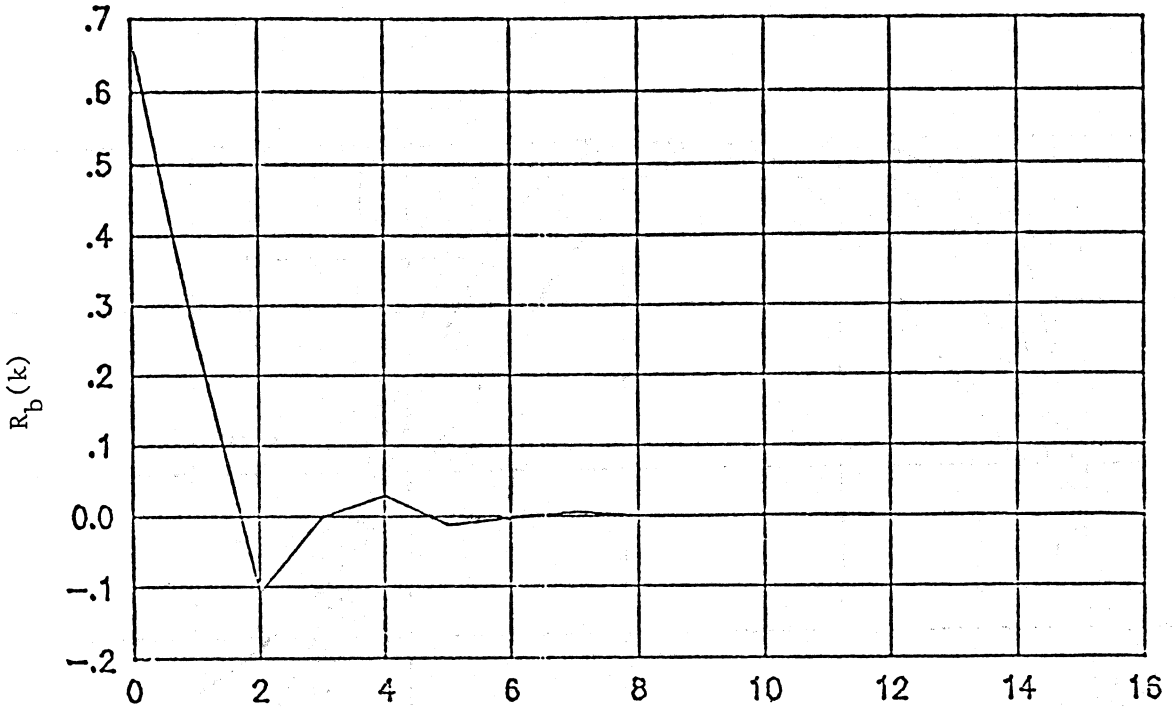

Figure 13(a). Central Butterworth Correlation Function: First Case (Q = 0, M = 1.5, P = 10, N = 1024)

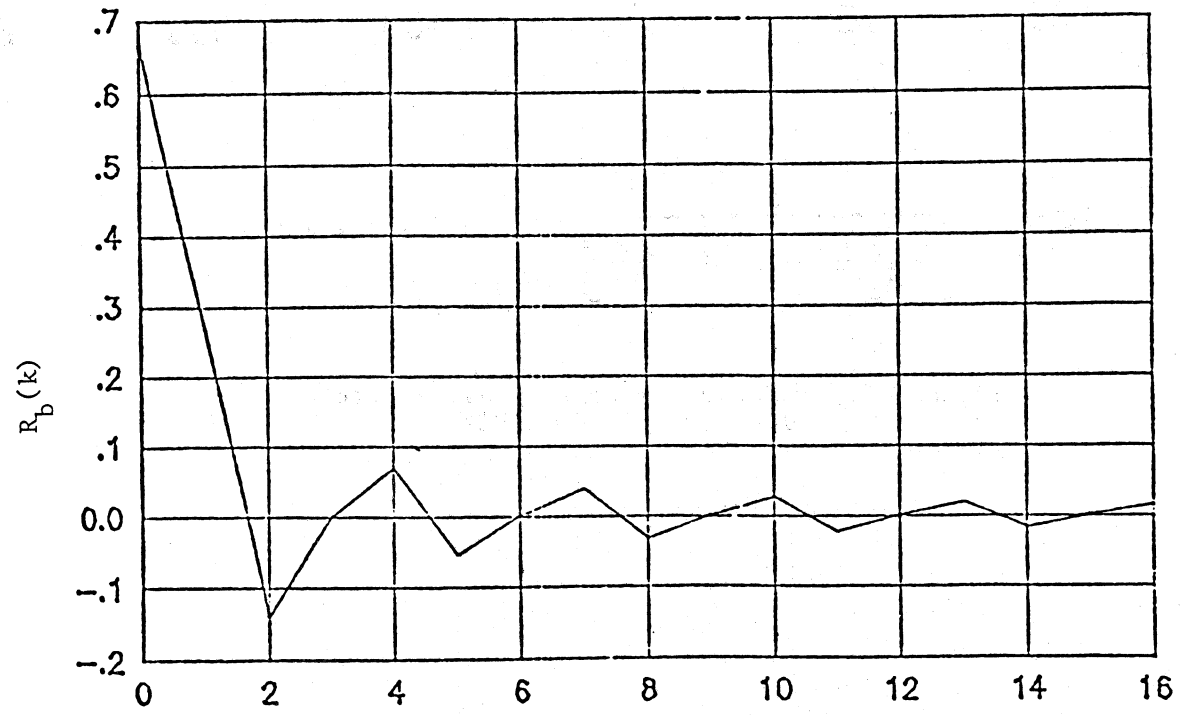

Figure 13(b). Central Butterworth Correlation Function: Second Case (Q = 0, M = 1.5, P = 100, N = 1024)

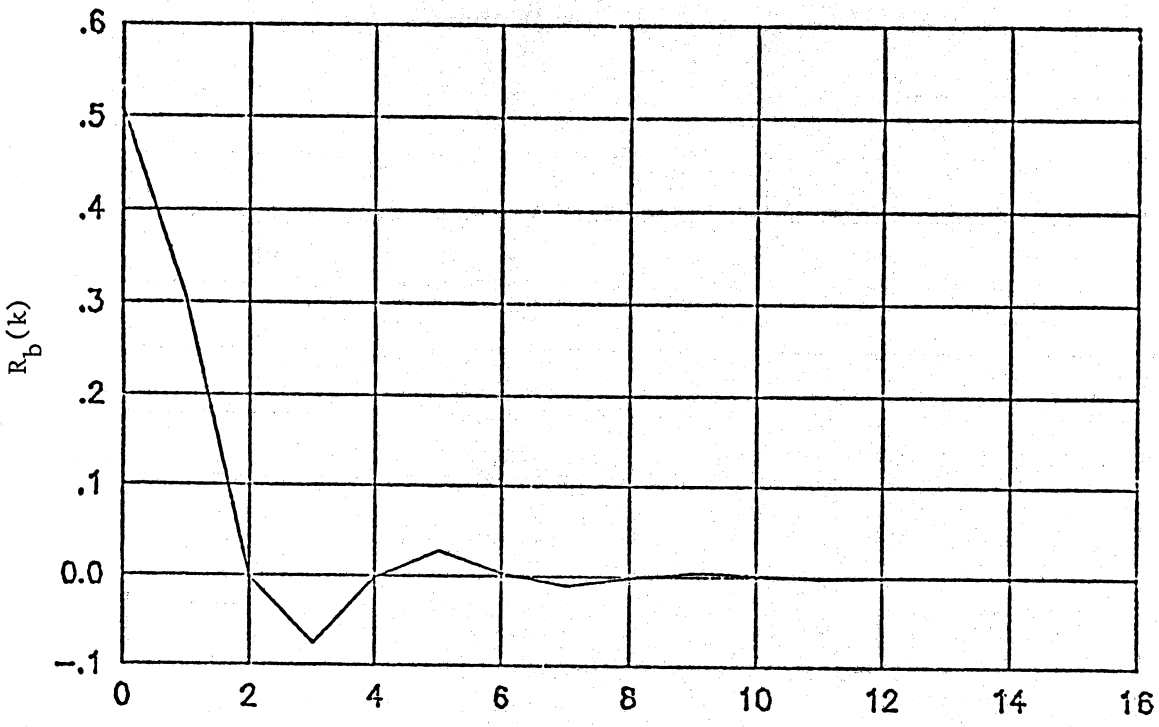

Figure 13(c). Central Butterworth Correlation Function: Third Case (Q = 0, M = 2, P = 10, N = 1024)

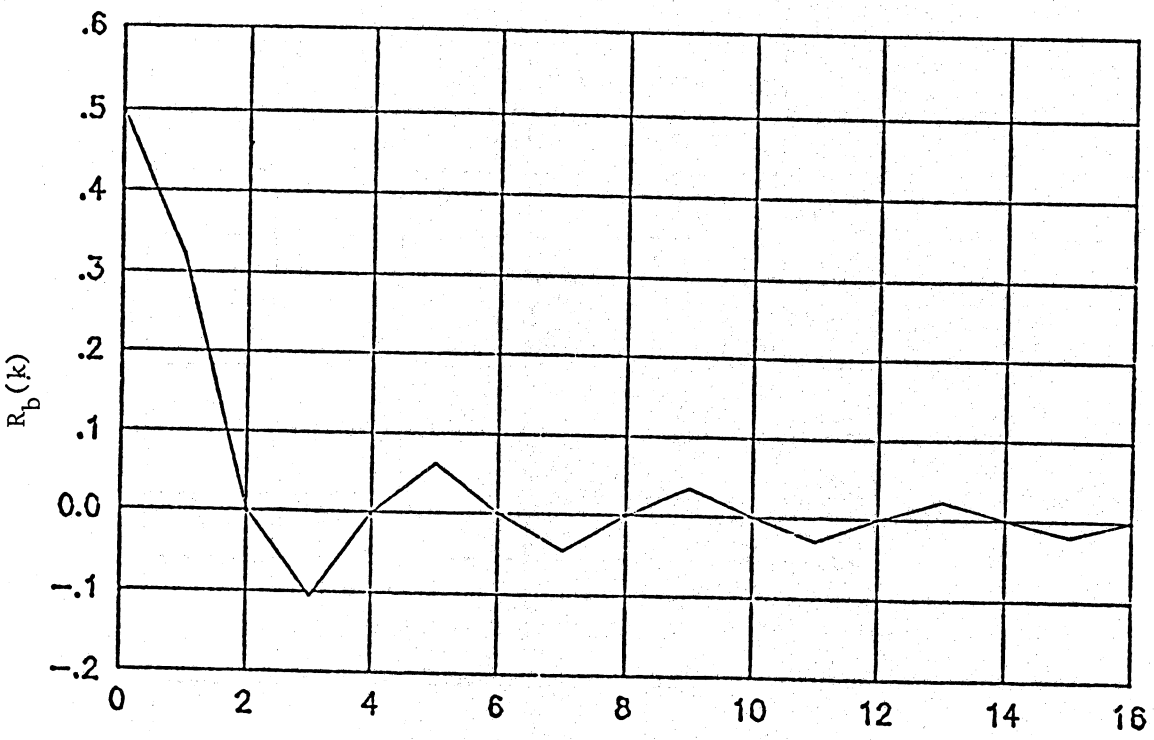

Figure 13(d). Central Butterworth Correlation Function: Fourth Case (Q = 0, M = 2, P = 100, N = 1024)

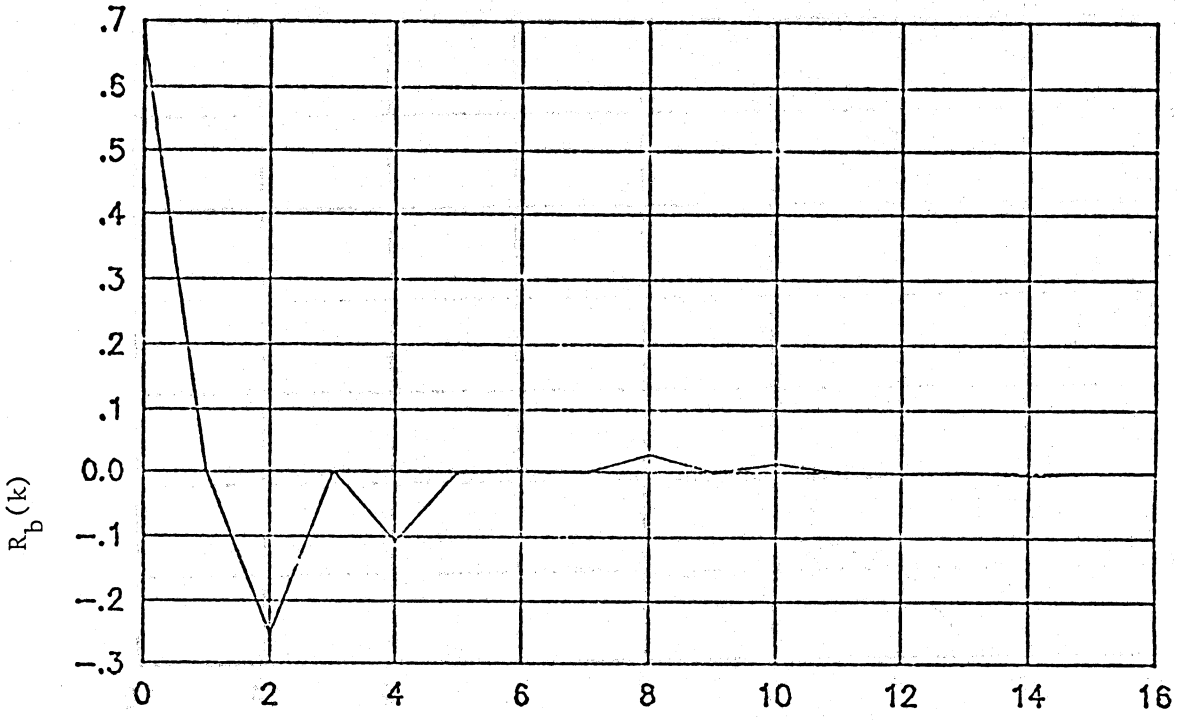

Figure 13(e). Noncentral Butterworth Correlation Function: First Case (Q = M = 1.5, P = 10, N = 1024)

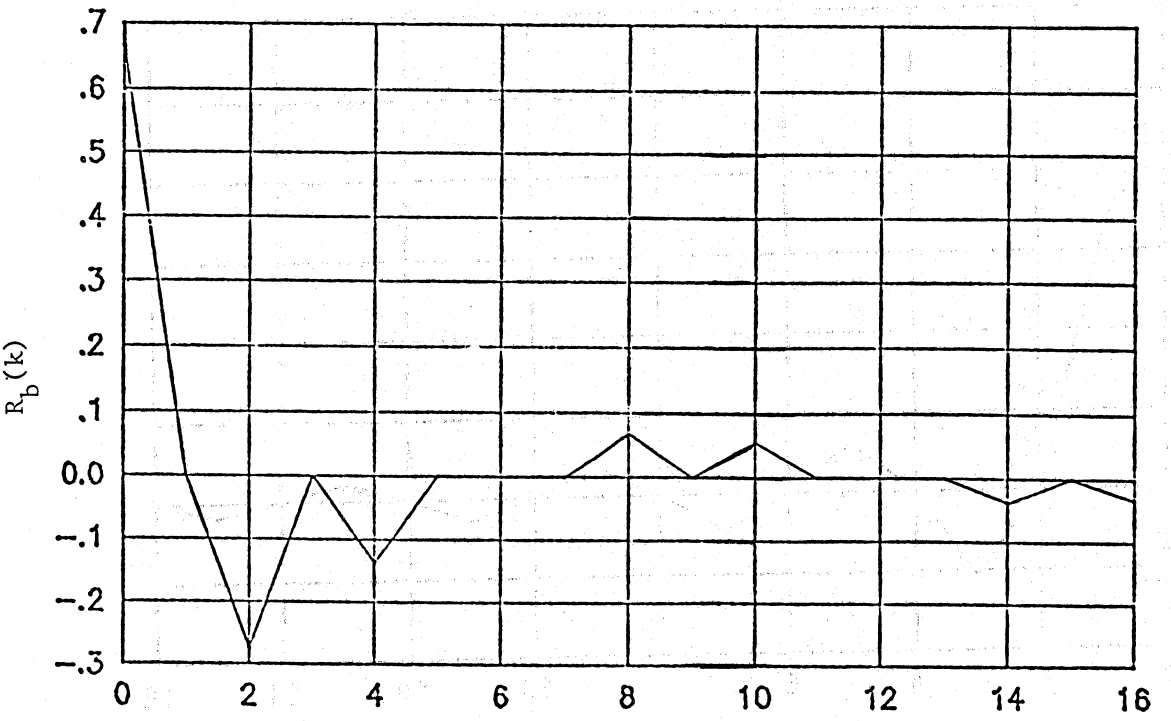

Figure 13(f). Noncentral Butterworth Correlation Function: Second Case (Q = M = 1.5, P = 100, N = 1024)

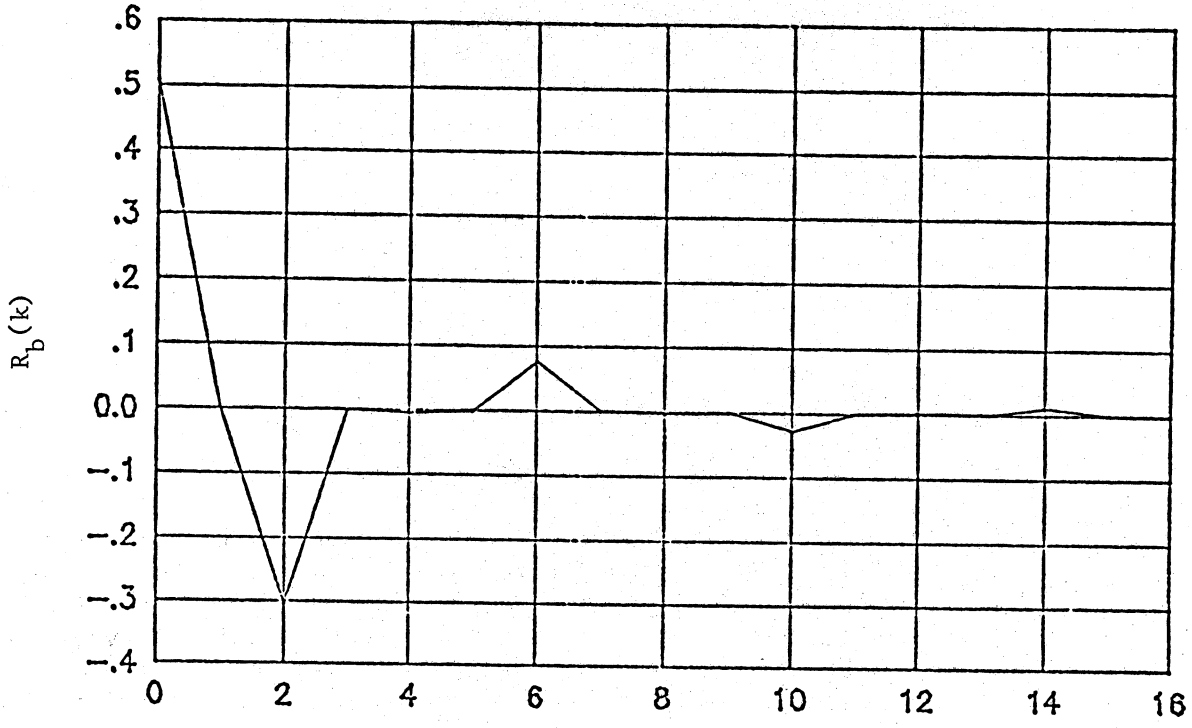

Figure 13(g). Noncentral Butterworth Correlation Function: Third Case (Q = M = 2, P = 10, N = 1024)

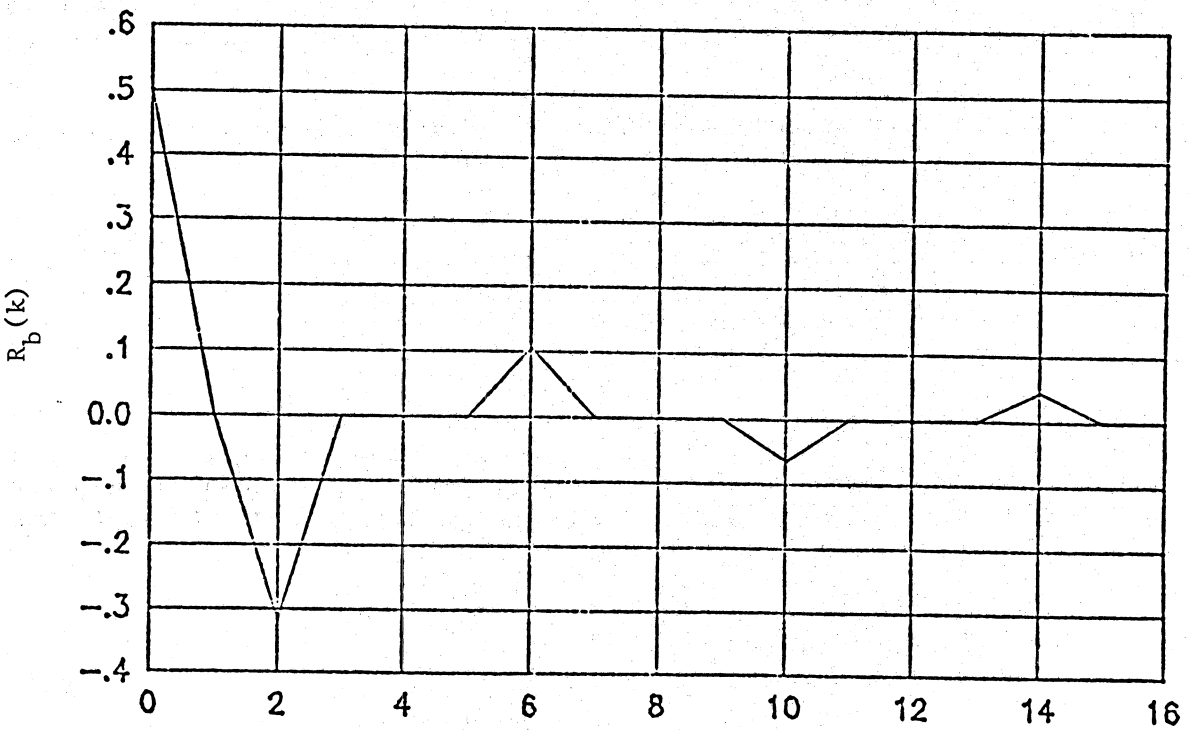

Figure 13(h). Noncentral Butterworth Correlation Function: Fourth Case (Q = M = 2, P = 100, N = 1024)

$$R_b(k) = A_o \text{sinc}\left(\frac{k\pi}{M}\right) \text{ for } Q = 0 \tag{16a}$$

and

$$R_b(k) = A_o \text{sinc}\left(\frac{k\pi}{Q+M}\right) \cdot \cos\left(\frac{k\pi Q}{Q+M}\right) \text{ for } Q \neq 0 \tag{16b}$$

Hence, the theoretical results predict that the zeroes of the discrete correlation function should occur at k = M, 2M, 3M . . . for the Q = 0 cases, and at k = (Q + M), 2(Q + M), 3(Q + M). . . plus k = (1/2) [(Q + M)/Q], (3/2)[(Q+M)/Q], (5/2)[(Q+M)/Q]. . . for the Q ≠ 0 cases. This behavior can indeed be verified in all the plots, and also that some of the zeroes are starting to exhibit a slight shift for the P = 10 cases relative to their P = 100 counterparts.

PREEMPHASIS AND FM/PM CONVERSION SIMULATIONS

The baseband input spectrum $S_b(f)$ is modified by the preemphasis characteristic T(f) and by the FM/PM conversion effect $(\Delta F/f)^2$ to become the equivalent phase modulating spectrum $S_x(f)$ of Figure 9. The use of a Butterworth baseband input must be verified to yield an effective $S_x(f)$ spectrum representative of that obtained with an ideal rectangular baseband. In particular, the Butterworth cutoff rate (P) must be sufficiently high to overcome the low frequency overshoots caused by the $(\Delta F/f)^2$ processor in the discrete program simulation.

The CCIR preemphasis network recommended for FDM/FM telephony applications has a voltage transfer characteristic given by (Panter, 1972).

$$V(s) = k_o \cdot \frac{1 + k_1 k_2 (s/\omega_r) + (s/\omega_r)^2}{1 + \frac{k_1 k_2}{1+k_1}(s/\omega_r) + (s/\omega_r)^2} \tag{17}$$

where $k_o^2 = 0.4$, $k_1 = 1.81$, $k_1 = (1/0.79)$, $\omega_r = 1.25\,\omega_h$, and $\omega_h = 2\pi f_h$ is the high baseband frequency in the rectangular spectrum model. The corresponding power transfer characteristic can be readily evaluated as $T(f) = |V(2\pi jf)|^2$ to yield the following:

$$T(f) = (0.4) \cdot \frac{1 + 2.0796(f/f_h)^2 + 0.4096(f/f_h)^4}{1 - 0.8545(f/f_h)^2 + 0.4096(f/f_h)^4} \tag{18}$$

This expression was simulated and tested with a uniform discrete input extending from zero to an arbitrary high frequency (f_h). The input was then modified to start at an arbitrary low frequency (f_1), thus simulating a rectangular baseband with low and high cutoffs. The preemphasized baseband spectrum is shown in Figure 14 where the abscissa has kHz units. The cutoff points agree with their predicted values in magnitude ($T(f_1) = 2.5$ and $T(f_h) = 0.4$) and location:

$$f_h = \frac{Q+1}{Q+M} \cdot \frac{N}{2} = \frac{5}{6}\ (512) = 426.6\overline{6}\ \text{(kHz)} \tag{19a}$$

$$f_1 = \frac{Q-1}{Q+M} \cdot \frac{N}{2} = \frac{1}{6}\ (512) = 85.3\overline{3}\ \text{(kHz)} \tag{19b}$$

The FM/PM conversion effect $(\Delta F/f)^2$ was next simulated, and its response when cascaded with the preemphasis characteristic was tested. The rectangular baseband spectrum with the same cutoff frequencies was used along with $\Delta F = 800$ (kHz units), and the output spectrum obtained is shown in Figure 15. The low and high cutoff locations are maintained as expected, and their max/min values can be noted to agree with the predicted values of $T(f_1) \cdot (\Delta F/f_1)^2 = 38.28$ and $T(f_h) \cdot (\Delta F/f_h)^2 = 8.79$.

The discrete Butterworth spectrum was then used as the input (instead of an ideal rectangle) into the preemphasis and FM/PM conversion cascade. All the parameter values remained as above, and the output spectra obtained for different P-values is shown in Figures 16(a) and 16(b). A comparison with the ideal response of Figure 15 shows that some significant distortion below the low frequency cutoff (f_1) can be introduced if the P - value is only moderately high as in Figure 16(b). Conversely, the ideal response becomes essentially reproduced in Figure 16(a) except for some slight attenuation at the low frequency edge. The use of $P \geq 50$ is thus motivated when using the Butterworth spectrum to simulate an ideal rectangular baseband spectrum.

The CCIR preemphasis characteristic (18) is expected to preserve the rms frequency deviation with or without preemphasis for a rectangular baseband input (Panter, 1972). This condition implies that the power content (areas) under the $S_b(f)$ and $S_p(f) = T(f) \cdot S_b(f)$ spectra are identical in principle. It is convenient to normalize the spectrum $S_p(f)$ by its power content, since then the ΔF parameter represents the rms frequency deviation. Hence, the normalization factor can be taken as the power content of $S_b(f)$, which is given by

$$P_b = \frac{2(f_h - f_1)}{\text{sinc}(\pi/P)} \approx 2(f_h - f_1) \tag{20}$$

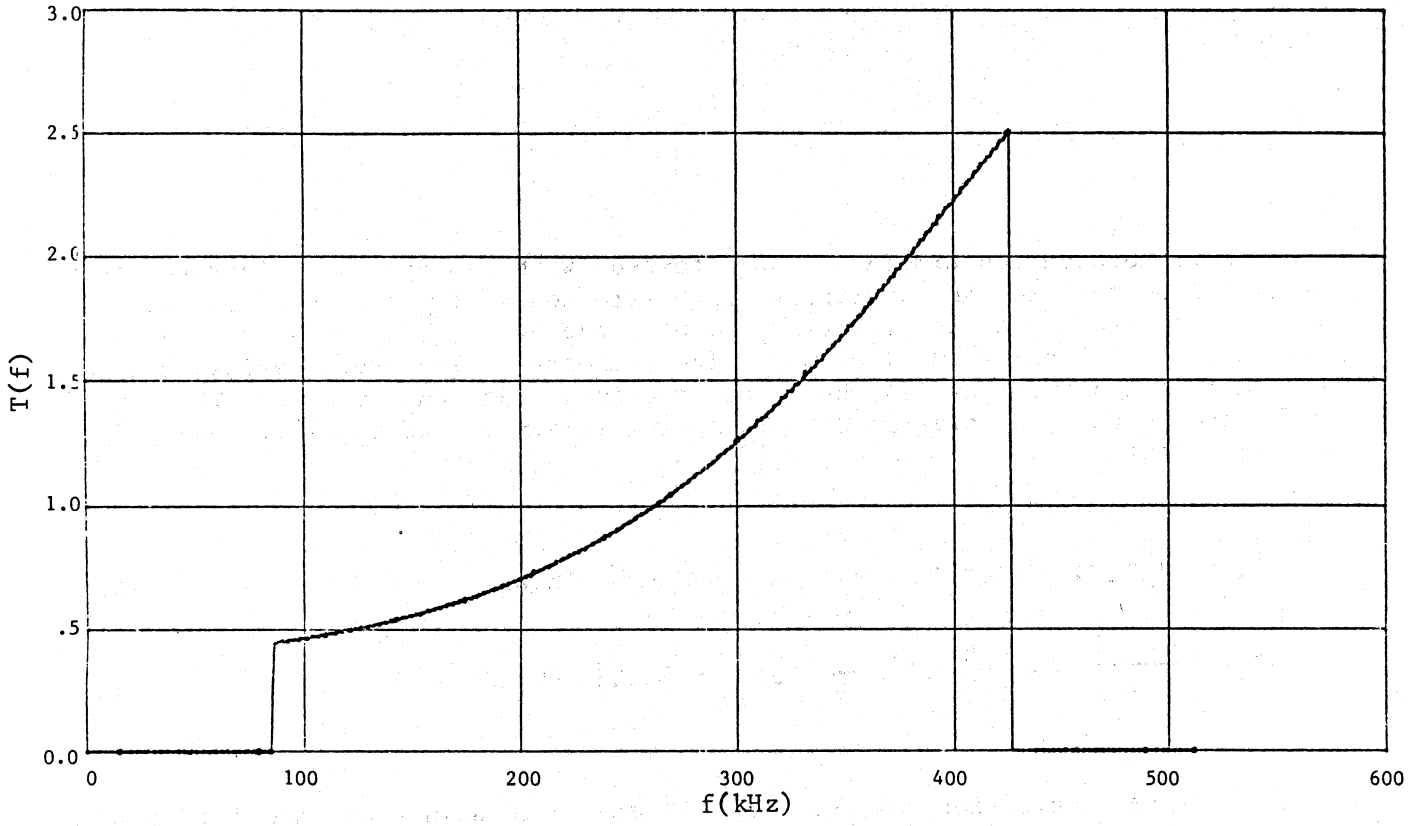

Figure 14. Preemphasized Baseband Spectrum with Rectangle Input (Q = M = 1.5, N = 1024)

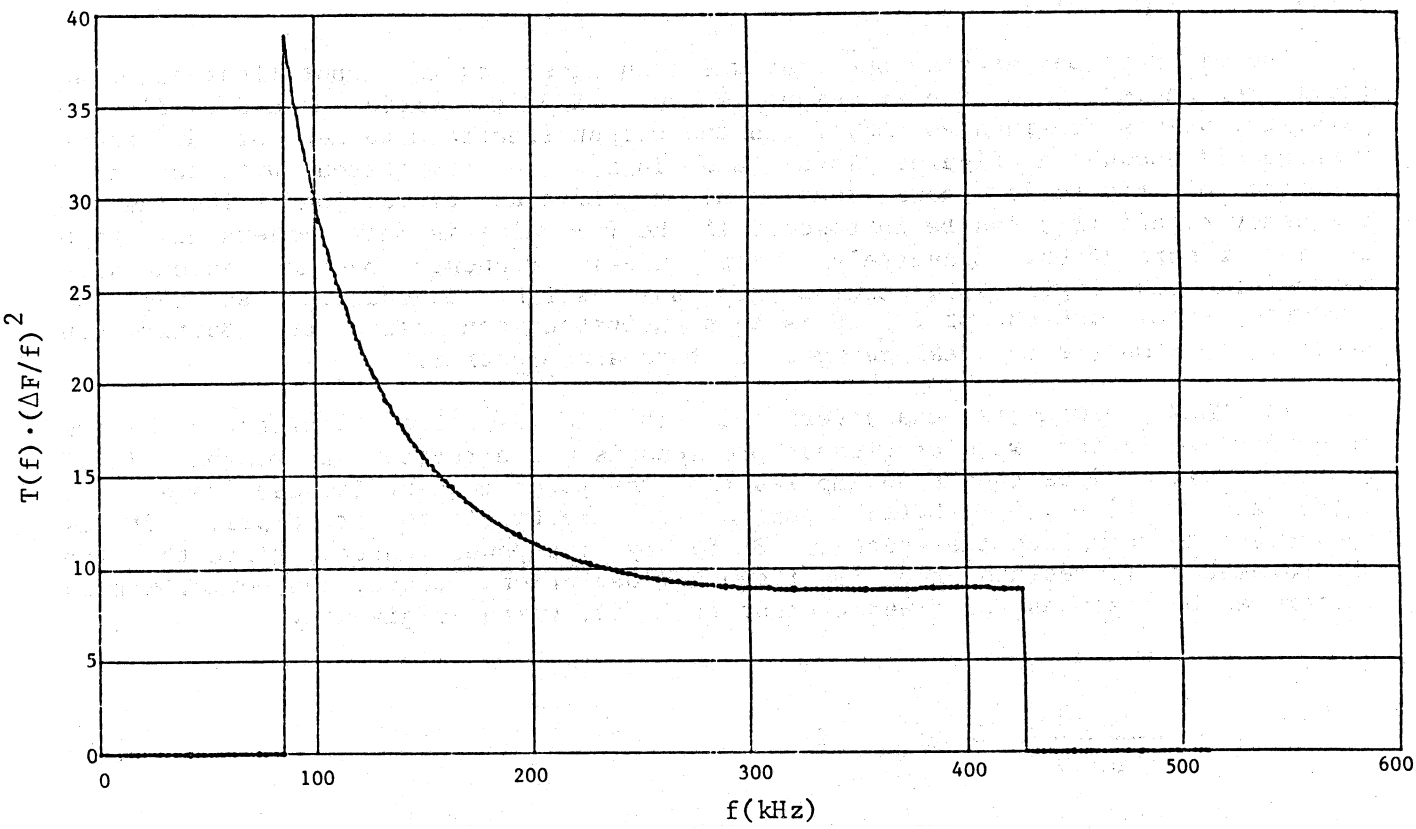

Figure 15. Equivalent Phase Modulating Spectrum with Rectangle Input (Q = M = 1.5, N = 1024)

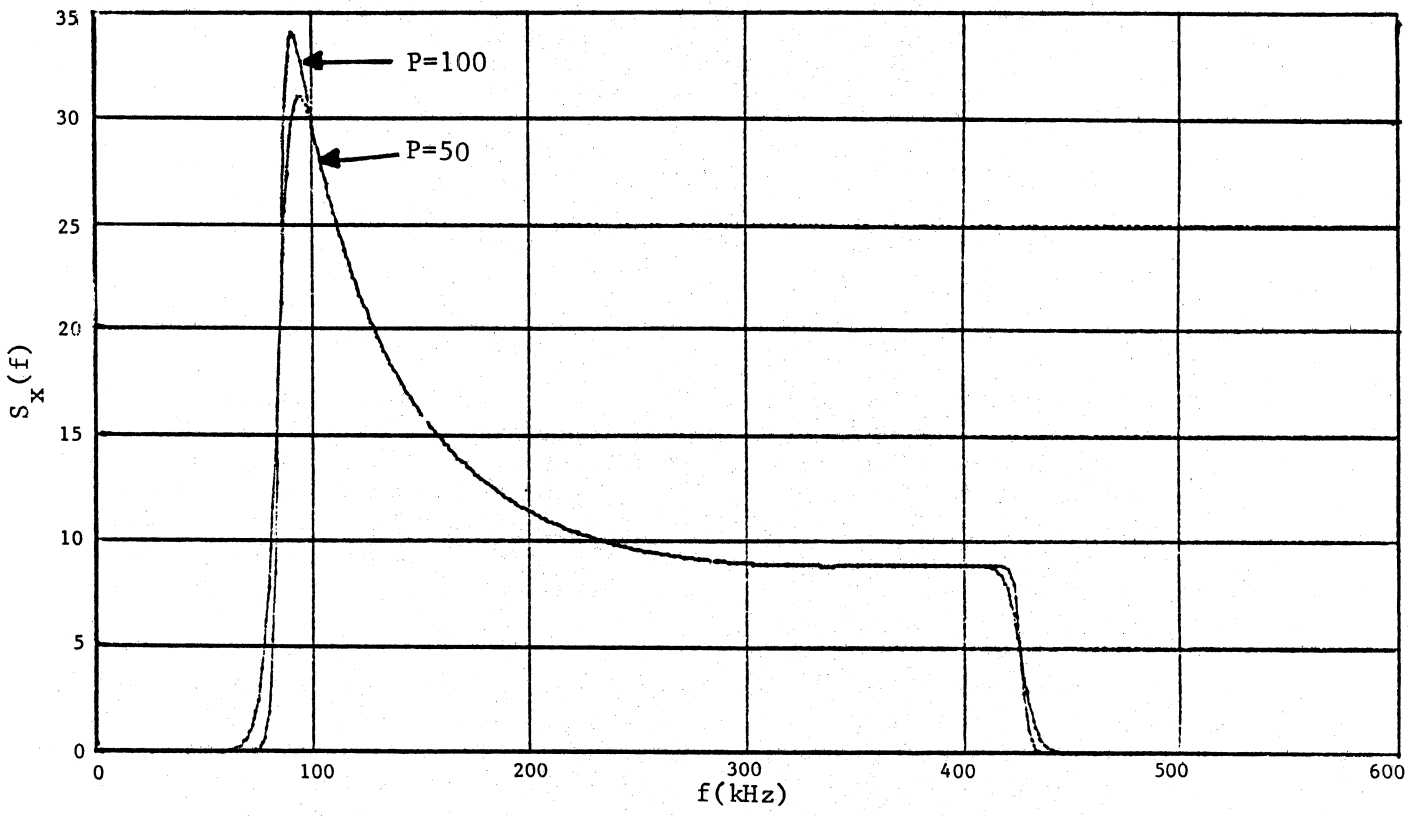

Figure 16(a). Equivalent Phase Modulating Spectrum with P = 50 and P = 100 Butterworth Inputs (Q = M = 1.5, N = 1024)

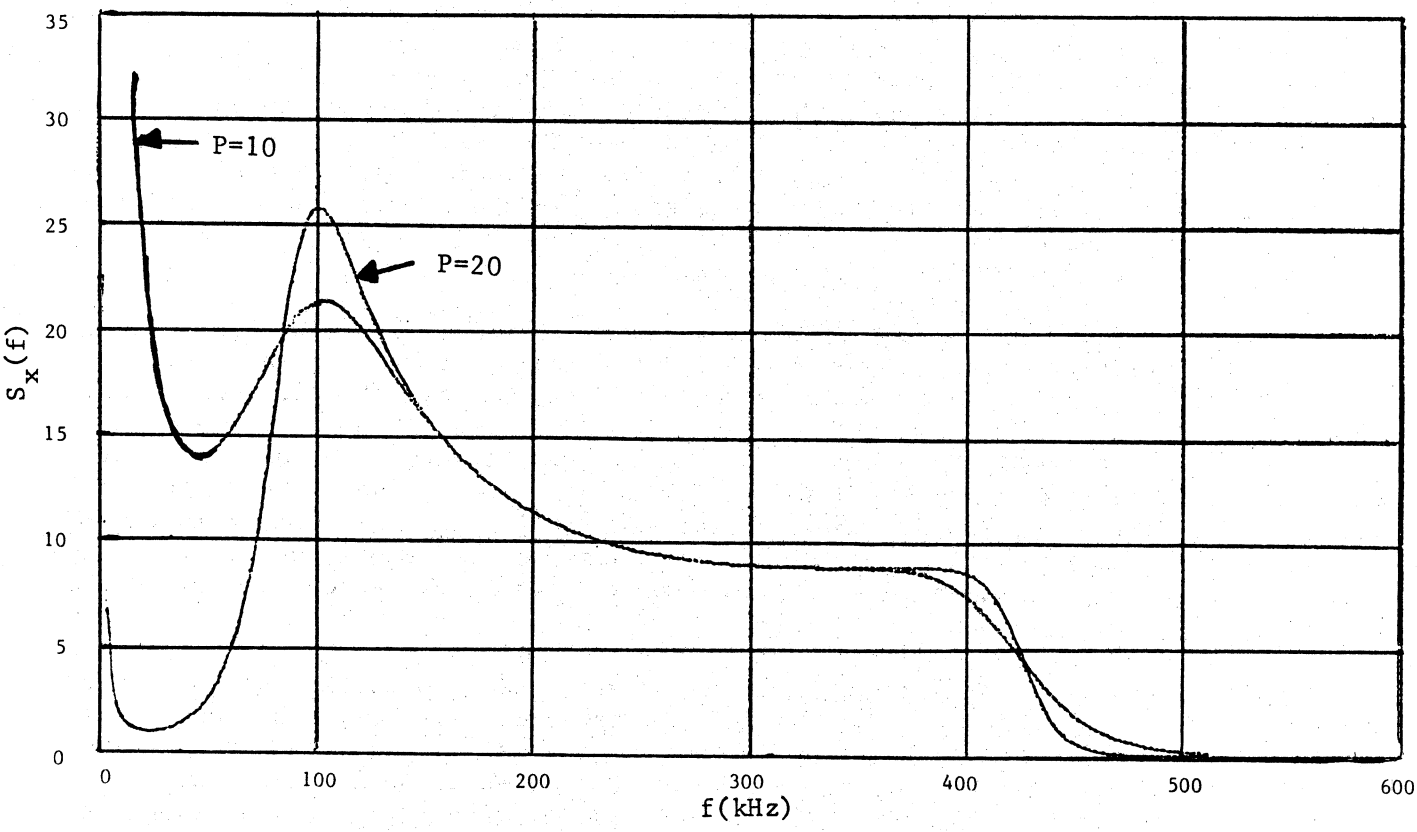

Figure 16(b). Equivalent Phase Modulating Spectrum with P = 10 and P = 20 Butterworth Inputs (Q = M = 1.5, N = 1024)

FDM/FM SPECTRAL SIMULATION RESULTS

The FM spectra obtained as outputs of the generalized simulation program are presented in this section. The input baseband spectrum consists of discrete samples from a noncentral Butterworth characteristic with P = 100. This input simulates an ideal rectangular baseband $S_b(f)$, while preserving its equivalent phase modulating spectrum $S_x(f)$ after preemphasis. The baseband cutoff frequencies are arbitrarily selected as $f_h = 426.66$ kHz and $f_l = 85.33$ kHz to illustrate the results. These values yield a representative Q = 1.5 and match the examples used in the last two sections.

The number of samples employed is established from the coverage condition $N(\Delta f) = 2\,(f_o + Mf_r) = 2(Q + M)f_r$, where $f_o = (1/2)\,(f_h + f_l)$ and $f_r = (1/2)\,(f_h - f_l)$. This condition can be rewritten as $N(\Delta f) = (M + 1)f_h - (M-1)f_l$, where the user selects the parameter $M > 1$ to provide enough bandwidth coverage. For $M \tilde{} 1$; the baseband input spectrum is just covered without any extra margin. The use of larger M values then provides for the additional coverage needed to account for the FM bandwidth expansion. For example, a coverage of $N(\Delta f) \tilde{} M(f_h - f_l)$ is provided for $M > > 1$, which represents a bandwidth expansion margin of about $M(f_h - f_l)/(2f_h)$.

The rms multichannel frequency deviation ΔF was varied from $42.\overline{66}$ to $2133.3\overline{3}$ kHz, so as to span an equivalent modulation index range of $m = (\Delta F/f_h) = 0.1$ to 5 radians. This index (m) is often referred to as the "rms modulation index", but should not be confused with the rms phase deviation (β) given by the root integral of (11). The critical implications of this distinction are discussed in the next section. A bandwidth expansion margin of about 0.4M occurs with M large, and the values of Q = 1.5, M = 46.5, N = 8192 and Δf = 2 kHz were used in the results next presented.

The FM output spectra obtained are shown in Figures 17(a) to 17(h), except for the discrete carrier component at f = 0 which is identified in the legend. The carrier magnitude was obtained from the limiting value of the correlation function $r_y(t)$ of the modulated signal, as specified from the sample value $r_y(n/2)$ in the discrete representation. The gaussian spectral approximation with standard deviation $\sigma = \Delta F$ is also included for each case. The spectral characteristic and cutoff frequencies of Figure 16(a) can be observed in the FM output spectra for the low index cases. The gaussian representation can be noted to be valid for the moderate or high index values as expected, with the transition occurring around m = 1 radian.

The generalized FM spectrum program was also used to obtain the normalized power spectra of various FDM/FM satellite telephony systems. The results are shown in Figures 18(a) to 18(l), along with the gaussian representation obtained with $\sigma = \Delta F$ for each case. The systems can be noted to span a wide variety of baseband modulation parameters (f_l, f_h, ΔF) corresponding to a range of $0.1 < m < 5$, with the gaussian spectral transition being evident as the index increases.

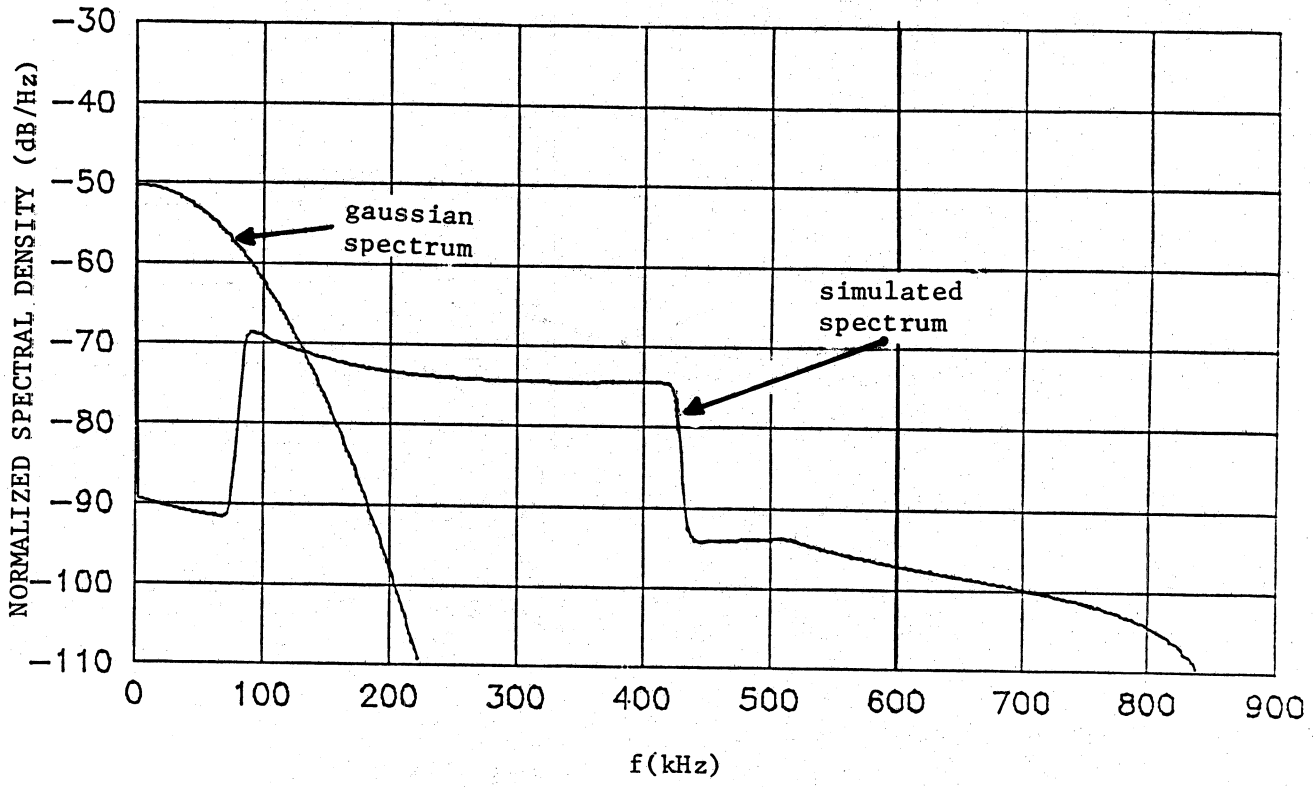

Figure 17(a). FDM/FM Spectrum for m = 0.10
(residual carrier = -0.157 dB)

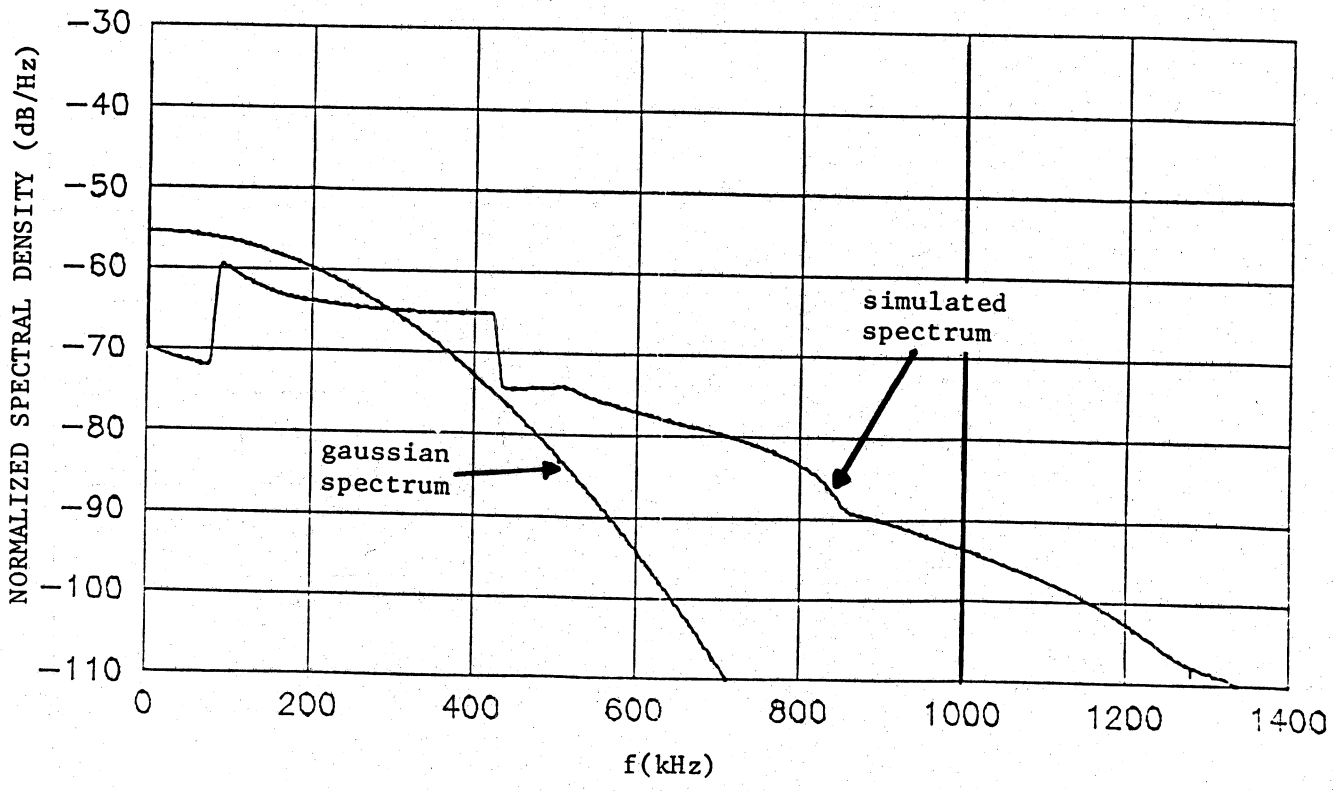

Figure 17(b). FDM/FM Spectrum for m = $0.3\overline{3}$
(residual carrier = -1.749 dB)

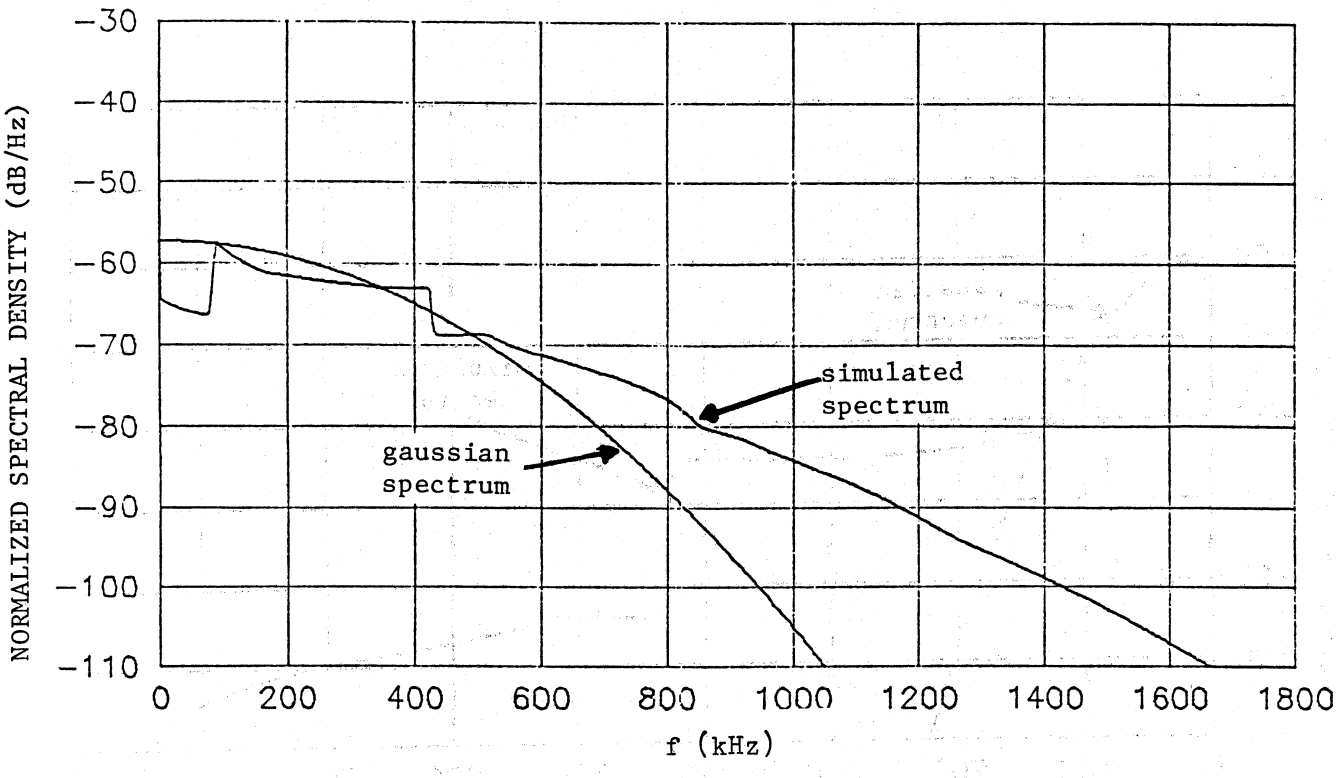

Figure 17(c). FDM/FM Spectrum for m = 0.5 (residual carrier = -3.935 dB).

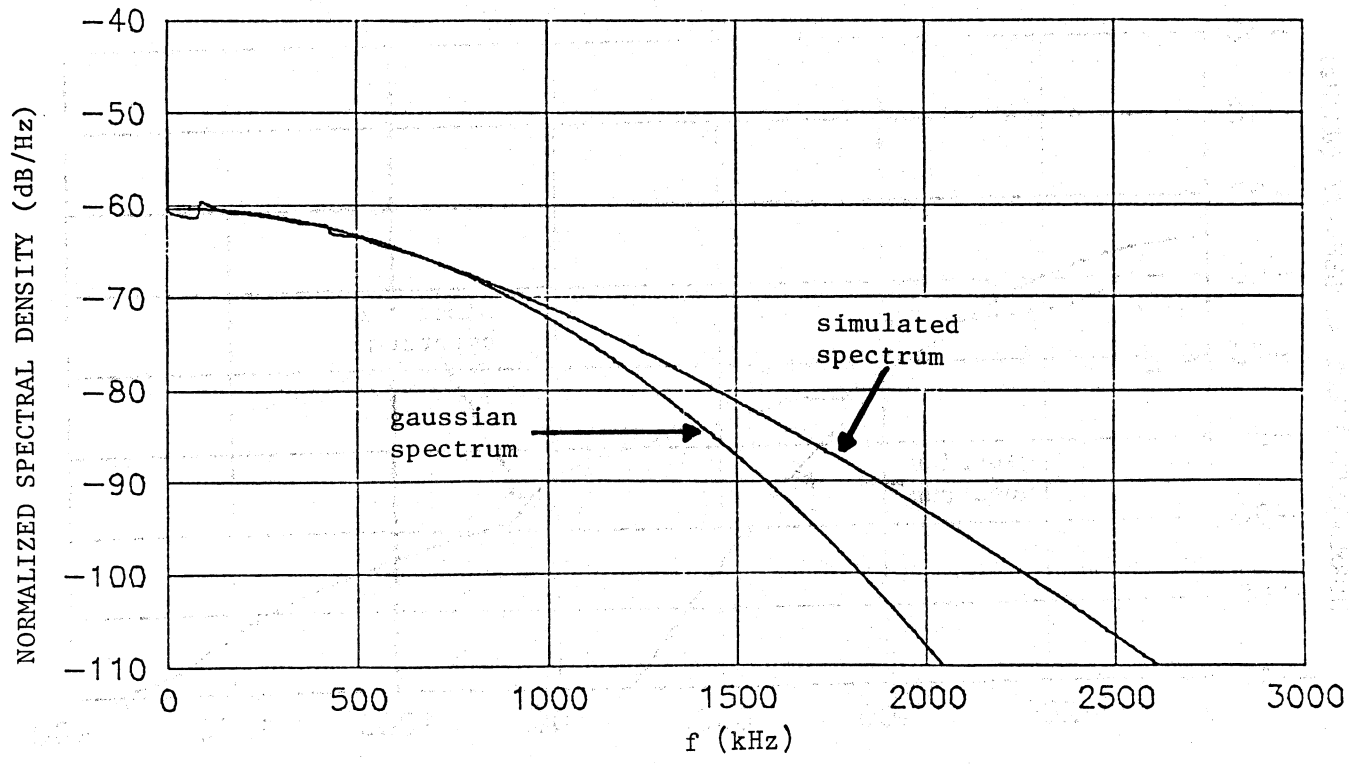

Figure 17(d). FDM/FM Spectrum for m = 1.0 (residual carrier = -15.741 dB).

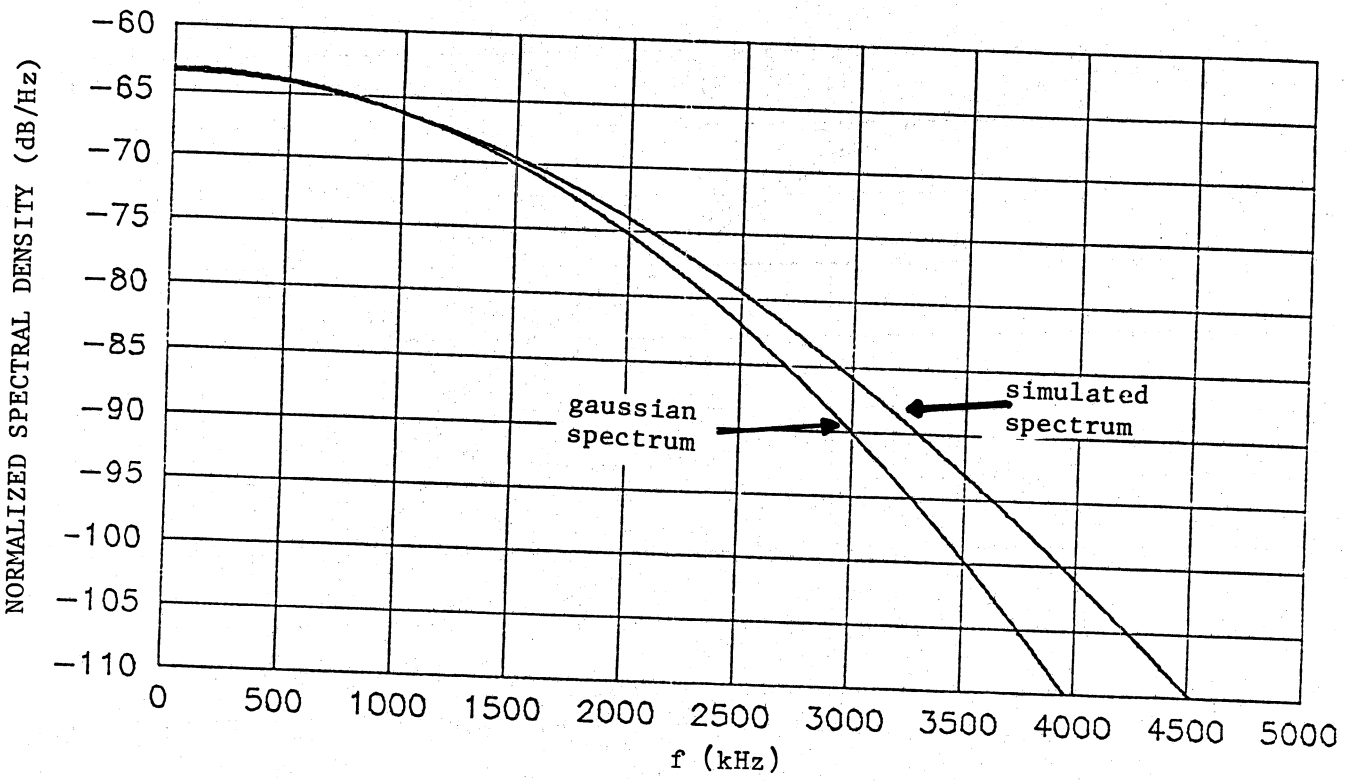

Figure 17(e). FDM/FM Spectrum for m = 2.0 (residual carrier = -62.964 dB).

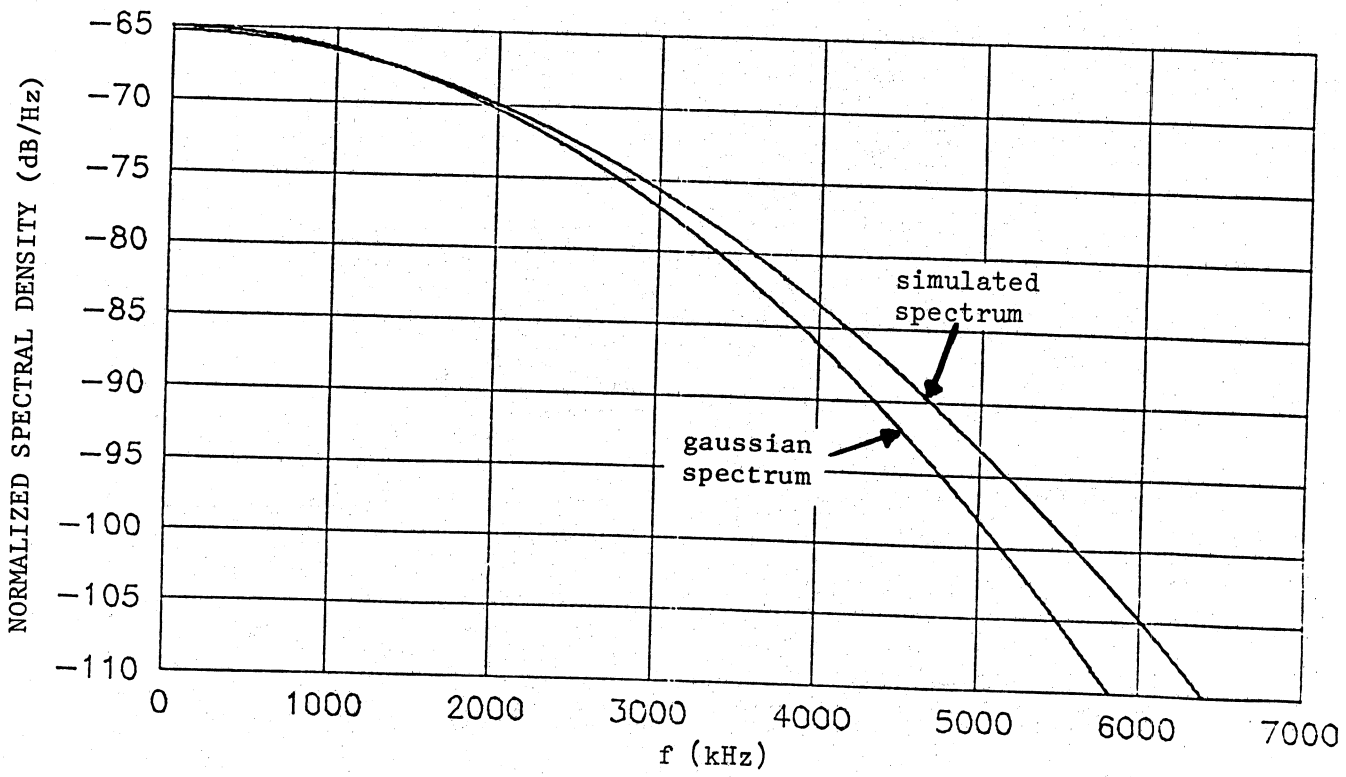

Figure 17(f). FDM/FM Spectrum for m = 3.0 (residual carrier = -141.669 dB).

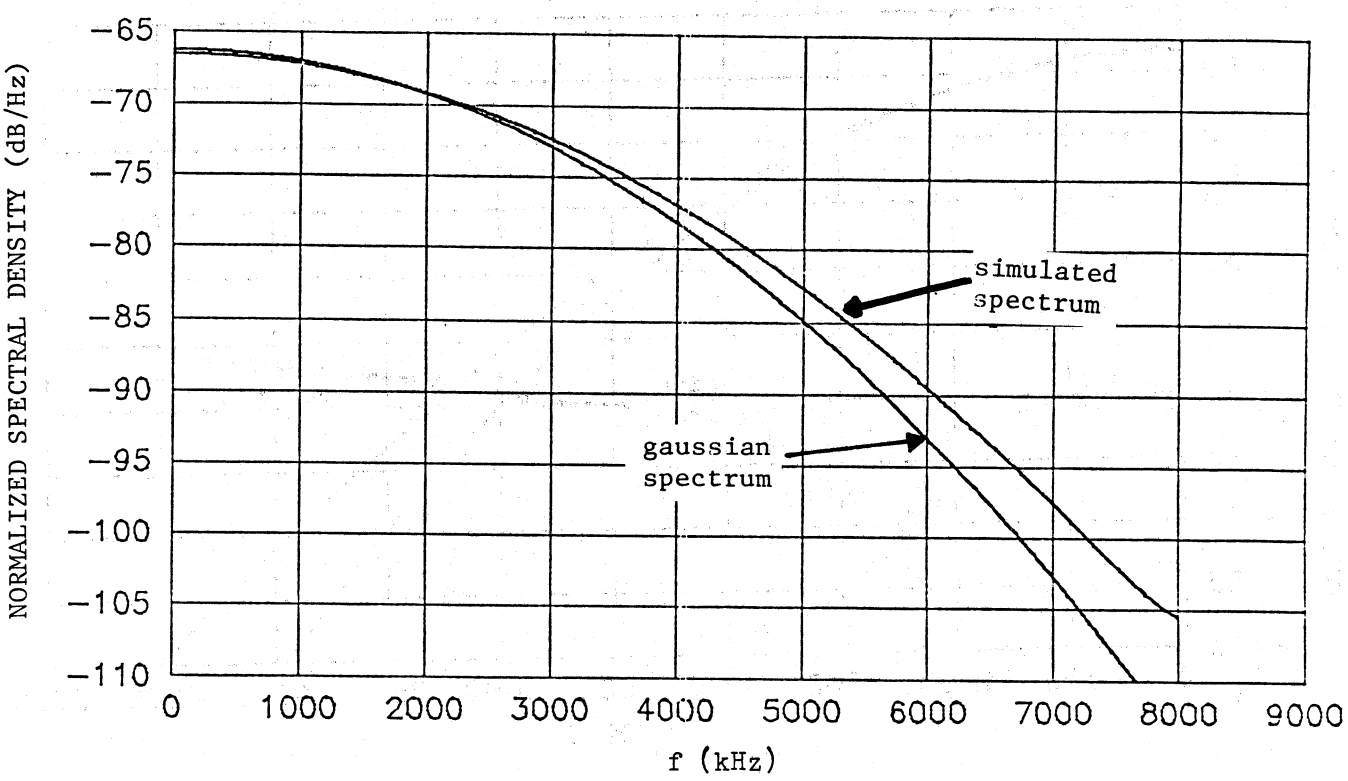

Figure 17(g). FDM/FM Spectrum for m = 4.0
(residual carrier = -251.857 dB).

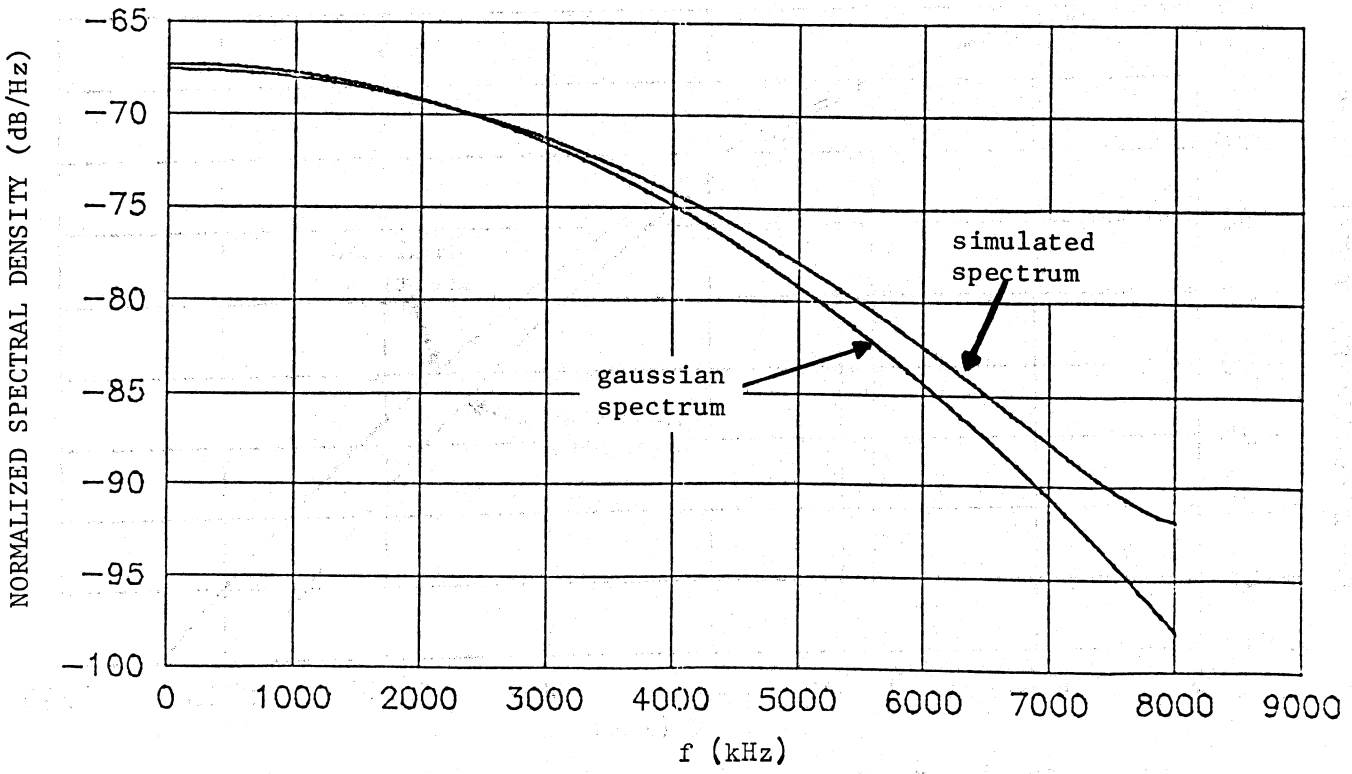

Figure 17(h). FDM/FM Spectrum for m = 5.0
(residual carrier < -390 dB).

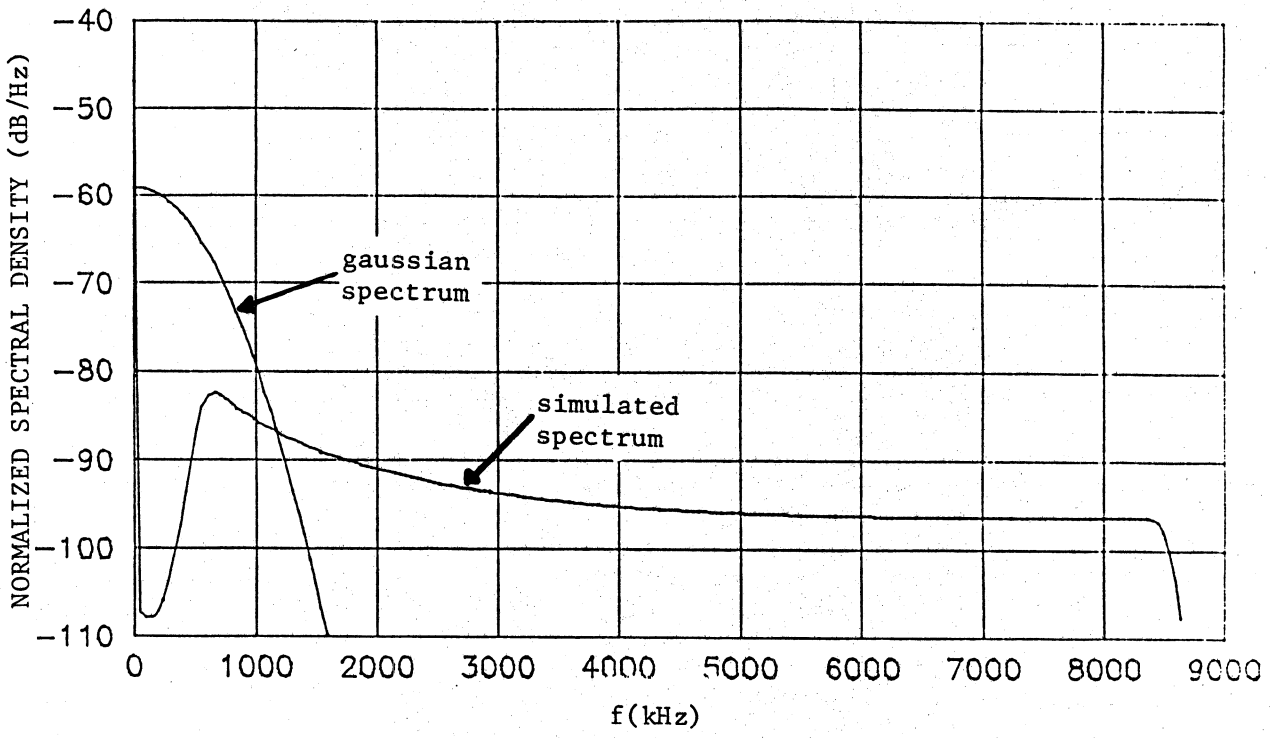

Figure 18(a). FM Spectrum of 1800-Channel Bell TD2 System (f_l=564 kHz, f_h=8524 kHz, ΔF=328.5 kHz, m=0.0385, residual carrier = -0.050 dB)

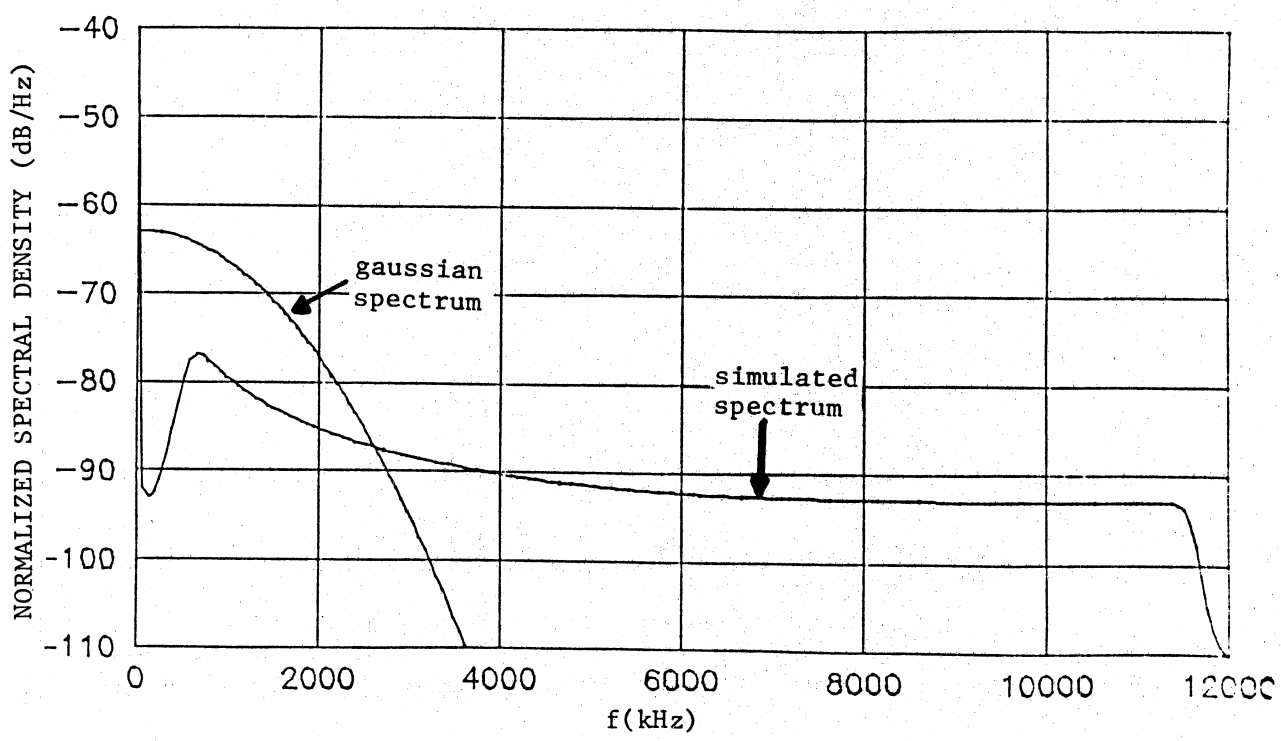

Figure 18(b). FM Spectrum of 2400-Channel Bell TH System (f_l=564 kHz, f_h=11596 kHz, ΔF=779.0 kHz, m=0.0672, residual carrier = -0.199 dB)

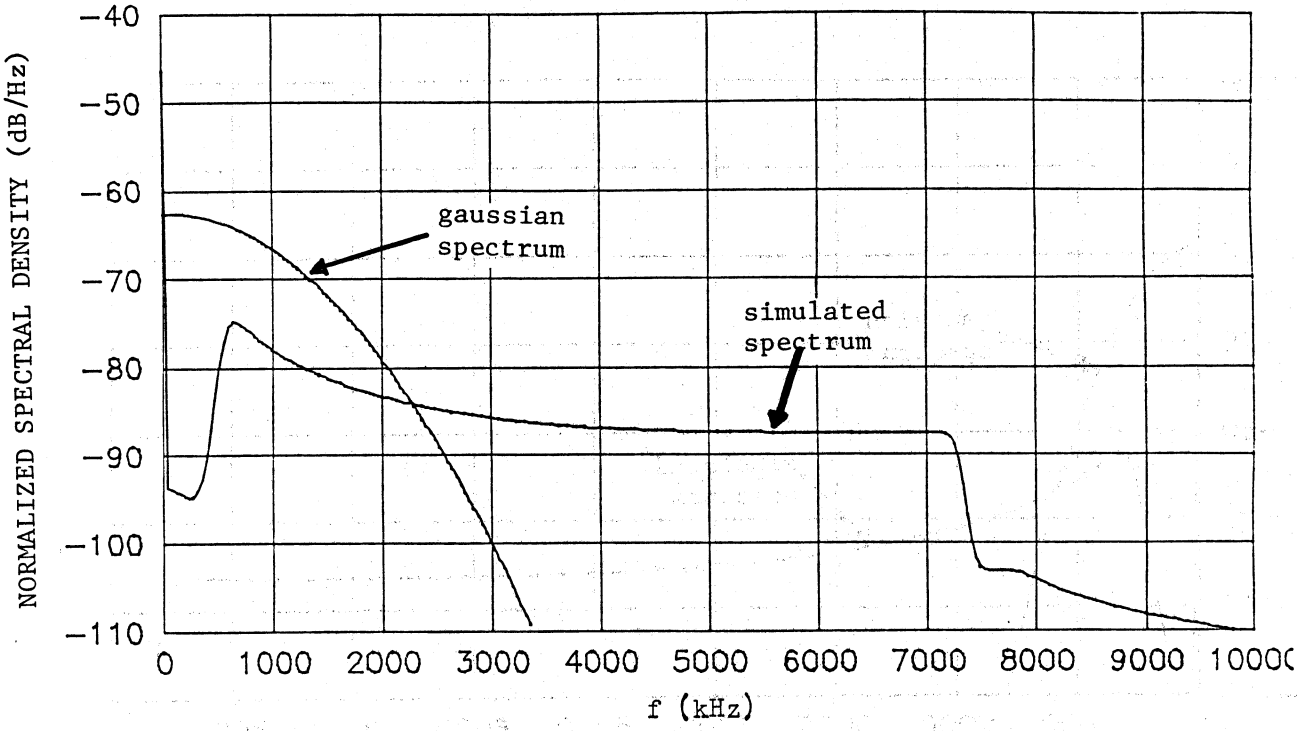

Figure 18(c). FM Spectrum of 1500-Channel Bell TD2 System (f_l=564 kHz, f_h=7284 kHz, ΔF=722.5 kHz, m=0.092, residual carrier = -0.291 dB)

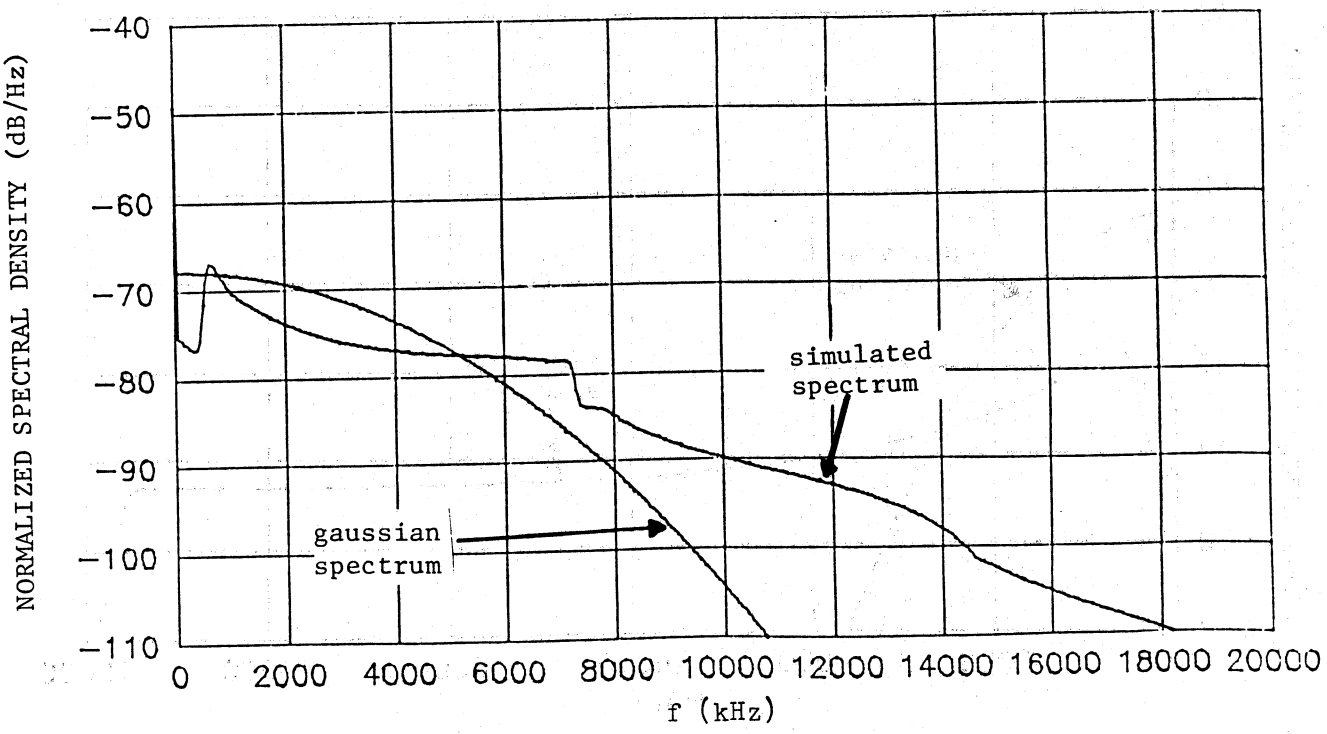

Figure 18(d). FM Spectrum of 1500-Channel AT&T System (f_l=564 kHz, f_h=7284 kHz, ΔF=2441.0 kHz, m=0.335, residual carrier = -3.320 dB)
(Note: carrier energy dispersal omitted)

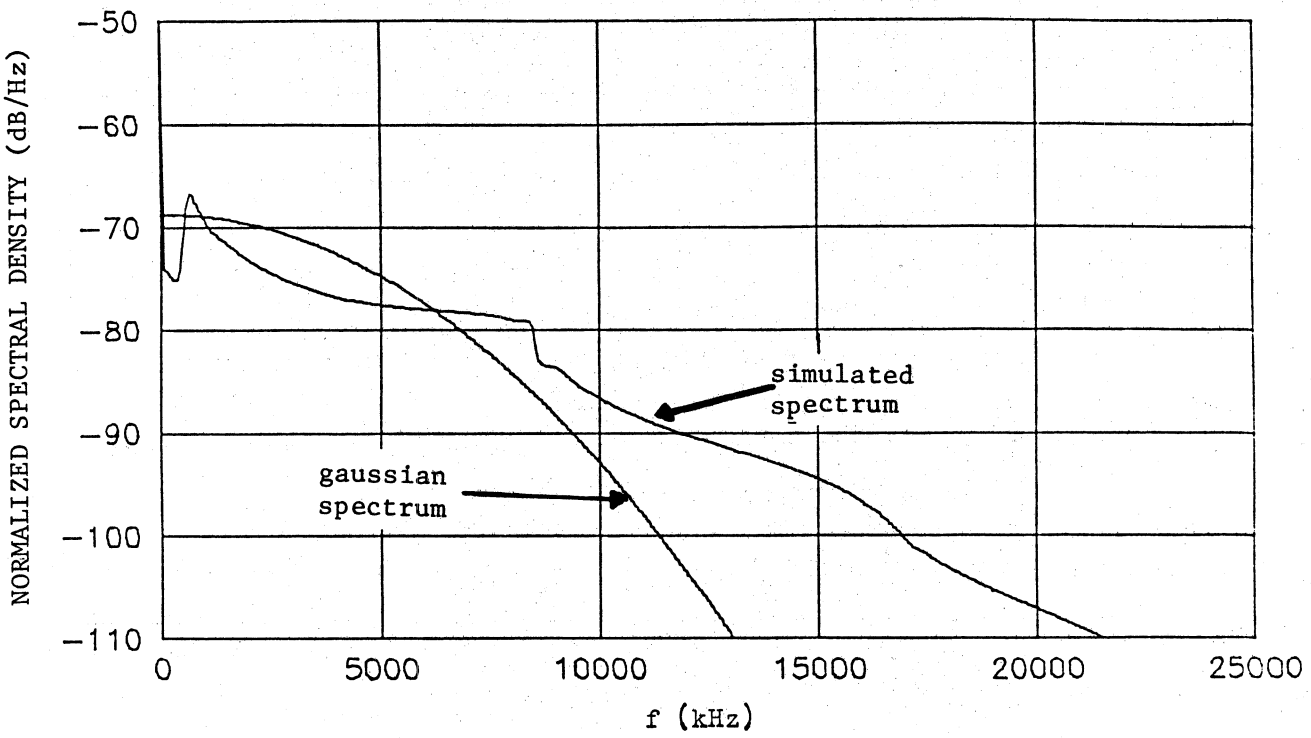

Figure 18(e). FM Spectrum of 1800-Channel AT&T System (f_l=564 kHz, f_h=8524 kHz, ΔF=2995.0 kHz, m=0.351, residual carrier = -4.145 dB) (Note: carrier energy dispersal omitted)

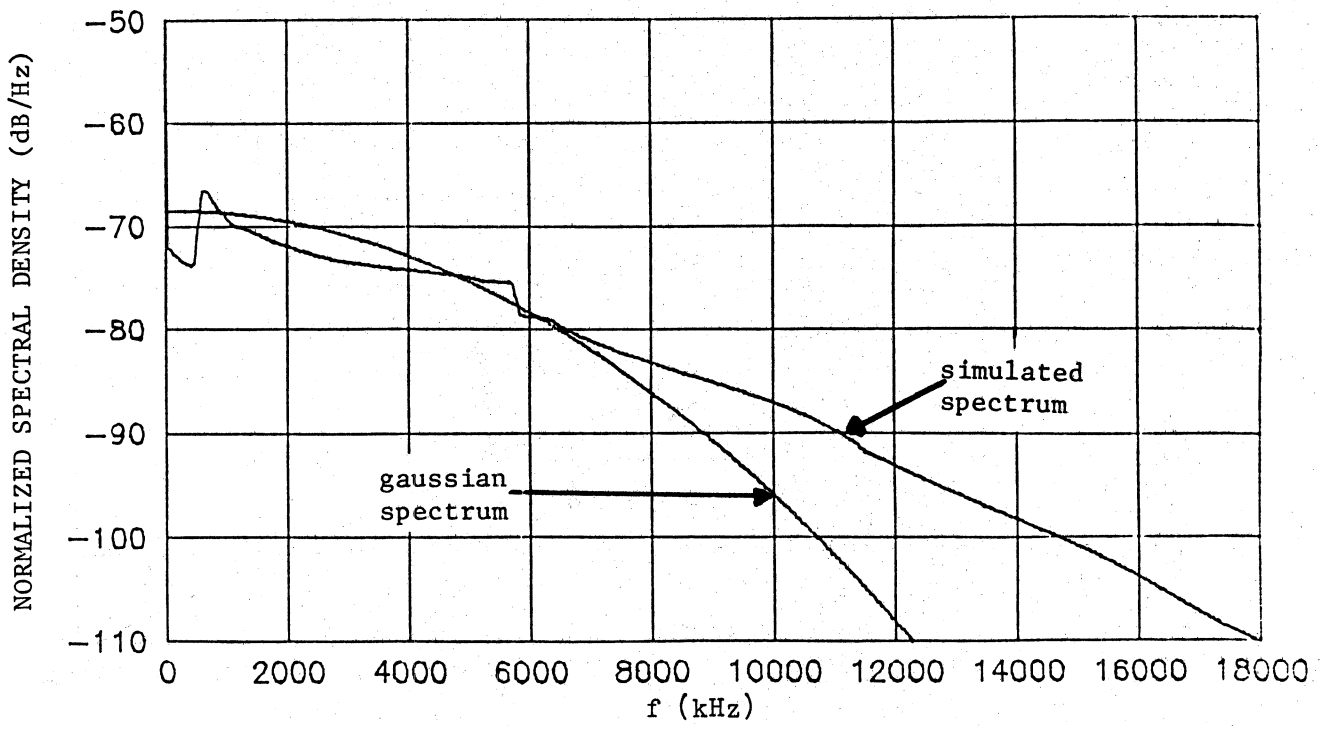

Figure 18(f). FM Spectrum of 1200-Channel AT&T System (f_l=564 kHz, f_h=5772 kHz, ΔF=2807.0 kHz, m=0.486, residual carrier = -5.858 dB) (Note: carrier energy dispersal omitted)

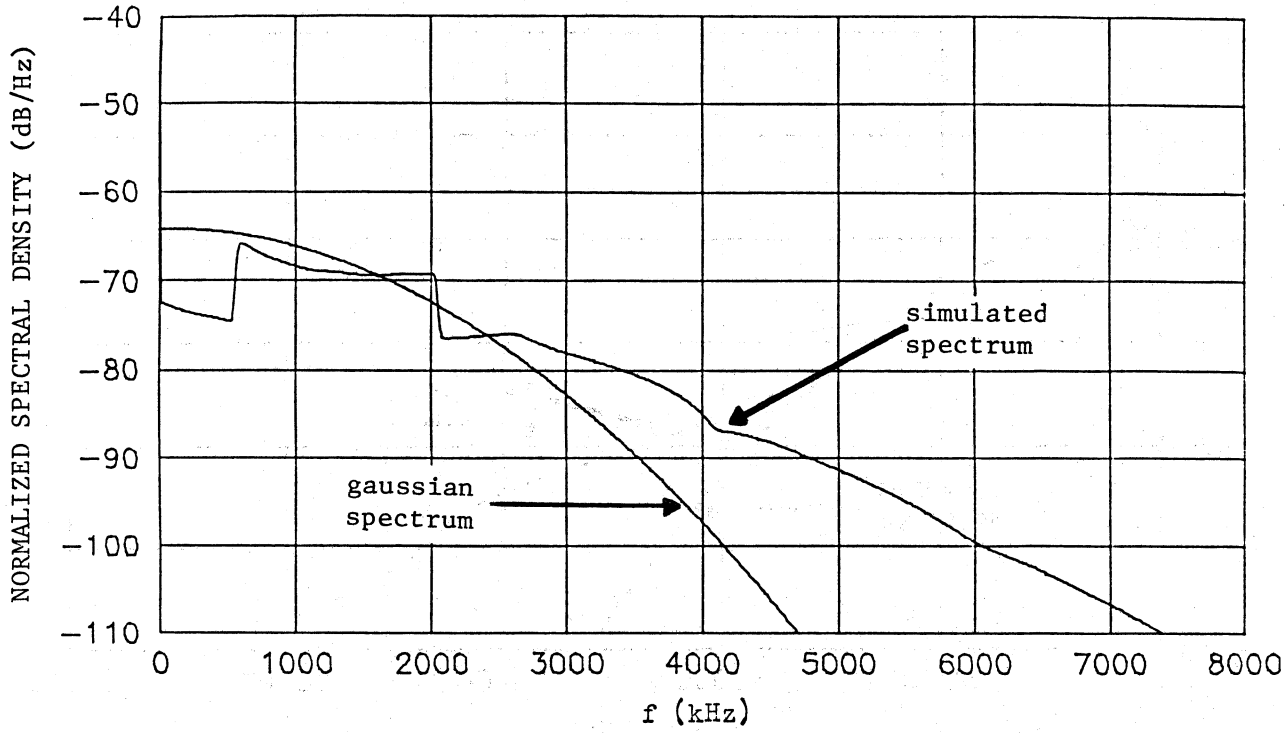

Figure 18(g). FM Spectrum of 360-Channel AT&T System (f_l=564 kHz, f_h=2044 kHz, ΔF=1022.0 kHz, m=0.500, residual carrier = -3.379 dB) (Note: carrier energy dispersal omitted)

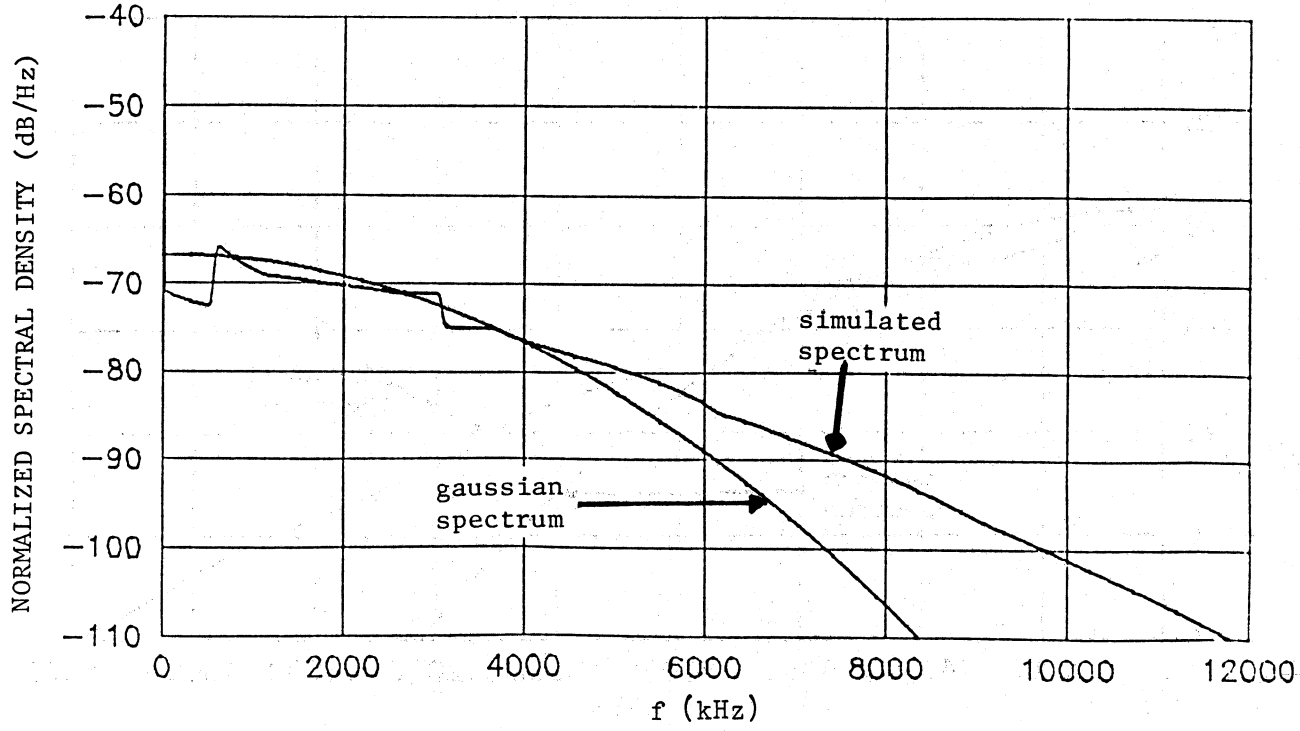

Figure 18(h). FM Spectrum of 600-Channel AT&T System (f_l=564 kHz, f_h=3084 kHz, ΔF=1871.0 kHz, m=0.607, residual carrier = -6.081 dB) (Note: carrier energy dispersal omitted)

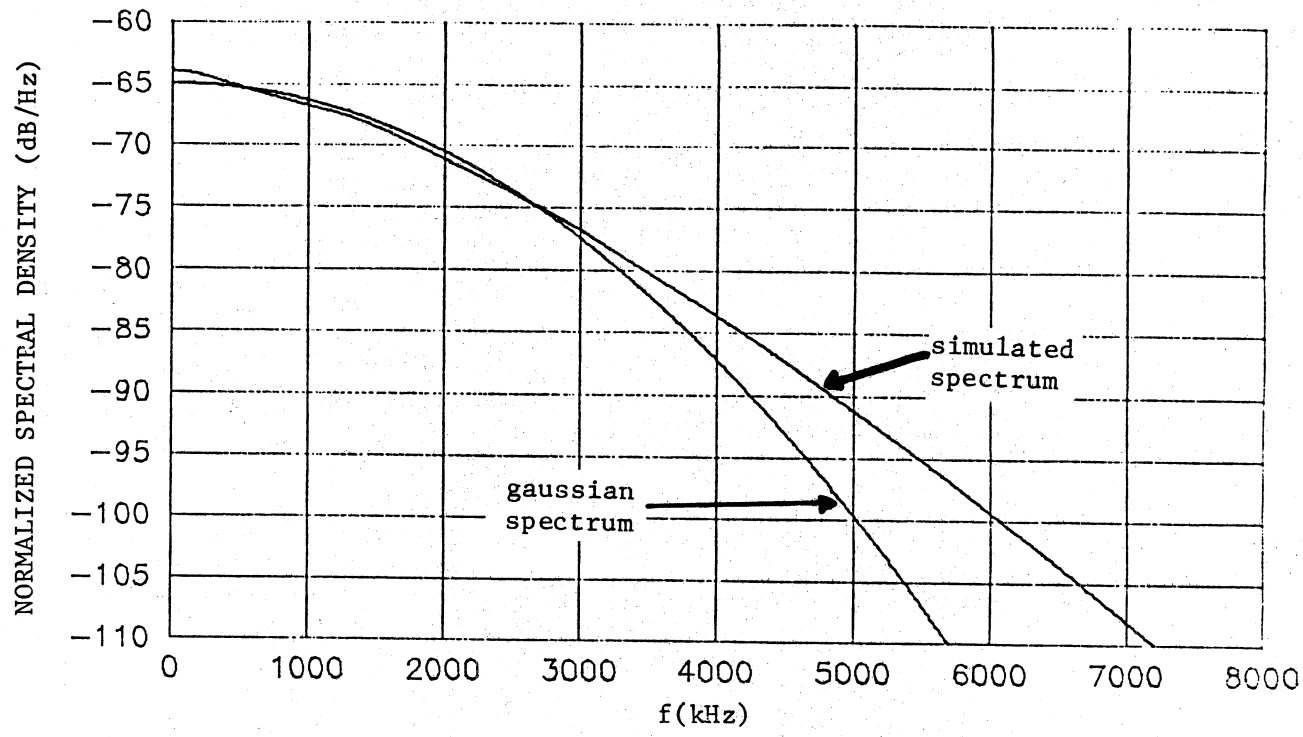

Figure 18(i). FM Spectrum of 360-Channel Western Union System (f_l=60 kHz, f_h=1550 kHz, ΔF=1250.0 kHz, m=0.806, residual carrier = -36.108 dB)

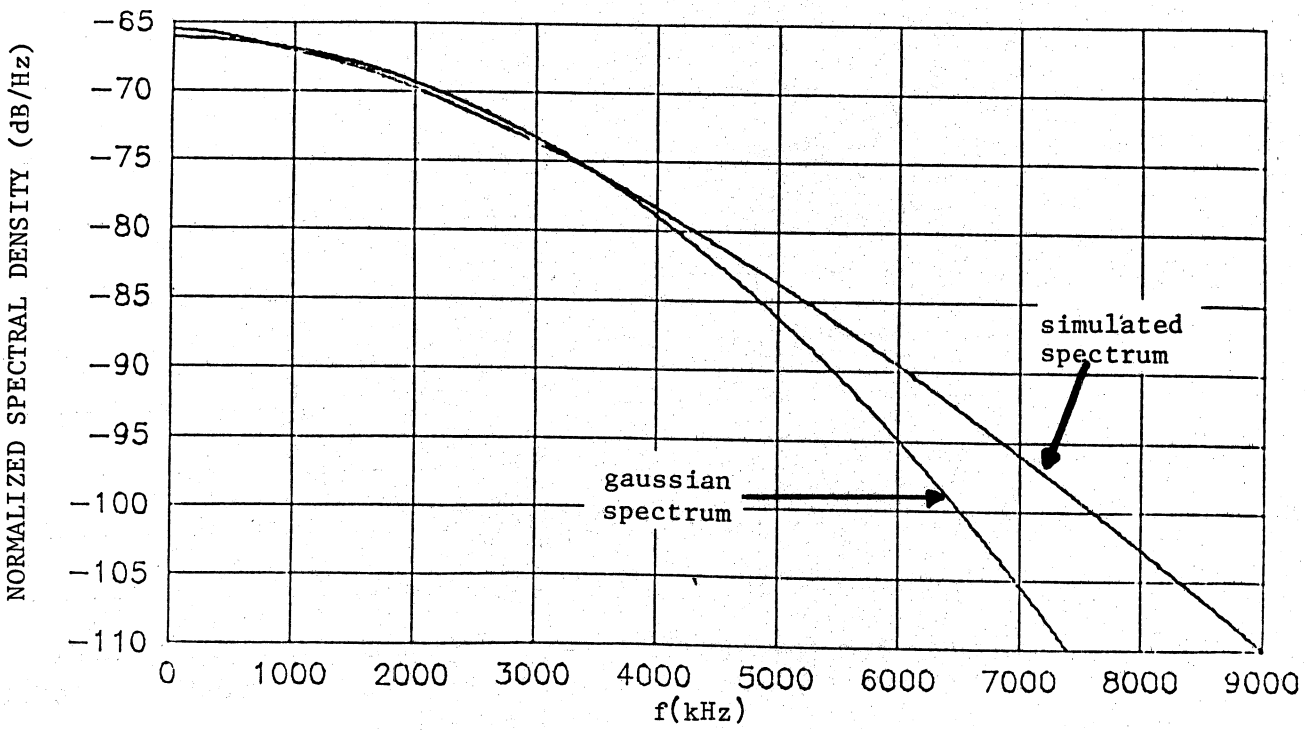

Figure 18(j). FM Spectrum of 420-Channel Western Union System (f_l=60 kHz, f_h=1796 kHz, ΔF=1645.6 kHz, m=0.916, residual carrier = -55.200 dB)

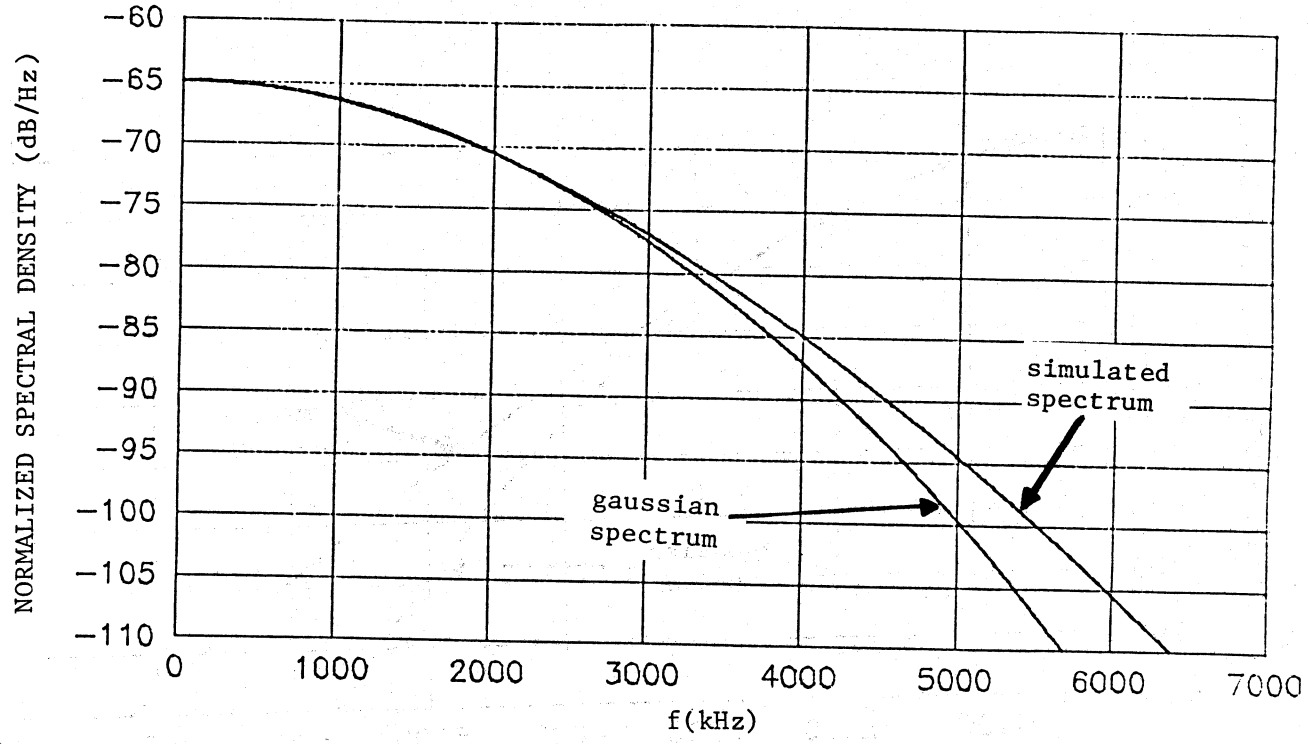

Figure 18(k). FM Spectrum of 180-Channel Western Union System (f_l=60 kHz, f_h=804 kHz, ΔF=1250.0 kHz, m=1.555, residual carrier = -73.562 dB)

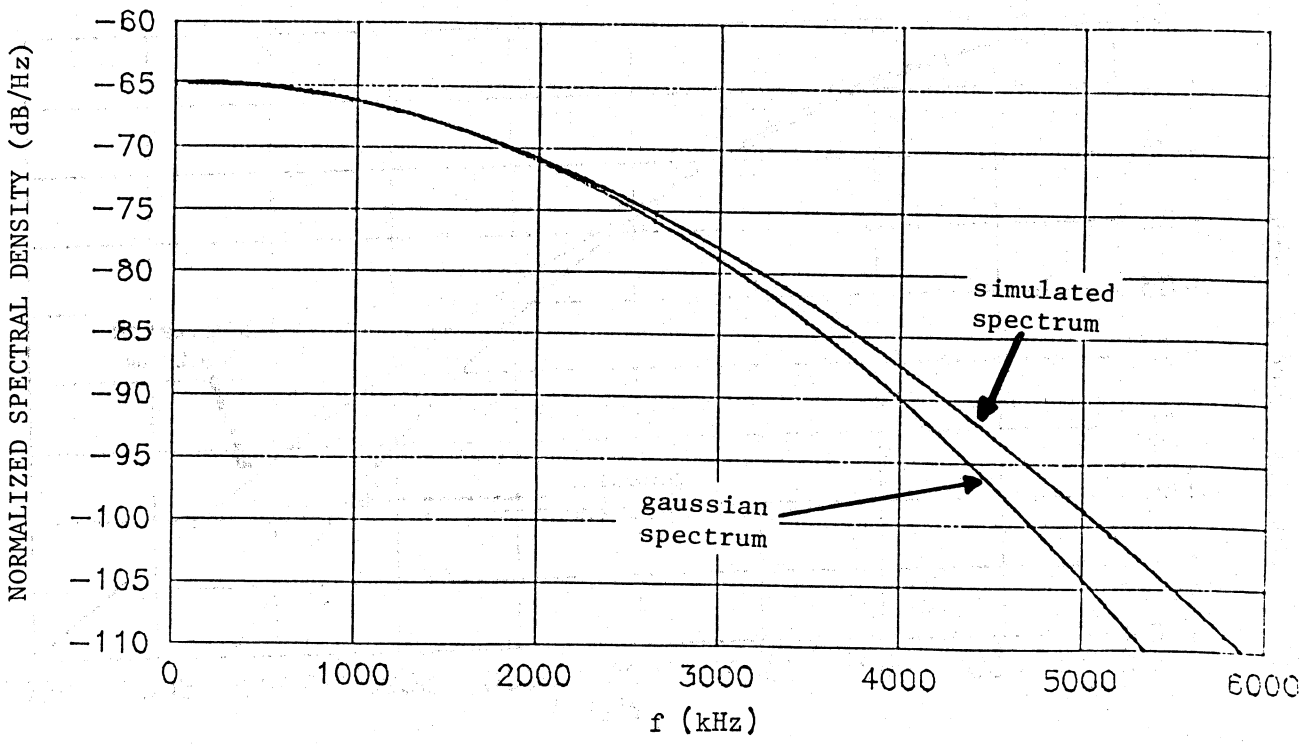

Figure 18(l). FM Spectrum of 120-Channel Western Union System (f_l=60 kHz, f_h=552 kHz, ΔF=1170.0 kHz, m=2.120, residual carrier = -103.099 dB)

The normalized power spectra of some of these FDM/FM systems have also been presented in a recent FCC document (Sharp, to be published). They were obtained via different simulation principles and procedures than those used here, and the results are included in Appendix B for comparison purposes. The cases presented have the following counterparts in this report:

COMSTAR 360 corresponds to Figure 18(g)
COMSTAR 600 corresponds to Figure 18(h)
COMSTAR 1200 corresponds to Figure 18(f)
TELSTAR 1800 corresponds to Figure 18(e)
WESTAR 120 corresponds to Figure 18(1)
WESTAR 180 corresponds to Figure18(k)

The first four cases all represent low-index modulations, and there is notable agreement with their counterparts in this report. The only distinction appears in the low-frequency peak being slightly higher in the FCC simulation, which is attributed to the higher peak in the preemphasized baseband spectrum when using an ideal rectangle instead of a Butterworth baseband as previously discussed. The last two cases represent higher-index modulations, and there is again general agreement between the two simulation results though the reference spectra are somewhat lower than their counterparts in this report. The discrepancies can be attributed to a higher spectrum arising from aliasing effects in the NTIA model, or to a lower spectrum arising from convolution series truncation in the FCC model. The distinction becomes academic, since the same gaussian spectral approximation holds well and is to be used in these higher-index cases.

SECTION 5

SUMMARY AND DISCUSSION OF RESULTS

The gaussian spectral approximation for high-index FM signals can be motivated in two ways, with a gaussian baseband modulation process of arbitrary spectrum being always assumed. One approach relies on Woodward's theorem, and identifies the limiting spectrum to the statistical distribution of the frequency modulating signal thus inducing the gaussian representation. The other approach uses Middleton's expansion to develop a weighted superposition of spectral convolution terms, which is manipulated into a gaussian approximation under high modulation index conditions.

The standard deviation (σ) of the gaussian spectral approximation represents the rms bandwidth of the modulated signal, and must be specified in terms of the modulation parameters for the spectral representation. The first approach (Woodward's theorem) yields $\sigma = \Delta F$ in terms of the rms frequency deviation (ΔF), while the second approach (Middleton's expansion) yields $\sigma = \beta . B_x$ in terms of the rms phase deviation (β) and the rms bandwidth (B_x) of the equivalent phase modulating signal. These two formulas are not always easily interchangeable, with the selection between them governed by the capability to quantitatively identify the parameters involved in each case.

The inclusion of a preemphasis network becomes a critical consideration, since it can be designed to preserve the rms phase (β) or frequency (ΔF) deviation but not both in general (and perhaps neither in a given application). For example, an ideal preemphasis characteristic (parabolic power transfer) makes the preemphasized FM baseband behave like a PM baseband so that $\sigma = \beta \cdot B_x$ becomes the natural approach. Conversely, the CCIR preemphasis for FDM/FM telephony preserves the rms frequency deviation and motivates using $\sigma = \Delta F$ to specify the gaussian spectrum parameter (Panter, 1972).

The rectangle convolution program was developed to analyze the gaussian spectral representation based on Middleton's expansion. The case of a rectangular baseband spectrum (down to zero frequency) and ideal preemphasis yields compact iterative expressions for the spectral convolution terms, thus bypassing the need to actually simulate the multiple convolution operations. These expressions were logically programmed along with the weighting coefficient distribution to generate the FM spectra as a function of the rms phase deviation (β). The number of spectral convolutions accounted is user selectable to provide any desired power preservation percentage. The results concluded that the gaussian spectral representation with $\sigma = \beta \cdot B_x$ becomes effective beyond $\beta \approx 1.5$ radians for the baseband modulation under consideration.

The generalized FM spectrum program was developed to analyze the gaussian spectral approximation based on Woodward's theorem. A rectangular baseband spectrum with low (f_l) and high (f_h) cutoffs was simulated via a noncentral Butterworth family that provides user selection of the location frequencies and cutoff rates, plus a spectral coverage parameter that accommodates the FM bandwidth expansion and controls the discrete representation aliasing. The

program again bypasses the multiple convolutions simulation by exploiting correlation function dependences and including discrete spectral transforms as needed. The gaussian representation with $\sigma = \Delta F$ was found to be become effective beyond $m = \Delta F/f_h \approx 0.7$ in both controlled parameter tests and existing systems simulations.

The normalized carrier component is always given by $-\beta^2(10 \log e)$ dB in terms of the rms phase deviation (β), so that the latter must be specified for a compact formulation (except for the β values where the carrier component becomes negligible). The rectangular baseband spectrum with low and high cutoffs yields $\beta = m/\sqrt{\varepsilon}$ without preemphasis, where $\varepsilon = f_1/f_h < 1$ so that $\beta > m$ always. The CCIR preemphasis case does not yield an exact compact result, but an effective functional approximation to the preemphasis characteristic has been used to develop the approximate relation (CCIR, 1978):

$$\beta \approx \frac{0.63m}{\sqrt{\varepsilon(1-\varepsilon)}} \left[1+2.89\varepsilon-3.17\varepsilon^2-0.72\varepsilon^4\right]^{1/2} \qquad (21)$$

A comparison between the normalized carrier component derived from this last expression and those obtained via the generalized FM simulation program is presented in TABLE 2. There is close agreement between the two results in all cases, including the 18(g) case where a large (m) relative to 18(e) or 18(f) is not accompanied by a larger (β) and the carrier magnitudes increase accordingly in both results. The functional approximation to the preemphasis characteristic was also compared to the actual characteristic (18) and found to overlap even under extreme (f_1, f_h) conditions representative of existing system specifications.

The ratio β/m obtained from (21) represents the conversion factor needed to determine the rms phase deviation (β) from the index $m = \Delta F/f_h$. This conversion factor is shown in Figure 19 as a function of $\varepsilon = f_1/f_h$. The parameter ε spans the range of $0.001 < \varepsilon < 0.275$ in existing system specifications, which corresponds to a range of $20 > \beta/m > 1.75$ for the conversion factor. The latter remains around $\beta/m \approx 2$ for $\varepsilon > 0.1$, but increases significantly for $\varepsilon < 0.05$ as shown in the figure.

The conversion factor β/m can be used to directly formulate the residual carrier component via $-\beta^2(10 \log e)$ dB, instead of deriving it from the correlation function measurement. The formula approach is preferable since the extreme baseband cases ($\varepsilon \ll 1$) can introduce a simulation compromise between incremental resolution (Δf small) and aliasing control ($N \cdot \Delta f$ large) that can affect the carrier measurement accuracy. The generalized spectrum program has now been modified to compute the carrier magnitude directly from the rms phase deviation (β), after such parameter is computed via (21) from the input baseband cutoffs (f_1, f_h) and the rms frequency deviation (ΔF).

The following procedure has now been implemented to generate the FM spectrum for given modulation parameters (f_1, f_h, ΔF). The values of $m = F/f_h$ and $\varepsilon = f_1/f_h$ are first computed to obtain the rms phase deviation (β) from the

TABLE 2

RESIDUAL CARRIER MAGNITUDES IN FM SPECTRA

Figure	m(rad)	β(rad)	Residual Carrier (dB) Formulation	Residual Carrier (dB) Simulation
17(a)	0.1	0.19	-0.16	-0.16
17(b)	0.33	0.63	-1.73	-1.75
17(c)	0.5	0.95	-3.90	-3.94
17(d)	1.0	1.90	-15.60	-15.74
17(e)	2.0	3.79	-62.39	-62.96
17(f)	3.0	5.69	-140.38	-141.67
17(g)	4.0	7.58	-249.57	-251.86
17(h)	5.0	9.48	-389.95	-390.00
18(a)	0.0385	0.106	-0.05	-0.05
18(b)	0.0672	0.209	-0.19	-0.20
18(c)	0.0992	0.256	-0.29	-0.29
18(d)	0.335	0.866	-3.26	-3.32
18(e)	0.351	0.966	-4.05	-4.15
18(f)	0.486	1.154	-5.78	-5.86
18(g)	0.500	0.877	-3.34	-3.38
18(h)	0.607	1.178	-6.03	-6.08
18(i)	0.806	2.769	-33.30	-36.11
18(j)	0.916	3.356	-48.91	-55.20
18(k)	1.555	4.076	-72.17	-73.56
18(l)	2.120	4.844	-101.89	-103.10

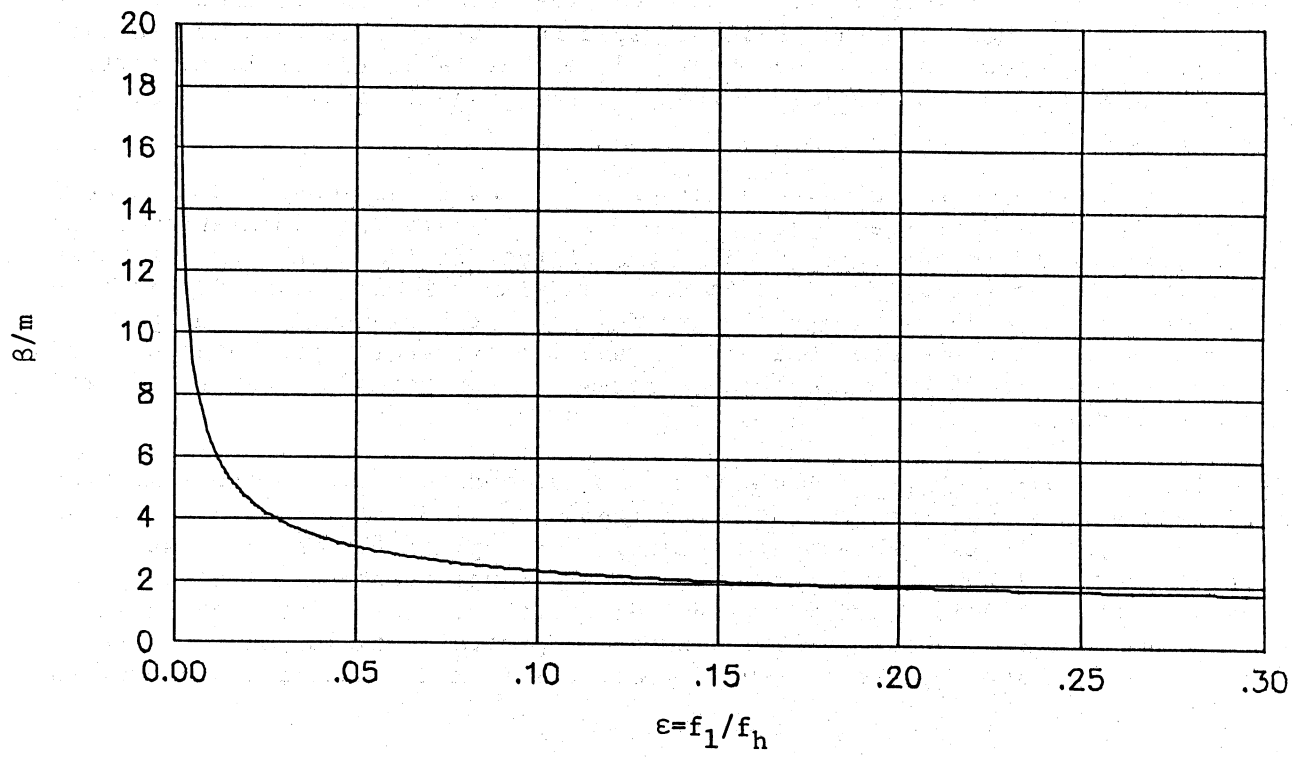

ε	β/m	ε	β/m
0.001	19.961	0.10	2.355
0.005	8.996	0.15	2.355
0.010	6.422	0.20	1.897
0.050	3.082	0.25	1.795

Figure 19. Conversion Factor (β/m) as a Function of Baseband Parameter (ε)

expression (21). If $\beta > 1.5$ (or any other bound selected), the gaussian spectral approximation with $\sigma = \Delta F$ is used to generate the continuous portion of the spectrum. If $\beta < 1.5$, then the generalized spectrum program is used to generate the continuous portion of the spectrum. In either case, the residual carrier component is generated as $-\beta^2(10 \log e)$ from the rms phase deviation (β) already computed.

The generalized spectrum simulation program is now operational and automated to deliver the FDM/FM system spectra from a set of equivalent modulation input parameters selected by the user. The program first decides on the gaussian spectral approximation validity, computes the gaussian standard deviation if such approximation is indeed valid, and generates the appropriate gaussian spectrum samples. Otherwise, the program negates the gaussian spectral representation and proceeds to deliver the proper spectral samples as generated by the generalized FM simulation process.

The FDM/FM simulation program has also been matched to drive another existing interference analysis program for FDM/FM telephony. The interference program computes the output NPR per telephony channel for a given FDM/FM input spectrum as the desired signal and a given arbitrary interference spectrum selected by the user. The FDM/FM simulation program reported here provides for the desired signal spectrum, and a set of interference spectral simulations are being developed to supplement those already available from the interference program menu.

REFERENCES

Abramson, N. (1963), "Bandwidth and Spectra of Phase and Frequency Modulated Waves," IEEE Transactions on Communication Systems, pp 407-414, December.

Algazi, V.R. (1968), "Bounds on the Spectra of Angle-Modulated Waves," IEEE Transactions on Communication Technology, Vol. COM-16, No. 4, pp. 561-566, August.

Blackman, N.M. and G.A. McAlpine (1969), "The Spectrum of a High-Index FM Waveform: Woodward's Theorem Revisited," IEEE Transactions on Communication Technology, Vol. COM-17, No. 2, pp. 201-207, April.

Cramer, H. (1945), "Mathematical Methods of Statistics," Princeton University Press, pp. 244-246.

CCIR (1978), Recommendations and Reports of the CCIR, Vol. IX, Report 792, Annex I, pp367-369.

Das, A. and G. Sharp (1975), "Convolution Method of Interference Calculation," Federal Communications Commission, Office of Chief Engineer, Research and Standards Division, Washington, D.C., Report No. RS 75-04, April.

De Rosa, J.K. (1976), "The Spectral Density of a Sinusoid Phase Modulated by a Gaussian-Filtered Gaussian Process," IEEE Transactions on Communications, pp. 935-938, August.

Feller, W. (1968), "An Introduction to Probability Theory and its Applications," Vol. 1, 3rd Edition, John Wiley & Sons, Inc., pp. 50-66.

Ferris, C. (1968), "Spectral Characteristics of FDM/FM Signals," IEEE Transactions on Communication Technology, Vol. COM-16, No. 2, April, pp. 233-238.

Jeruchim, M.C. and D.A. Kane (1970), "Orbit/Spectrum Utilization Study," Vol. IV, General Electric, Space Systems Organization, Valley Forge Space Center, Philadelphia, Pa., Document No. 70SD4293, December.

Panter, P.F. (1972), "Communication Systems Design," McGraw-Hill Book Company, pp. 234-236 and 262-266.

Pontano, B.A., J.C. Fuenzalida and N.M. Chitre (1973), "Interference into Angle-Modulated Systems Carrying Multichannel Telephony Signals," IEEE Transactions on Communications, Vol. COM-21, No. 6, pp. 714-727, June.

Sharp, G.L. (to be published), "Reduced Domestic Satellite Orbital Spacings at 4/6 GHz," Federal Communications Commission, Office of Science and Technology, Document No. FCC OST R83-2.

APPENDIX A

FM BANDWIDTH AND POWER DISTORTION

The identification of a finite bandwidth measure for the FM signal spectra implies a spectral tail truncation and a power preservation compromise. The effectiveness of a bandwidth measure to accommodate the FM signal spectrum is also critical from an analytical simulation standpoint. The number of point samples involved in discrete representations is necessarily finite, so that it induces aliasing and distortion effects that limit the spectral analysis accuracy.

The approach usually employed for analog FM bandwidth assignment has been Carson's Rule. The FM bandwidth is given by $B = 2(\Delta F_p + f_m) = 2(\alpha+1)f_m$, where ΔF is the peak frequency deviation, α is the peak modulation index and f_m is the peak modulating frequency. This rule represents an additive combination of the bandwidth expressions for extreme high ($B \approx 2\Delta F_p = 2\alpha f_m$) and low ($B \approx 2f_m$) index conditions. One of these two expressions prevails over the other for $\alpha >> 1$ or $\alpha << 1$, so that their linear superposition always yields the bandwidth measure for extreme index conditions.

The distortion implications of Carson's Rule as a function of the modulation index remains an open issue. There is no distortion measure or criterion that is generally accepted for evaluation purposes, with the difficulties arising from the variety of modulating signal characteristics and models that occur in practice. The discussion that follows concentrates on power preservation as a distortion measure for a deterministic (single sinewave) and random (uniform spectrum) baseband modulation cases.

One distortion criterion is based on the magnitude of the sidebands preserved or rejected when band-limiting the modulated signal spectrum. In the case of single sinusoidal modulation, the number $M_\upsilon(\alpha)$ of significant sideband pairs to be preserved can be established as a function of the index (α) for a given significance level (υ) from the condition $|J_M(\alpha)| \geq \upsilon$ where $J(\cdot)$ is the Bessel function of the first kind. The FM bandwidth measure is then given by $B_\upsilon(\alpha) = 2M_\upsilon(\alpha)f_m$, and varies with the level (υ) selected besides the index (α). This bandwidth allocation procedure has been compared to Carson's Rule to show that the latter represents an FM bandwidth assignment with a significance level in the $0.01 < \upsilon < 0.1$ range for all practical modulation indices when the modulation is a single sinusoid.

Another distortion criterion consists of the power percentage being preserved or rejected when band-limiting the modulated signal spectrum. For a single sinusoidal modulation, the power percentage preserved is given by

$$P_M(\alpha) = J_o^2(\alpha) + 2 \sum_{n=1}^{M} J_n^2(\alpha) \qquad \text{(A-1)}$$

when n = 1 to M sideband pairs are maintained. The number of pairs $M_p(\alpha)$ needed

for a given power percentage (p) can be found from this relation, and the FM bandwidth measure is then given by $B_p(\alpha) = 2M_p(\alpha)f_m$. The normalized bandwidth $2M_p(\alpha)$ can be evaluated independently of the modulating frequency (f_m).

The normalized bandwidth is shown in Figure A-1 for various power percentages to be preserved. Each step function corresponds to a fixed power percentage (p), with the solid step function representing p = 99% power preserved. The normalized bandwidth assignment based on Carson's Rule is given by $2(\alpha + 1)$, which is represented in the figure by the solid straight line. The rule is noted to essentially follow the p = 99% curve steps for indices in the $0.9 < \alpha < 4.3$ range. It also preserves more power at lower indices, but falls progressively below the 99 percent power curve at higher indices outside this range.

The case of a random modulating signal with a uniform baseband spectrum has also been analyzed using preserved power as the band-limiting distortion criterion. A peak to rms load ratio of 11 dB has been assumed to simulate representative conditions of FDM/FM telephony, and the resultant bandwidth measure $B_q(\alpha) = 2M_q(\alpha)f_m$ is obtained from the following relation

$$M_q(\alpha) \simeq \alpha \left[\sqrt{1 - \log\left(q^{5/7}.\alpha^3\right)} - 0.05\right] + 0.75 \qquad \text{(A-2)}$$

where $q = 1 - (p/100)$ represents the power fraction rejected. This expression is an effective approximation to a complicated integral formulation for moderate index values ($1 < \alpha < 5$). The normalized bandwidth $2M_q(\alpha)$ is shown in Figure A-2 for various (q) values, along with the bandwidth assignment corresponding to Carson's Rule. The latter can be noted to represent a power rejection in the $10^{-10} < q < 10^{-8}$ range, which is negligible.

The two modulation cases analyzed here correspond to extreme distribution conditions, in that one has all the baseband energy concentrated on a single frequency while the other has it spread uniformly over a frequency band. The implication of Figures A-1 and A-2 is that Carson's Rule represents a rather effective approach to the analog FM bandwidth assignment from a power preservation standpoint when modulation indices below five radians are considered. The results also indicate that Carson's Rule preserves considerably more power when the baseband modulation has a spread rather than concentrated spectral characteristic.

References

(A.1) Carlson, A.B. (1968), "Communication Systems," McGraw-Hill Book Company, pp. 239-243.

(A.2) Plotkin, S.C. (1967), "FM Bandwidth as a Function of Distortion and Modulation Index," IEEE Transactions on Communications Technology, pp. 467-470 (June).

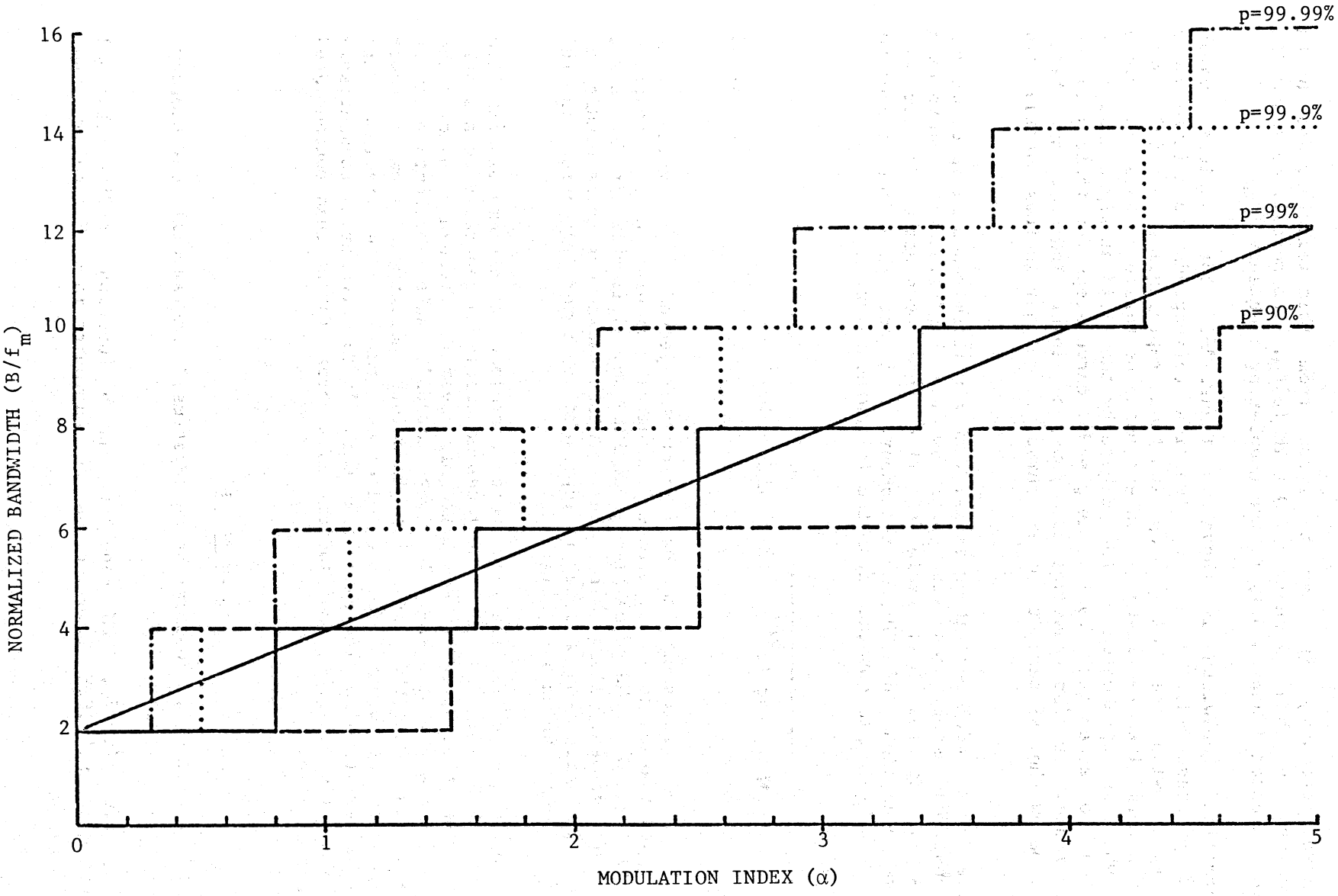

Figure A-1. FM Bandwidth Occupancy and Power Preservation with Sinusoidal Modulation.

(Note: Carson's Rule is the Straight Line)

(Legend: p is the Power Percentage Preserved)

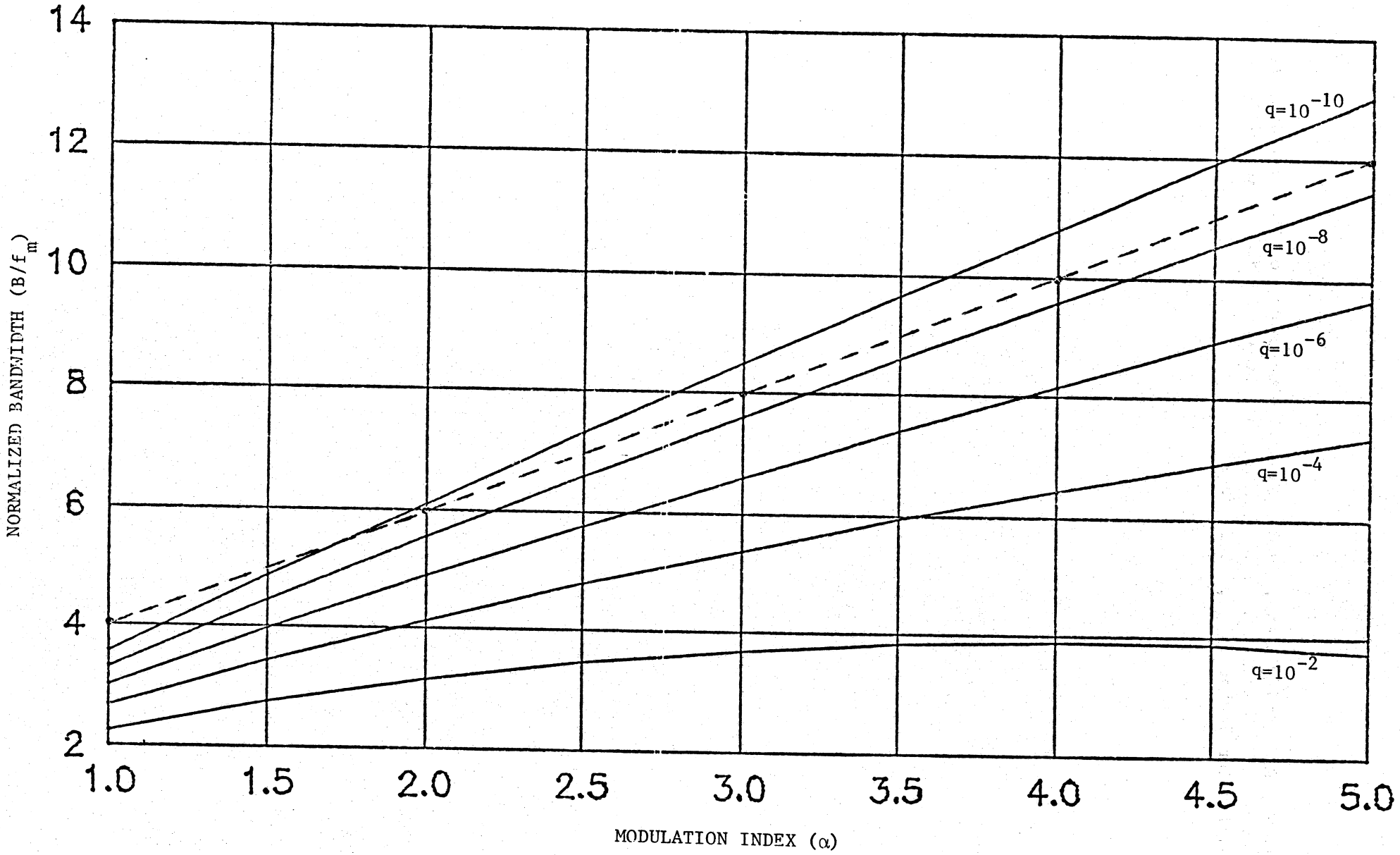

Figure A-2. FM Bandwidth Occupancy and Power Preservation with Band-Limited White Modulation.
(Note: Carson's Rule is the Dotted Line)
(Legend: q is the Power Fraction Rejected)

(A.3) Medhurst, R.G. and Plotkin, S.C. (1968), "Comments on FM Bandwidth as a Function of Distortion and Modulation Index," IEEE Transactions on Communication Technology, p. 500 (June).

APPENDIX B

COMPARISON OF FDM/FM SPECTRAL SIMULATIONS

The following pages present a comparison of the FDM/FM normalized power spectra generated by the FCC and NTIA spectral simulation programs. Each page contains the simulation results for the same satellite communication system, as obtained using both programs. The FCC simulation results correspond to the top graph of each page, while the NTIA simulation results correspond to the bottom graph.

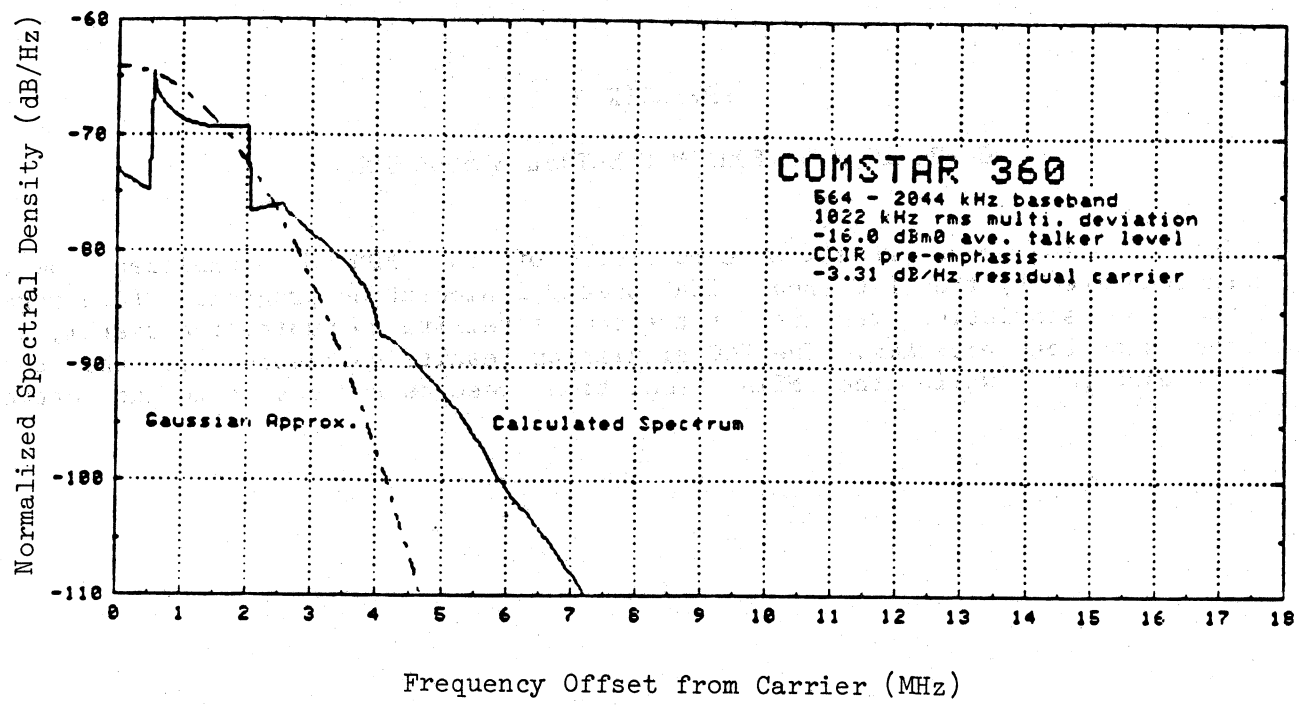

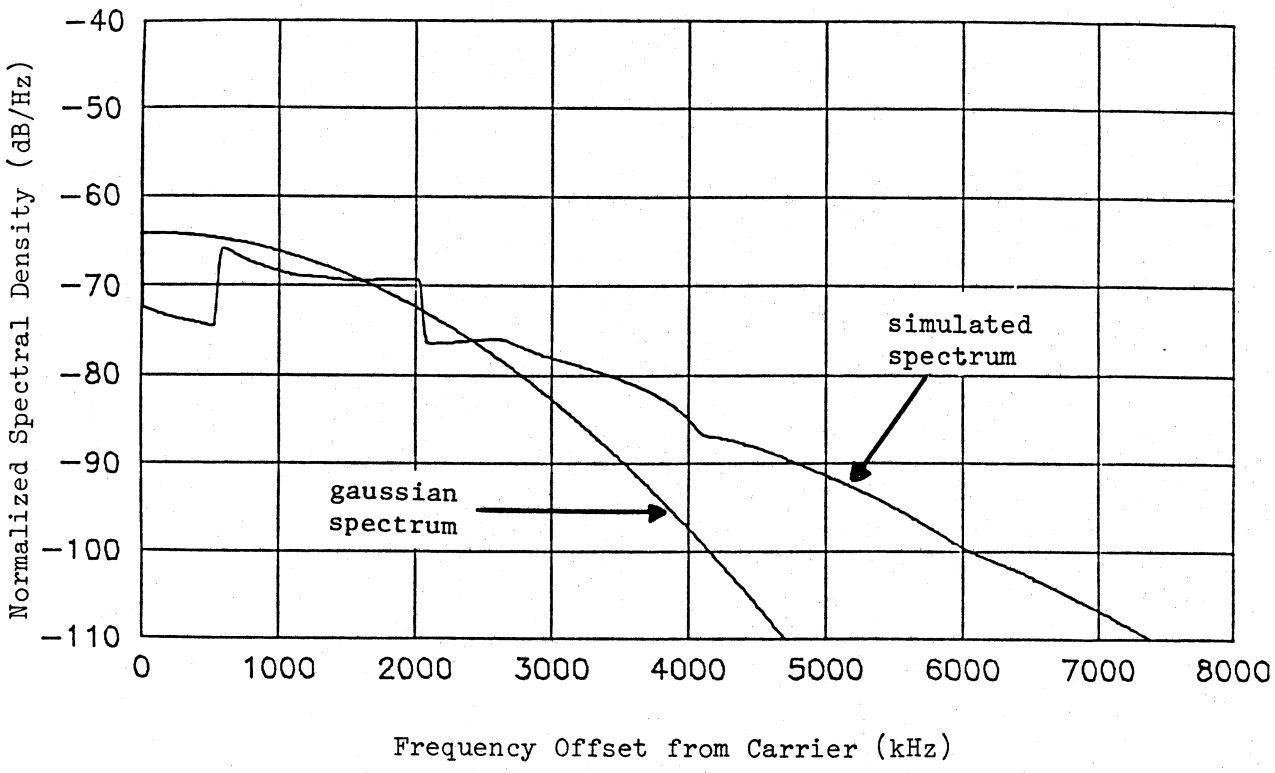

Figure B-1. Comparison of Comstar 360 Spectral Simulations (FCC top, NTIA bottom)

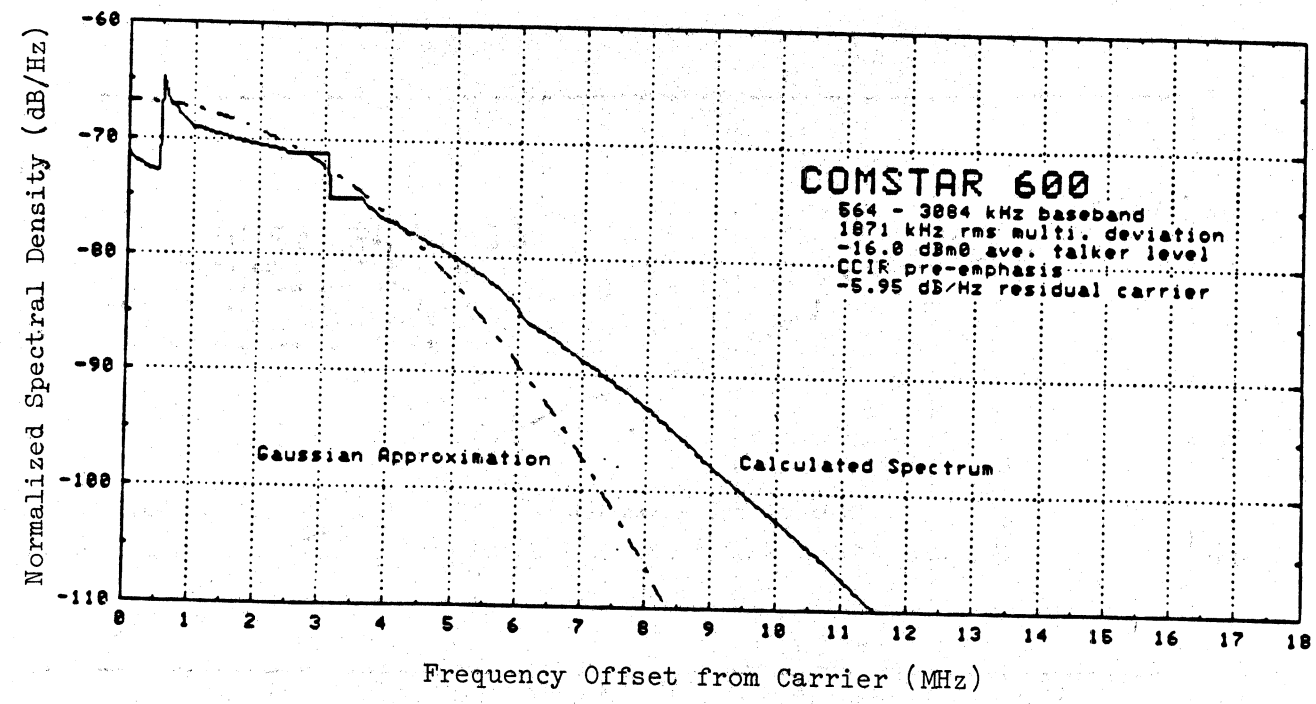

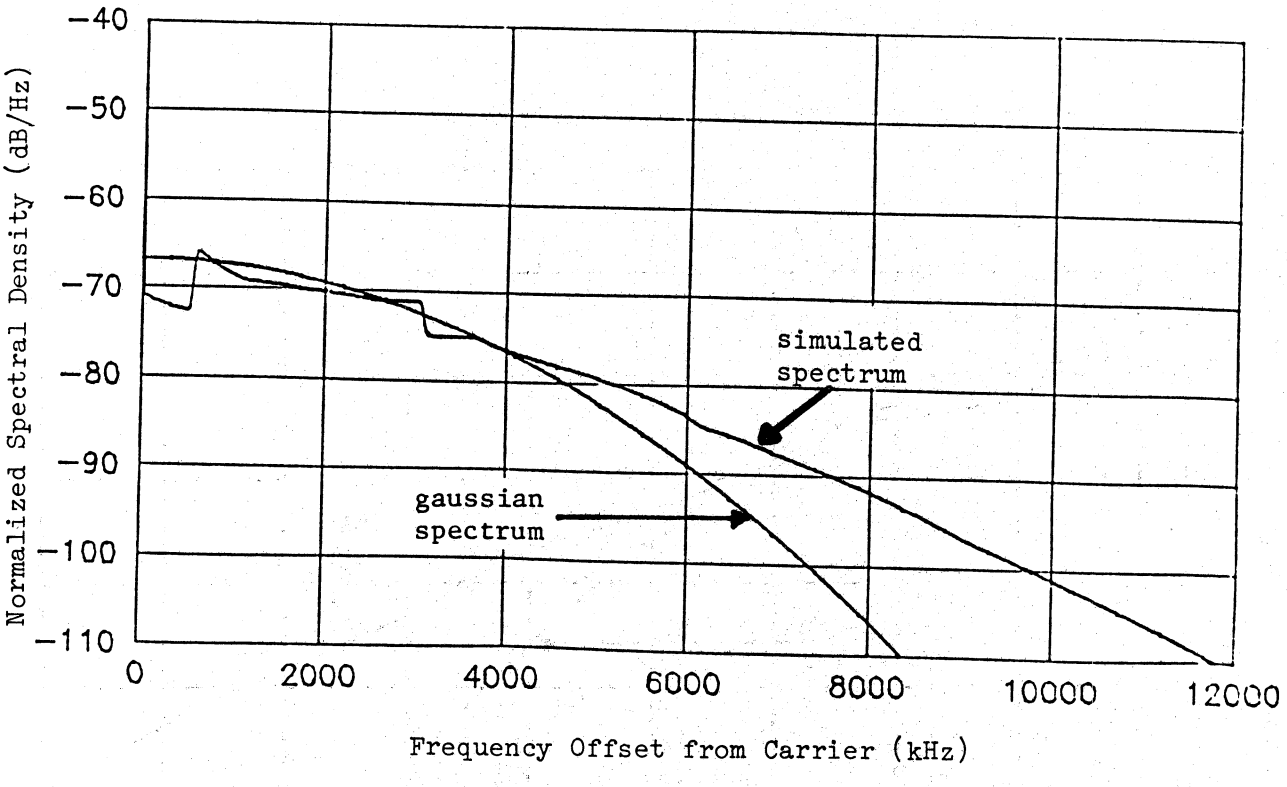

Figure B-2. Comparison of Comstar 600 Spectral Simulations (FCC top, NTIA bottom)

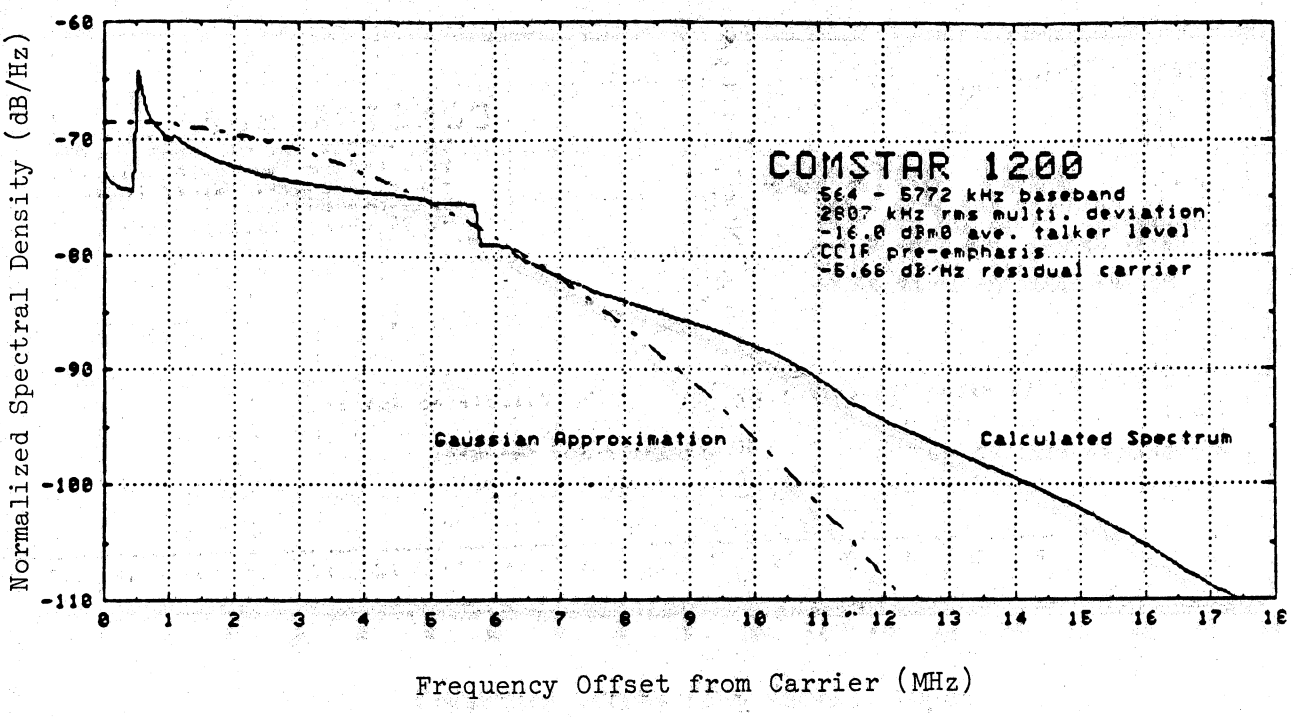

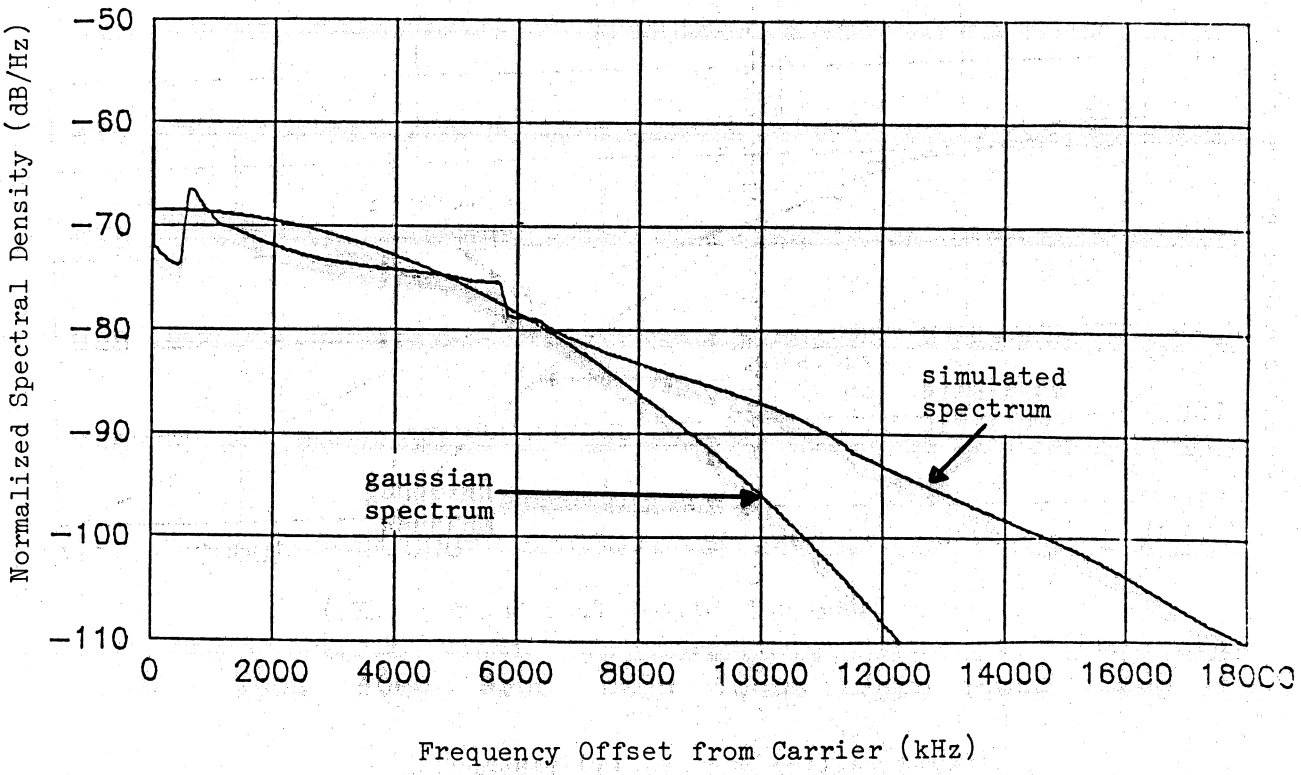

Figure B-3. Comparison of Comstar 1200 Spectral Simulations (FCC top, NTIA bottom)

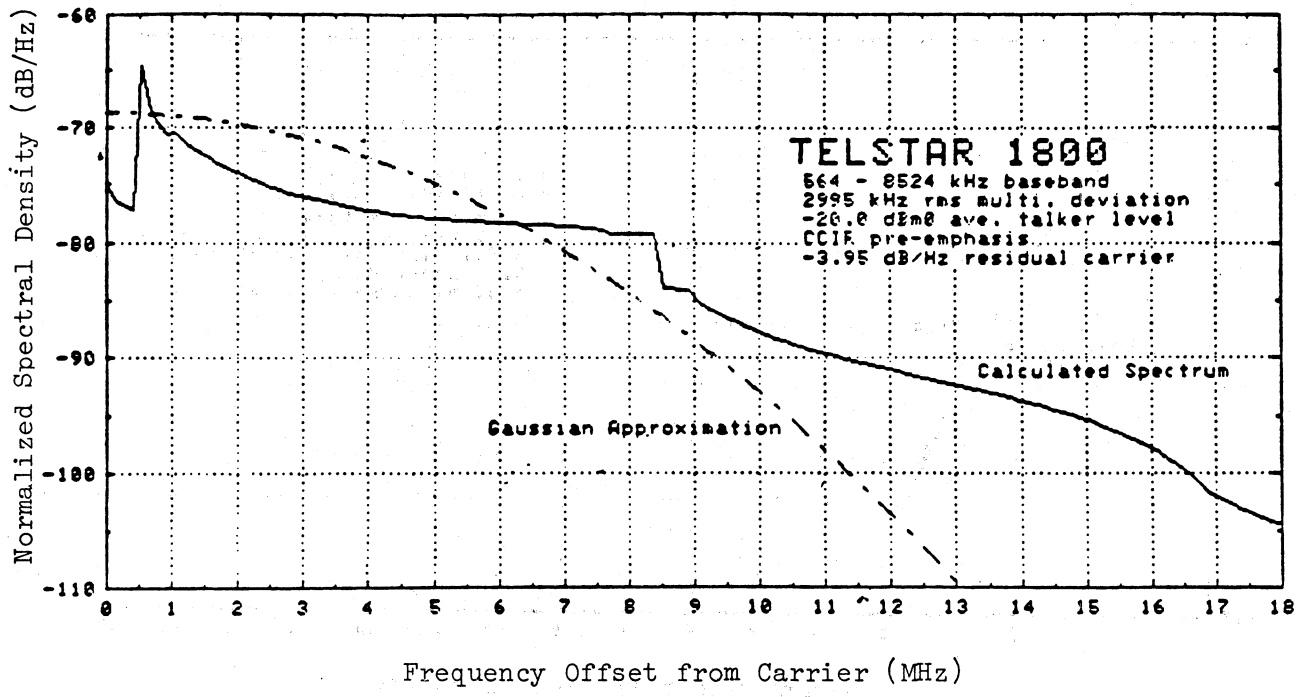

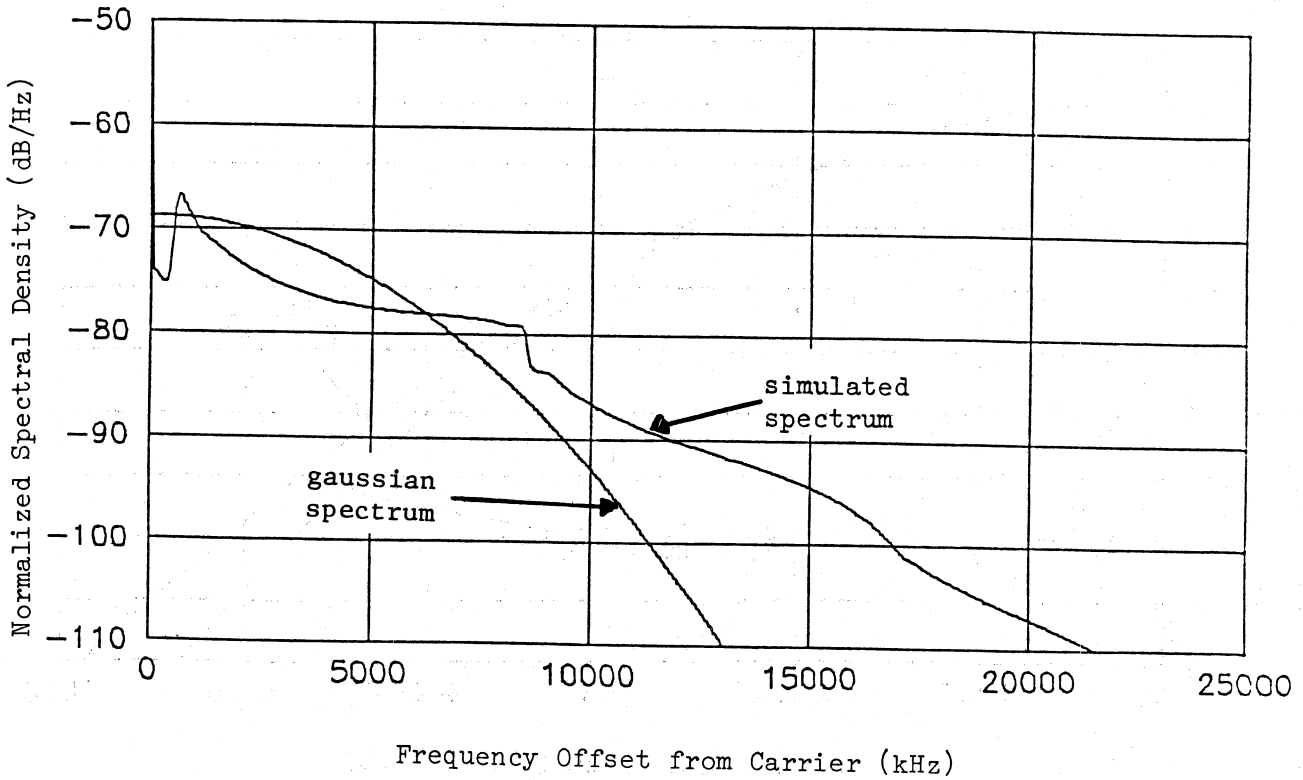

Figure B-4. Comparison of Telstar 1800 Spectral Simulations (FCC top, NTIA bottom)

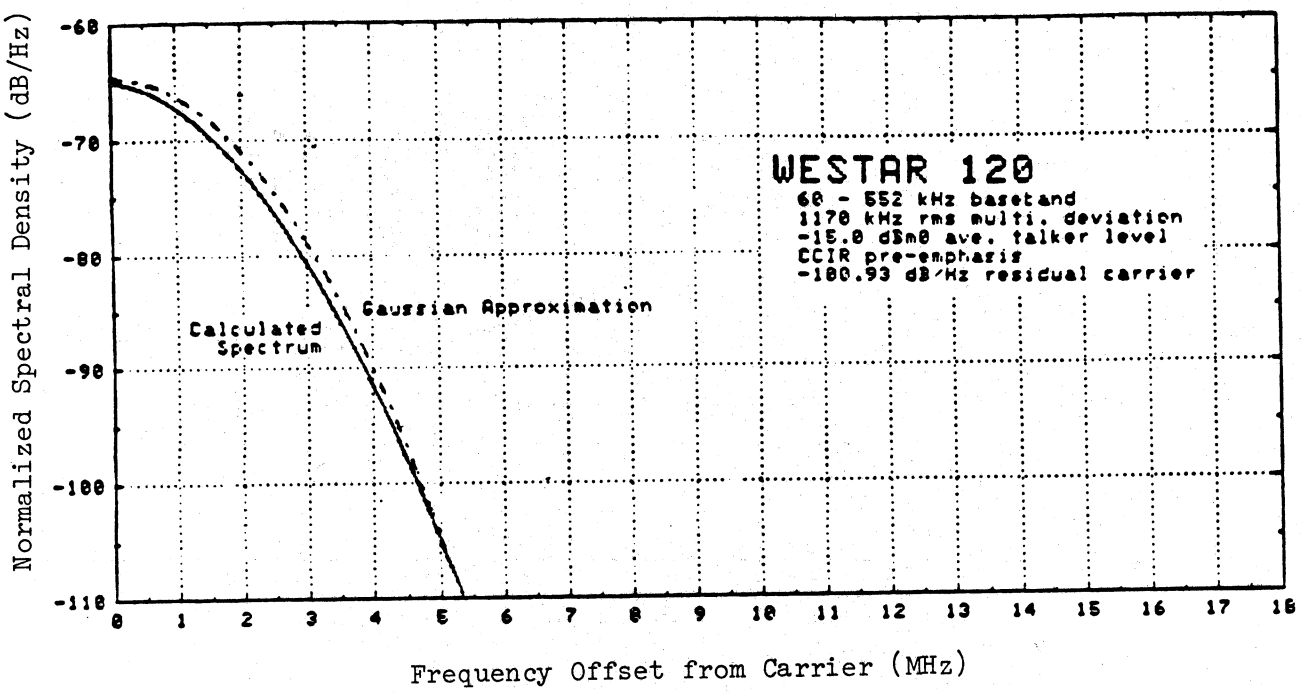

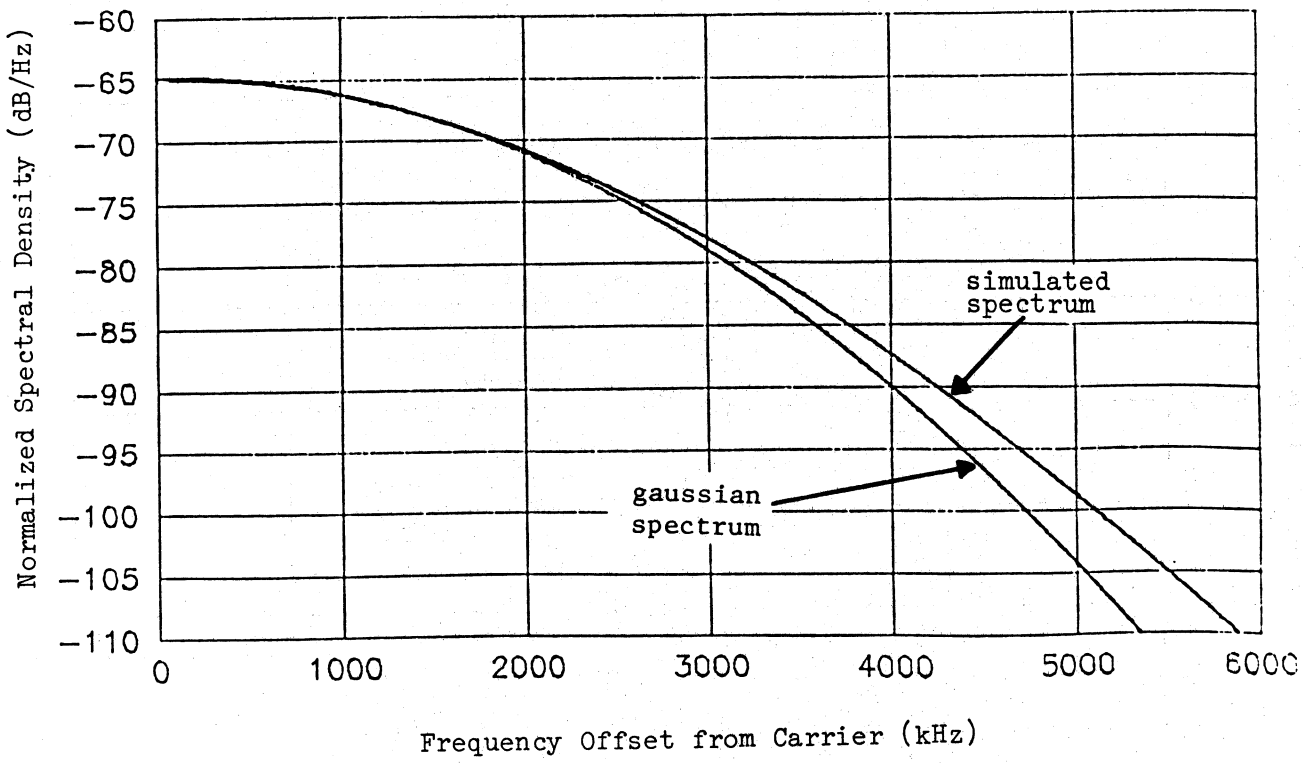

Figure B-5. Comparison of Westar 120 Spectral Simulations (FCC top, NTIA bottom)

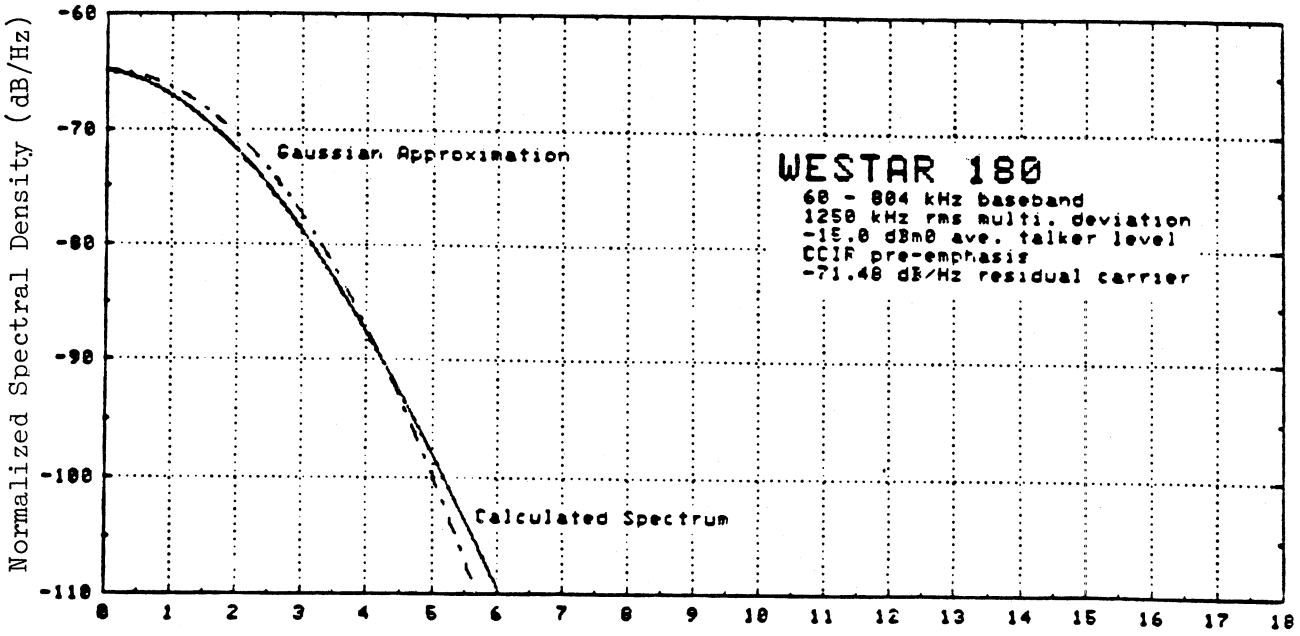

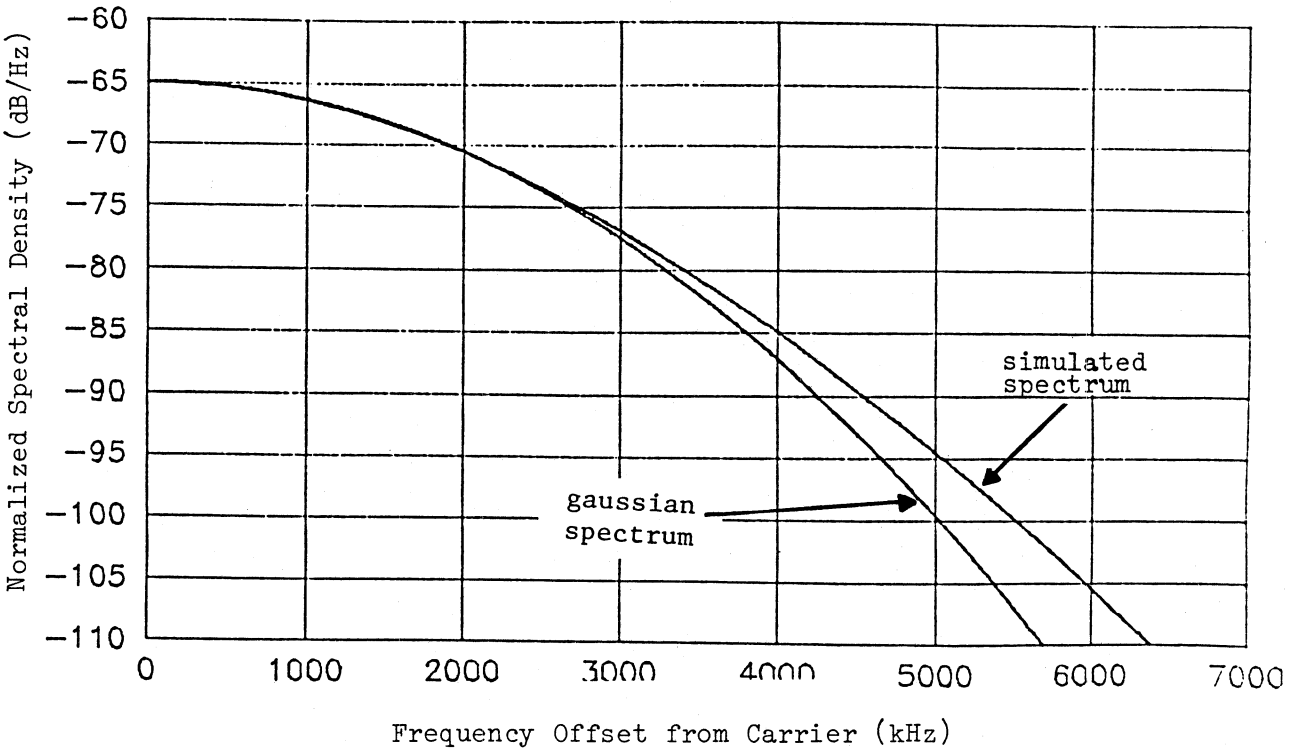

Figure B-6. Comparison of Westar 180 Spectral Simulations (FCC top, NTIA bottom)

FORM **NTIA-29**
(4-80)

U.S. DEPARTMENT OF COMMERCE
NAT'L. TELECOMMUNICATIONS AND INFORMATION ADMINISTRATION

BIBLIOGRAPHIC DATA SHEET

	1. PUBLICATION NO.	2. Gov't Accession No.	3. Recipient's Accession No.
	NTIA REPORT 83-134		

4. TITLE AND SUBTITLE

FM SPECTRUM MODELING AND FDM/FM SIMULATION PROGRAMS

5. Publication Date
September, 1983

6. Performing Organization Code

7. AUTHOR(S)
Cesar A. Filippi

8. PERFORMING ORGANIZATION NAME AND ADDRESS
National Telecommunications and Information Administration
179 Admiral Cochrane Drive
Annapolis, Maryland 21401

9. Project/Task/Work Unit No.
9014101

10. Contract/Grant No.

11. Sponsoring Organization Name and Address
U.S. Dept. of Commerce/NTIA
179 Admiral Cochrane Drive
Annapolis, Maryland 21401

12. Type of Report and Period Covered
Technical

13.

14. ~~SUPP~~LEMENTARY NOTES

15. ABSTRACT *(A 200-word or less factual summary of most significant information. If document includes a significant bibliography or literature survey, mention it here.)*

This report is concerned with the spectral representation of analog FM signals, with particular attention to FDM/FM satellite communication systems. The FM spectral modeling and gaussian approximation principles are analyzed and extended to develop computer simulation programs capable of providing representative FM spectra. A generalized program is developed to accommodate a variety of baseband and preemphasis characteristics, and adapted to generate FDM/FM telephony spectra. The program features the automatic validation and generation of the gaussian spectrum model if applicable, or the automatic simulation of the modulation process to generate the FM spectrum samples otherwise. The program is used to simulate a collection of satellite FDM/FM telephony spectra, which are to be applied as input data into other available interference analysis programs, as part of a major automated computer capability dedicated to the comprehensive assessment of orbital congestion and spectrum resource management concerns pertinent to national and international satellite communication systems scenarios.

16. Key Words *(Alphabetical order, separated by semicolons)*

FM Spectrum Models; Gaussian Spectral Approximation; FM Spectrum Simulation; FDM/FM Telephony Spectra

17. AVAILABILITY STATEMENT

☒ UNLIMITED.

☐ FOR OFFICIAL DISTRIBUTION.

18. Security Class. *(This report)*	20. Number of pages
UNCLASSIFIED	92
19. Security Class. *(This page)*	21. Price:
UNCLASSIFIED	